THE MECHANICAL PROPERTIES AND STABILITY OF RADIATA PINE STRUCTURAL TIMBER

A thesis
Submitted to the University of Canterbury
in partial fulfilment of the requirement for the degree of
Doctor of Philosophy

by

Ping Xu

School of Forestry
University of Canterbury, New Zealand

November 2000

THE MECHANICAL PROPERTIES AND STABILITY OF RADIATA PINE STRUCTURAL TIMBER

Ping Xu
The New Zealand School of Forestry
University of Canterbury

ABSTRACT

Investigating stiffness, strength and stability in radiata pine structural timber is significant to the civil engineering, forestry industry and genetic selection in New Zealand due to the following reasons:

1. Radiata pine provides about 90% structural timber for industry and is one of the major incomes of the forestry industry in New Zealand.
2. Stiffness, strength and stability are major quality criteria of structural timber.
3. Radiata pine stem has large proportion of corewood that tends to be low in stiffness, strength and stability.

This study first presents the maps of average stiffness, average strength and average warp in radiata pine structural timber, obtained from sixty-two 27-year old, unpruned radiata pine trees. From these maps, one can conclude that the butt logs are problem logs, because the butt logs displayed the lowest stiffness, as well as the maximum bow and spring within the stems. The stiffness and strength distributions were compared with the typical distribution of wood density, which reveals that the wood density alone does not reflect the mechanical properties of radiata pine structural timber, because: 1) the denser butt logs exhibited the lowest stiffness among all log types; 2) the butt logs were not the strongest logs compared with other log types.

Knots are found to be the most important factor weakening the mechanical properties and causing extra distortion in structural timber. 99% of the boards broke at a knot that is associated also with lower local stiffness. 70% of maximum bows and 40 % of

maximum springs occurred off the expected mid-span, which may be attributed to the deflections introduced by larger margin and edge knots.

In order to estimate the failure strength non-destructively, this study examined the failure features of the weakest point in detail, including the local stiffness at the failure zone, the failure pattern of knots and the failure frequency in relation to growth and features of knots. The results of this study reveal that non-destructive estimation of strength at the likely weakest point in structural timber is possible.

ACKNOWLEDGEMENTS

I am grateful to Professor J. C. F. Walker, the principal supervisor, for his guidance, inspiration and brilliant advice during my Ph.D study. Many thanks to Assoc. Professor A. H. Buchanan, the co-supervisor, for his help in understanding the problems in relation to the construction industry. The encouragement and consistent support from my supervisors and their willingness to discuss the research problems are sincerely appreciated.

Appreciation is given to the Unversity of Canterbury for a doctoral scholarship.

Thanks are also given to Mr. Michael Weavers and Mr. Richard Newton, technical staff of the Department of Civil Engineering, Mr. Bob Bullsmith, Mr. David K. Clark, Mr. Karl Schasching and Mr. Paul Fuller, technical staff in School of Forestry, for their professional assistance in the last three years.

I would like to take this opportunity to express my gratitude to all staff members and postgraduates at the New Zealand School of Forestry. Their support and friendship have made the stay at Canterbury University memorable.

Finally, special thanks are given to my husband Huawu Liu and my daughter Yingzhi Xu for their understanding and tolerance during many evenings and weekends when I spent the time in the laboratory and office for my research. Their support cheered me up in the last three years, especially when the things went tough.

CONTENTS

Chapter 8 Overall summary and recommendation

LIST OF TABLES

LIST OF FIGURES

Chapter 1

INTRODUCTION

1.1. INTRODUCTION

Improving wood quality of radiata pine (*Pinus radiata D. Don*) species is very significant to the economy of New Zealand, for the following reasons.

- Radiata pine is the most important forest plantation species in New Zealand and radiata pine sawn-timber comprises about 90% of New Zealand's sawn timber production (Department of Statistics, New Zealand, 1996; Kinimonth and Whitehouse, 1991).
- Radiata pine stem has large proportion of corewood that produces low quality timber. For example, corewood consists of nearly half of a 25-year old radiata pine stem if the corewood zone is defined as the wood zone in the first ten growth rings from the pith. Also the proportion of corewood would increase with any reduction of the rotation lengths of radiata pine specices (Sorensson, *et al.*, 1997; Shelbourne, 1997; Zhang, 1997; Cown, 1992; Kinimonth and Whitehouse, 1991; Bier and Colins, 1985; Walford, 1982). According to the report of Sorensson, *et al.* (1997), the rotation length for radiata pine could drop below 20 years in the next two decades.
- Radiata pine contains larger knots than other species, which weakens the mechanical properties and stability of radiata pine structural timber (Kinimonth and Whitehouse, 1991; Fenton, 1967; Kinimonth, 1961).

Improving wood quality of radiata pine species is related to: 1) establishing objective methods to evaluate the wood quality characteristics; and 2) finding efficient ways to increase the value of radiata pine stems. Considering the application of radiata pine structural timber, this thesis concentrates on the investigations of mechanical properties and stability of radiata pine stems. The investigation presented here makes specific contributions in the following areas.

1) Genetic selection

This study investigated the relationship between the log volume and log stiffness in radiata pine. The results reveal that fast growth itself is not a disadvantage in genetic selection after isolating the effects of species, harvesting age and growth environment. It is encouraging for the selection of fast growing genes.

2) Log sorting and allocation

This study provides detailed wood quality maps in terms of stiffness, strength and warp, which give an insight into the relevance of growth features and wood quality variations to primary processing. From these maps, one can concludes that the butt logs are problem logs due to the lowest stiffness, poor strength in corewood, and the maximum values of bow and spring. Thus this study recommends cutting the stem at about 2.7 m above groundline for other end uses, which may minimize reprocessing and waste at mills, thus driving down the production costs and upgrading the value of the remaining part of the stem.

3) Estimating failure strength of structural timber

This study presents the correlation between the failure strength and the local failure stiffness in boards, which is useful to estimate the failure strength in terms of stiffness that can be measured non-destructively. In addition, this study explored the failure features of knots in timber specimen. Two major failure patterns, i.e. boundary-broken pattern (around the knot) and plane-broken pattern (across the knot) in structural timber, are first identified and the failure angles of the broken knots are first characterized, which could be valuable to predict the likely weakest point of board. Combining the prediction of the weakest point and stiffness-strength relation, the strength of structural timber can be estimated. This would benefit visual grade and civil engineering.

4) Investigation of warp

This study first gives the distributions of bow and spring within log types according to the radial distance from the pith in radiata pine.

Kinking is found to be a major factor causing extra bow and spring in structural timber. This gives a clue for further investigation on warp.

1.2. MECHANICAL PROPERTIES OF STRUCTURAL TIMBER

Important mechanical properties for building materials would include stiffness (or modulus of elasticity i.e. the stress-strain relation within the linear region), strength (i.e. ability of timber withstanding stress without failure), hardness (i.e. capacity of timber to withstand denting and abrasion) and toughness (i.e. the ability of the material to absorb energy) (Walker, 1993; Walford, 1985b). Among those mechanical properties, the hardness is considered if severe surface wear is involved (e.g. floor and furniture) and toughness is the major consideration of brittle materials (Walker, 1993; Harris, 1989; Gordon, 1978). Structural timber neither suffers severe surface wear, nor is it usually brittle. Therefore, only stiffness and the strength are investigated in this study.

Forestry industry, civil engineers, and wood scientists have different concerns regarding the investigation of stiffness and strength. A reliable distribution map for average stiffness and average strength in stems is important for the forestry industry, because saw mills can improve log sorting and allocation according to such information. Civil engineers mainly concern non-destructively predicting how weak the board might be and where the weakest point might occur, since beam failure at the weakest point would be catastrophic. For wood scientists, the investigation for the influence of the natural factors on stiffness and strength is significant, due to the needs of genetic selection. Therefore, the strategy of this study is to focus on three aspects for investigating the stiffness and the strength:

1) Showing wood quality maps of radiata pine in terms of stiffness and strength.
2) Estimating the strength of board at the weakest point non-destructively.
3) Investigating the effect of knots on the strength of board.

Machine stress grading and tensile testing were used to investigate the stiffness and the strength in this study due to following main advantages (a full description of the advantages are presented in Chapter 3 and Chapter 4). Machine stress grading can

provide the variations of the local stiffness at 152 mm intervals along the length of each piece of timber, which is important for profiling a detailed stiffness map and studying the features of the stiffness at the weakest point. The ultimate tensile strength indicates the strength at the weakest point, which meets the requests of the construction industry, i.e. knowing how weak the board might be and where the weakest point occurs.

Sixty-two radiata pine trees were taken randomly from a 27-year old, unpruned single stand on the Mamaku Plateau in the Central North Island of New Zealand for this study. The trees were cut to give 1,988 structural timber specimens with dimensions 90 × 35 × 4,200 mm for machine stress grading to study stiffness, and 1,919 these timber specimens were employed for tensile testing to study strength (69 broke during machine stress grading due to large knots on the board). Based on the experimental data, detailed timber quality maps in terms of averaged stiffness and averaged strength are presented in this thesis, and the mechanical properties at the weakest point and the failure features of the knots are also exhibited in this thesis in detail.

1.3. STABILITY OF STRUCTURAL TIMBER

Stability is the ability of timber to sustain deformation during moisture sorption without excessive dimensional change. In contrast, instability of timber is a description of dimensional change during moisture sorption.

Three separate facets, i.e. shrinkage in drying, movement in service and responsiveness to a fluctuating environment, are used to evaluate the instability of timber (Walker, 1993). Shrinkage is defined as the ratio of dimensional change to the green (swollen) dimension. Movement is defined by measuring the swelling or shrinkage of dried wood between the relative humidities 60% to 90% at 25 °C (Walker, 1993). Responsiveness is the efficiency (speed) of wood in response to a fluctuation in atmospheric moisture content (Walker, 1993; Harris, 1961). Movement and responsiveness are related to the effect of environment on timber in service. From the sawmill's point of view, the shrinkage and shrinkage-induced warp are the major concerns regarding down-grading wood quality, and hence are commonly used as guides of instability in current studies

(Cown *et al.*, 1991b; Kinimonth and Whitehouse, 1991). This study only investigated warp for two reasons:

1) warp results in degrade, wastage and rejection of structural timber, and hence a major annual loss to sawmills (Walker, 1993).
2) shrinkage has been well documented in previous research (Siau, 1995; 1984, 1971; Walker, 1993; Nestic and Miler, 1991; Kinimonth and Whitehouse, 1991; Cown *et al.*, 1991a; Skaar, 1988, 1972), while the detailed information related to the warp of radiata pine is very limited.

Warp is classified into six typical forms including diamond, cup, bow, spring (or crook), twist and kink (ASTM, Designation: D9-87, 1995; Ministry of Forestry, New Zealand, 1995; U.S. Forest Products Laboratory, 1955). Considering the diamond and cup are not main warp forms in radiata pine, this study focused on the investigation of bow, spring, twist and kink. The influence of spiral grain on the twist and the extra warp caused by knots were also studied in this study. After machine stress grading, the warp in 1,919 structural timber specimens ($90 \times 35 \times 4{,}200$ mm) were examined carefully. The timber quality maps of radiata pine species in terms of bow, spring and twist are presented in this thesis. And this thesis also comments on the effect of the spiral grain and the length of board on the twist.

1.4. OVERVIEW

This thesis is divided into eight chapters. Chapter 1 briefly introduces the significance, objectives, and methodology of this study. Chapter 2 introduces a method to evaluate log volume. The volumes of 239 radiata pine log are used to study the relationship between the log volume and the log stiffness, in order to identify whether log volume can be treated as a potential predictor of the log stiffness. Chapter 3 explores the stiffness gradient in 62 radiata pine trees. A detailed stiffness map is presented in this chapter, which includes the variations of local average stiffness, board stiffness within different log types according to radial distance from pith. Research regarding the relationship between the log volume and log stiffness is also displayed. Chapter 4 describes the advantages of investigating ultimate tensile strength in structural timber,

then the variations of the tensile strength is displayed within log types according to radial distance from the pith. In Chapter 5, the best indicator of the failure strength is determined after examining correlations between the failure strength and various suggested indicators of the failure strength. Based on the experimental facts, Chapter 6 first presents two failure patterns of the broken knots. In addition, efficient methods for measuring the failure angle of broken knots are introduced. Chapter 7 gives timber quality maps in terms of bow, spring and twist. The significance of kink for unpruned radiata pine species is also discussed in this chapter. An overall summary and recommendations for future research are given in Chapter 8.

1.5. OBJECTIVES

The goals of this study were evaluating structural timber quality in terms of stiffness, strength and stability in radiata pine to meet the requests of forestry industry, civil engineering and genetic selection. The specific objectives of this study were as follows:

1) Determining average values and variation trends of stiffness, strength and warp within stems.
2) Examining the relationship between the log volume and the log stiffness.
3) Identifying the best indicator of failure strength of structural timber from amongst the variables, e.g. average bending stiffness, average tensile stiffness, F-grade mark, maximum knot area ratio and local failure stiffness.
4) Predicting the weakest point of board, which includes investigations of the failure features of knots, i.e. percentage of failed board due to knots, the types of failed knots, the knot area ratio of failed knot, the failure angle of the knot and the failure pattern of the knot.
5) Investigating the effect of natural defects on the warp.

Chapter 2

THE VOLUME OF RADIATA PINE LOGS

2.1. INTRODUCTION

A larger yield volume of logs is desirable in the forest harvest. However, fast growing species that can be harvested early are associated with poor wood quality, because younger trees contain a higher proportion of corewood (Matheson *et. al.*, 1997; Bendtsen and Senft, 1986). Slow grown trees are generally thought to be denser and stiffer when they reach harvesting age (Cown and McConchie, 1983; Harris 1965).

A concern of this study is whether fast growth itself is a disadvantage in genetic selection, i.e. whether the poor mechanical properties are related to growth rate after isolating the influences of species, age and growth conditions. Thus, an investigation of the relationship between log volume and log stiffness in a single stand of 27-year old, unpruned radiata pine was conducted. The experimental results for log volume are presented in this chapter, in order to compare with the distribution of log stiffness in the next chapter.

A number of methods have been introduced to estimate the merchantable log volume. However, the existing methods are not satisfactory in terms of the accuracy and convenience to users as reviewed in Section 2.2. Therefore, an alternative method for calculating the log volume is considered in this study. 239 radiata pine logs were employed for this study, which are shown in Section 2.3. The optimal method for calculating log volume is introduced in Section 2.4. Section 2.5 displays the experimental results, and a summary is given in Section 2.6.

2.2. REVIEW OF PREVIOUS STUDIES

In the forestry industry, a number of formulae (Avery and Burkhart, 1994) have been used for the estimation of the volume of a single log:

Huber's: Volume of log = A_M L (2.1)

Smalian's: Volume of log = $\frac{(A_B + A_S)}{2}$L (2.2)

Newton's: Volume of log = $\frac{(A_B + 4A_M + A_S)}{6}$L (2.3)

where

L is the length of log, m;

A_B, A_M and A_S are areas of the big end, the midpoint cross-section and the small end progressively, m^2.

By assuming the log as a cylinder, replacing A_m with $\pi(\frac{D_m}{2})^2$, Hamilton (1985) presented a simplified form of Huber's formula in the Forest Mensuration Handbook as:

Hamilton's Volume of log = $\frac{\pi D_m^2}{4}L$ (2.4)

where

L is length of log, m;

D_m is the diameter of middle cross-section, m.

Note: if D_m measured in cm, L measured in m, formula (2.4) is changed to the form:

Volume of log = $\frac{\pi D_m^2}{40{,}000}L$ **(2.4)'**

Formulae (2.1), (2.3), (2.4) are inconvenient and inaccurate for measuring and calculating due to the following difficulties.

- The mid-diameter and midpoint area may not be assessable when a log is in piles.
- Even if the logs are not in piles, the mid-diameter can only be obtained overbark. Therefore, errors of measured mid-diameter and estimated midpoint area are

significant due to the uncertainty of bark thickness, taper of log and irregular shape of cross-section (Avery and Burkhart, 1994).

- log does not always appear in a cylinder shape. In fact, the logs are tapered and elliptical (Liu, 1998; Kinimonth and Whitehouse, 1991; McAdoo, 1969).

Formula (2.2) could be even less accurate than the other formulas i.e. (2.1), (2.3) and (2.4), especially when a log with flared ends (Avery and Burkhart, 1994).

Ellis and Kimbeerley (1995) introduced the fifth method in Japanese Agricultural Standard (JAS), by replacing the D_m^2 with $\frac{4}{\pi}D_S^2$ to Formula (2.4). Huber's formula is further simplified to the form:

$$V = D_S^2 L \qquad (2.5)$$

where

V is the log volume in cubic metres for length less than 6 m;

D_S is the small-end diameter inside bark, m; L is the length of the log, m.

Note: if D_S is measured in cm and L is measured in m, formula (2.5) has the form:

$$\mathbf{V = D_S^2 L/10{,}000} \qquad \mathbf{(2.5)'}$$

Ellis and Kimbeerley's formula (Formula 2.5) avoids the measurement of mid-diameter. However, their method also oversimplifies a log as a cylinder with diameter $\sqrt{\frac{4}{\pi}}D_S$. Consequently, the sum of the deviation is accumulated to a very large value when Formula (2.5) is used to calculate the total volume of many logs.

Summarising the above, the existing methods for estimating the volume of log have obvious shortcomings -- either inconvenient or inaccurate. Hence, the first task of this study is to seek a reliable and accurate method for the calculation of log volume, which can assess the volume of individual logs.

2.3. MATERIALS

Sixty-two radiata pine trees were selected and felled randomly from a single stand of 27-year old, unpruned radiata pine on the Mamaku Plateau in the Central North Island of New Zealand. Every stem of fifty–three trees was cross-cut to give four 4.2 meter logs (butt, middle, top and upper top) (Fig.2.1), whereas each stem of the other nine shorter trees was cross-cut into just three 4.2 meter logs (butt, middle, top) (Fig. 2.2). Total number of logs used in this study is 239. The identity of each log, such as tree number, log type, was retained by tagging them on the larger end of each log.

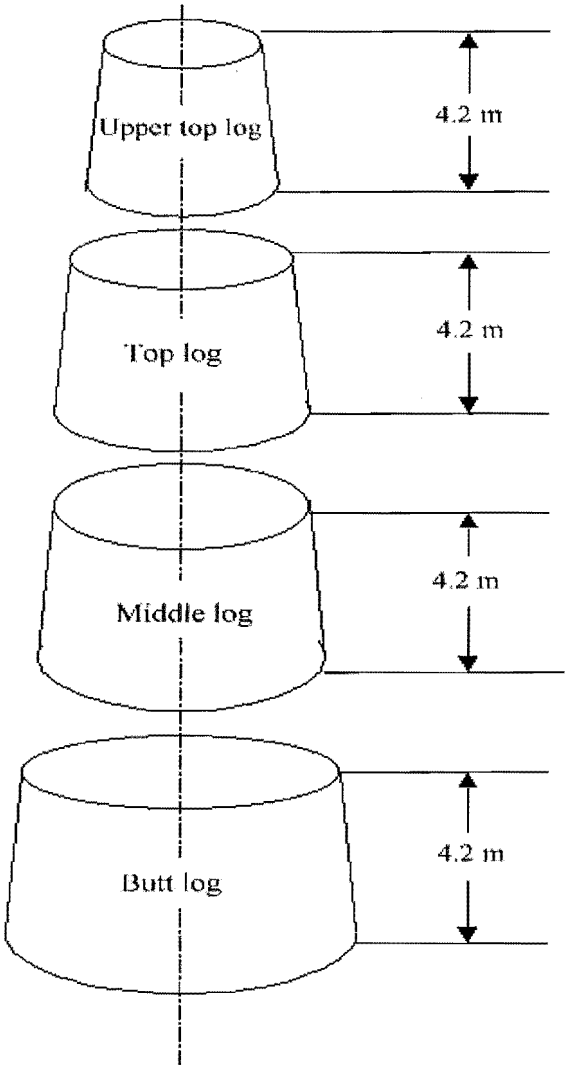

Fig. 2.1. Cutting pattern of 53 stems.

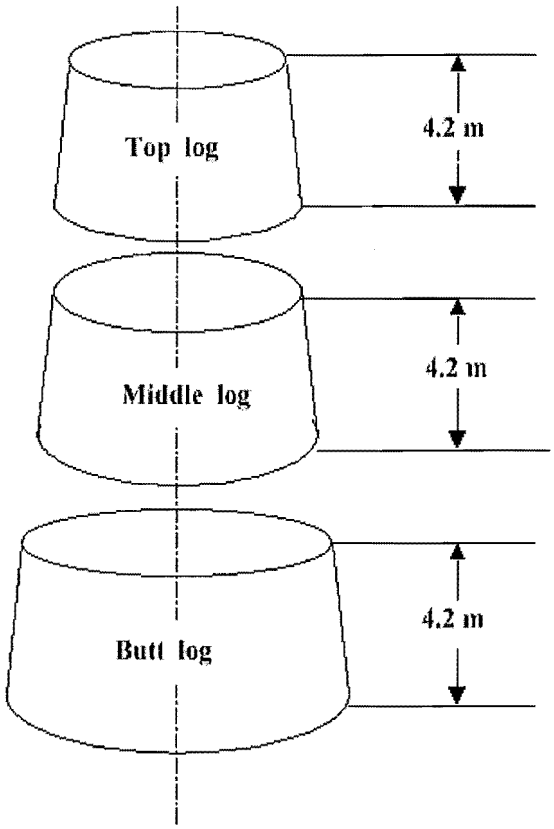

Fig. 2.2. Cutting pattern of other 9 stems.

2.4. METHODS

This section introduces two formulae, i.e. the formula for the circular cone-shaped log and the elliptic cone-shaped log, to calculate the volume of the log. The derivation of the formulae and the measurement of the log diameter are also presented in this section.

2.4.1. Calculating for merchantable volume of logs

A radiata pine log is better treated as a truncated elliptical cone or a truncated circular cone rather than as a cylinder because of the following two reasons:

1) large taper (Walker and Butterfield, 1995; Cown, 1992);
2) the cross-sections of the stems were best approximated as either ellipses or circles (Liu, 1998; Kinimonth and Whitehouse, 1991; McAdoo, 1969).

Hence, this study calculated the log volumes according to following formulas:

$$\text{Volume}_{\text{circular cone}} = \frac{\pi h}{12}(\overline{D}_B^2 + \overline{D}_T^2 + \overline{D}_B\overline{D}_T) \quad (2.6)$$

$$\text{Volume}_{\text{elliptical cone}} = \frac{\pi h}{12(D_{BL} - D_{TL})}(D_{BL}^2 D_{BS} - D_{TL}^2 D_{TS}) \quad (2.7)$$

where

h is the length of the log, m;

$\overline{D}_B$ and $\overline{D}_T$ are the mean diameters at the base (big end) and top (small end) respectively, m;

D_{BL} and D_{BS} are the longest and shortest diameters at the base (big end), m;

D_{TL} and D_{TS} are the longest and shortest diameters at the top (small end), m.

2.4.2. Derivation of the formulas for the volume of a single log

The volume of a circular cone is given by

$$\text{Volume} = \frac{\pi}{3}R^2L \quad (2.8)$$

where

R is the radius in the base, m;

and L is the length of the cone, m.

The volume of a truncated circular cone (Fig. 2.3) can be calculated from

$$\text{Volume} = \frac{\pi}{3}R_B^2L - \frac{\pi}{3}R_T^2(L-h) \quad (2.9)$$

where

R_B and R_T is the radii of the base and the top of the log, m;

h is the length of the log, m;

L is the length of the cone, m.

From the theory of similar triangles shown in Fig. 2.3, one obtains

$$\frac{L}{R_B} = \frac{L-h}{R_T} \qquad \text{or} \qquad L = h\,R_B/(R_B - R_T) \tag{2.10}$$

Substituting Equation (2.10) into (2.9), we have

$$\text{Volume} = \frac{\pi h}{3}\left[\frac{R_B^3 - R_T^3}{R_B - R_T}\right]$$

$$= \frac{\pi h}{3}[R_B^2 + R_T^2 + R_B R_T]$$

$$= \frac{\pi h}{12}[\overline{D}_B^2 + \overline{D}_T^2 + \overline{D}_B\overline{D}_T]$$

and Equation (2.6) is derived.

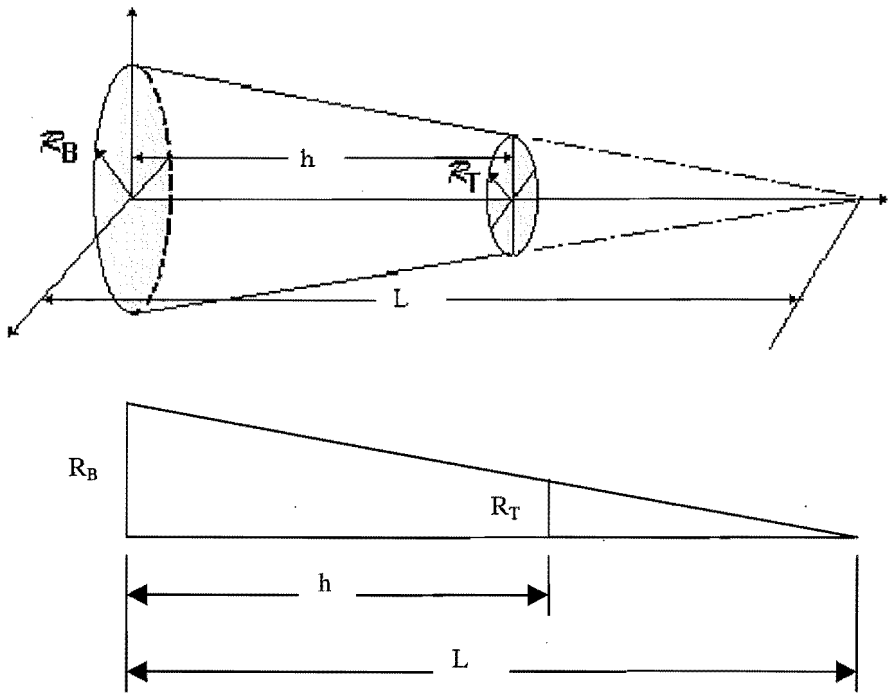

Fig. 2.3. A truncated circular cone.

The volume of an elliptical cone is given by

$$\text{Volume} = \frac{\pi}{3} abL \qquad (2.11)$$

where

a and b denote the major and minor semi-axes, m;

L is the length of the cone, m.

The volume of a truncated elliptical cone (Fig. 2.4) can be calculated from

$$\text{Volume} = \frac{\pi}{3} a_B b_B L - \frac{\pi}{3} a_T b_T (L - h) \qquad (2.12)$$

where

a_B and b_B are the major and minor-axes at the base, m;

a_T and b_T are the major and minor-axes at the top, m;

L is the length of the cone, m;

h is the length of the log, m (Fig. 2.4).

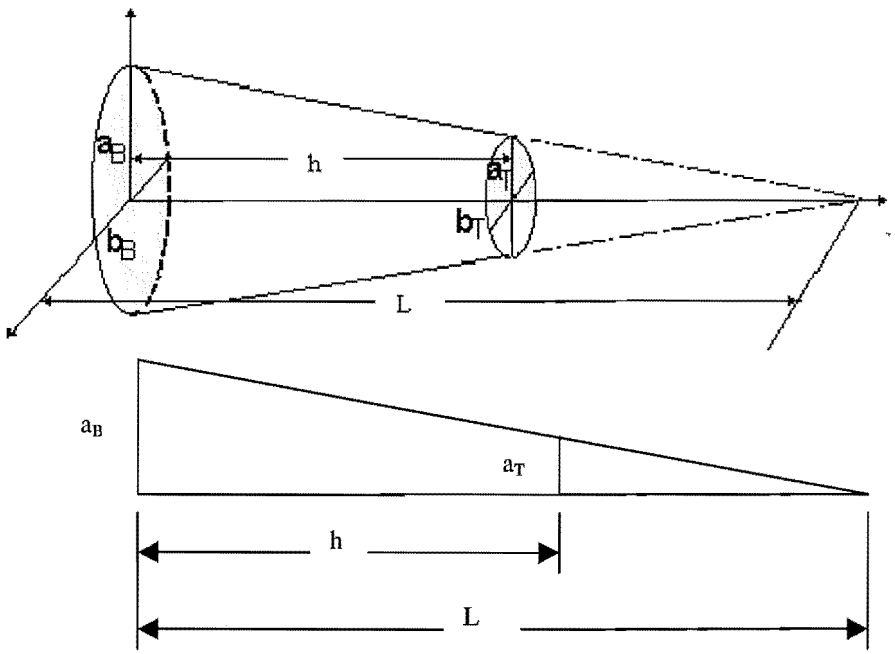

Fig. 2.4. A truncated elliptical cone.

From the theory of similar triangles shown in Fig. 2.4, one obtains

$$\frac{L}{a_B} = \frac{L-h}{a_T} \qquad \text{or} \qquad L = h\, a_B/(a_B - a_T) \tag{2.13}$$

Substituting Equation (2.13) into (2.12), we have

$$\text{Volume} = \frac{\pi h}{3\,[a_B - a_T]}[a_B{}^2 b_B - a_T{}^2 b_T] \tag{2.14}$$

Because $a_B = D_{BL}/2$, $a_T = D_{TL}/2$, $b_B = D_{BS}/2$ and $b_T = D_{TS}/2$, Equation (2.7) is derived.

2.4.3. Measurement of log diameter

The following two situations were considered in this study during measurement of diameters of logs:

- in a truncated circular cone-shaped log, the average diameters ($\overline{D}_B$, $\overline{D}_T$) inside bark were measured at the big end and small end respectively;
- in a truncated elliptical cone-shaped log, the shortest diameters ($\overline{D}_{BS}$, $\overline{D}_{TS}$) and the largest diameters ($\overline{D}_{BL}$, $\overline{D}_{TL}$) inside bark were measured at the big end and the small end respectively.

Then the volumes of the logs were calculated according to either formula (2.6) or (2.7).

2.5. EXPERIMENTAL RESULTS

2.5.1. Probability of logs being truncated elliptical cones

As with previous studies, this investigation found that the cross-sections of the logs were best approximated as either ellipses or circles. Table 2.1. shows that the percentage of the logs being truncated elliptical cones in the 62 bottom logs is 66%; and about half of middle logs appear as the truncated elliptical cones. And the probability of truncated elliptical cones decreases on moving up the stems. In the upper top logs, the probability of logs being truncated elliptical cones reduces to 19%.

Table 2.1. Percentage of the logs being truncated elliptical cones.

Log type	Number of logs with elliptical ends	Number of logs with circular ends	Percentage of truncate elliptical cone
62 bottom logs	41	21	66%
62 middle logs	28	35	45%
62 top logs	15	47	24%
53 upper top logs	11	42	21%

Note: A cross-section is determined as elliptical if the difference between the largest and smallest diameter is more than 20 mm.

2.5.2. Merchantable volume of logs

As already mentioned, in this study, the fifty–three stems were cut into butt, middle, top and upper top logs; and the other nine stems were cut into butt, middle and top log due to their shorter lengths. The volume of each log was calculated according to formula (2.6) or (2.7).

The results of the experiments show the merchantable volumes ranging from 0.049 m^3 to 0.979 m^3 in all 239 logs. The average volumes of butt, middle, top, and upper top logs are 0.428 m^3, 0.306 m^3, 0.249m^3 and 0.194 m^3 respectively.

Fig. 2.5. indicates the number of logs in different volume ranges. For this 27- year old radiata pine stand, 64.4% of all 239 logs fall into the range from 0.142 m^3 to 0.328 m^3; 20.5% of 239 logs are in the volume range from 0.359 m^3 to 0.514 m^3. There are just 5% of 239 logs that have smaller volume than 0.142 m^3 and 10% of 239 logs that have larger volume than 0.514 m^3.

Fig. 2.5. The number of logs in different volume intervals.

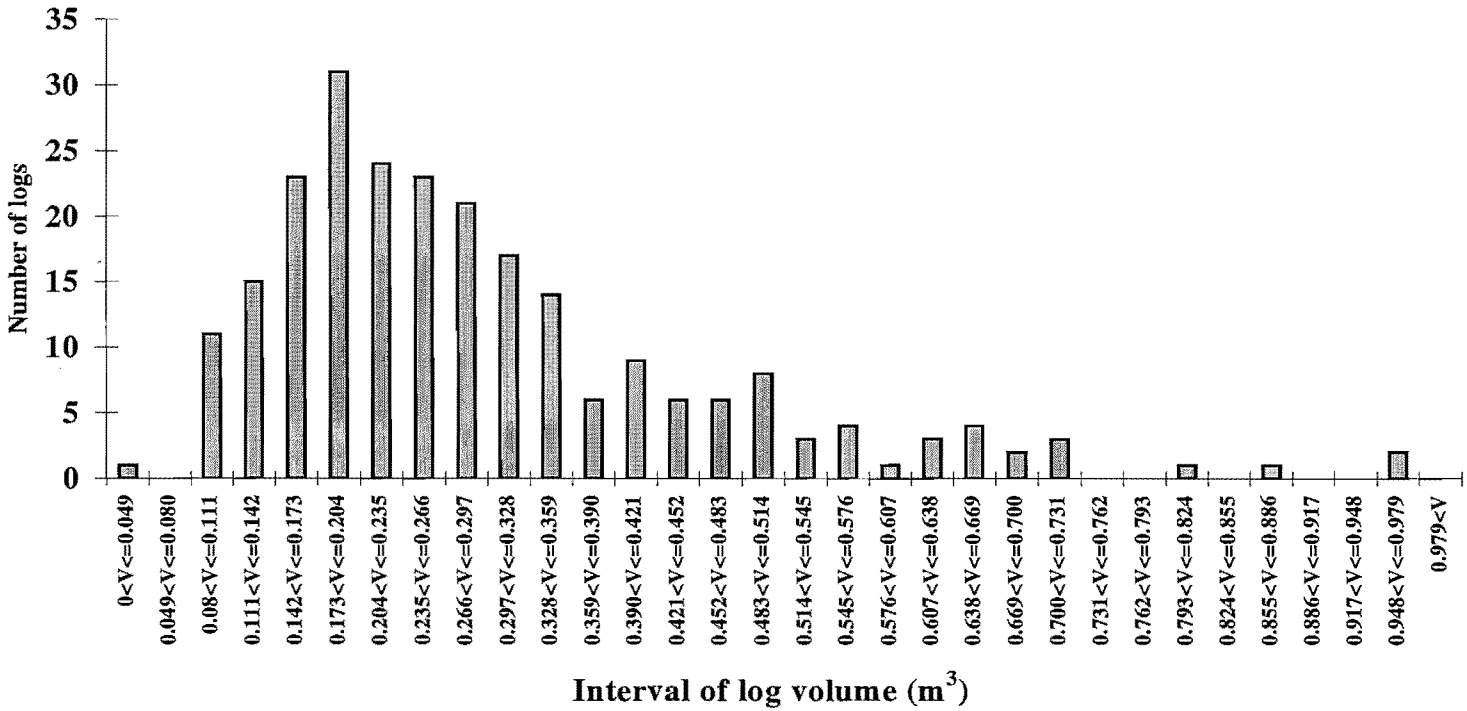

2.6. SUMMARY

Considering the ends shape and the taper of radiata pine stems, this study suggests calculating the volume of radiata pine log using either a formula of the truncated circular cone or a formula of the truncated elliptical cone in order to improve the accuracy and efficiency of previous methods. The derivations of these formulas are given in detail in this chapter. According to these alternative methods, a distribution of log volume in a single stand of 27-year old, unpruned radiata pine is presented in this chapter, which provides useful information for analyzing the influence of the log volume on the log stiffness in next chapter.

Chapter 3

STIFFNESS IN RADIATA PINE STEMS

3.1. INTRODUCTION

Stiffness or modulus of elasticity (i.e. the ratio between stress and strain within the elastic region) has long been recognized as a key quality standard of wood and timber. The published literature regarding the stiffness gradient in small clear wood is rich (Cave and Walker, 1994; Walker, 1993; Bodig and Goodman, 1973; Gunnerson *et al.*, 1972; Goodman and Bodig, 1970; Cave, 1969). Compared with the small clear wood, the investigation regarding the stiffness gradient in structure timber is more complex due to the natural defects and the variation of microfibril angle in the stem. However, providing a reliable stiffness map in the stem is very necessary and useful for the wood industry. A reliable distribution of the stiffness can improve log sorting and allocation, which minimizes reprocessing and waste at mills, thus driving down the production costs with significant benefits for the forestry industry. Therefore, one objective of this study is targeted on the distribution pattern for stiffness, in order to obtain a wood quality map in terms of stiffness gradient in radiata pine stems.

Addis Tsehaye (1995) provided some information about the variation of mean stiffness in 915 structural timber specimens from a 25-year old, unpruned radiata pine plantation on the Canterbury Plains near Dunsandel in the South Island of New Zealand. Addis Tsehaye (1995) reported that: the mean stiffness of boards increased with the radial distance from the pith to the bark; and there was no obvious difference for the mean stiffness in different log types along the vertical direction of the stems.

This study investigated the mean stiffness gradient in 1,988 structural timber specimens with the dimensions 90 × 35 × 4,200 mm that were from a single stand of 27-year old, unpruned radiata pine on the Mamaku Plateau in the Central North Island of New Zealand. A detailed stiffness map is first presented in this chapter, which includes the variation of log stiffness in vertical direction, the mean stiffness gradient of boards within log types according to the distance from the pith, and the variation of local

average stiffness at 152 mm intervals over the stems. Based on the experimental data, this study concludes that butt logs are problem logs due to their lowest log average stiffness in the stems, and the worst stiffness part is from the bottom to 2.7 m. After isolating the least-stiff 20%, the average stiffness of boards from the remaining logs is enhanced with the largest gain being in the butt log (1.9 GPa) and the minimum gain in the upper top logs (1.1 GPa). These improvements for stiffness show that "boxed-pith" board is unsuited for structural purpose, because the highest average stiffness value in boxed-pith boards for all log types is still lower than the boundary stiffness value of F5 structural grade (6.9 GPa), even if the least-stiff 20% of logs has been isolated. Based on the experimental data of the log volume shown in Chapter 2, this chapter also displays the relationship between the log volume and the log stiffness. The results reveal that log volume is not a good potential indicator of log stiffness because of the poor correlation between them. This is encouraging for radiata pine species, as it means that larger log volume does not result in less log stiffness under the same growth conditions (same harvesting age, same location and same environment).

The general principles, and the equations to determine stiffness are reviewed in Section 3.2. The experimental materials and methods of this study are listed in Section 3.3 and Section 3.4. Section 3.5 presents the experimental results; and there is a summary in Section 3.6.

3.2. PRINCIPLES AND EQUATIONS TO DETERMINE STIFFNESS

The stiffness or MOE (modulus of elasticity) defines the relationship between stress and strain within the elastic region. The stress is the load or force per unit area and the strain is the dimensional change of a sample under load divided by the original dimension (Bodig and Jayne, 1982). According to Hooke's law for an isotropic material, the stress increases proportionally to the strain within the elastic limit, i.e.

$$\sigma = E\gamma \qquad (3.1)$$

where

σ = the stress, Pa;

E = the stiffness (modulus of elasticity), Pa;

γ = the strain, decimal.

Timber is considered to be an orthotropic material with three mutually perpendicular axes in the longitudinal (L), radial (R), and tangential (T) directions (Fig. 3.1). Consequently, there are three different elastic moduli that are denoted as (E_L), (E_R) and (E_T) along the three axes (Bodig and Jayne, 1982; Goodman and Bodig, 1970).

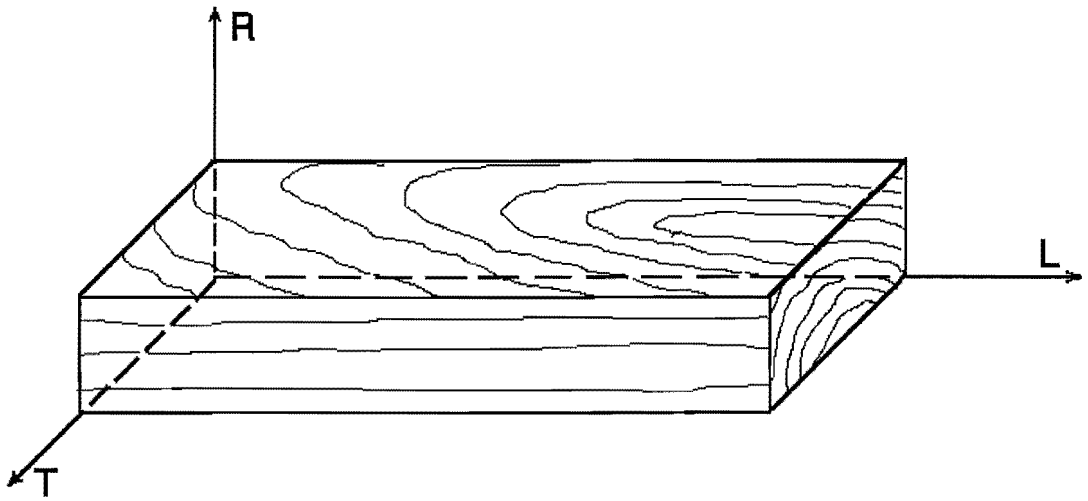

Fig. 3.1. Wood beam in an orthogonal coordinate system (Bodig and Jayne,1982).

E_L is measured as the ratio of a normal stress to the normal strain in longitudinal direction i.e.

$$E_L = \sigma_L / \gamma_L \qquad (3.2)$$

where

E_L = the stiffness in the longitudinal direction, Pa;

σ_L = the axial stress, Pa;

γ_L = the corresponding strain, decimal (Bodig and Jayne, 1982).

Similarly, the moduli of elasticity in radial and tangential directions can be expressed using the following formulae:

$$E_R = \sigma_R / \gamma_R \quad (3.3)$$

$$E_T = \sigma_T / \gamma_T \quad (3.4)$$

where

E_R = modulus of elasticity in radial direction, Pa;

E_T = modulus of elasticity in tangential direction, Pa;

σ_R = stress normal to radial direction, Pa;

σ_T = stress normal to tangential direction, Pa;

γ_R = radial strain, decimal;

γ_T = tangential strain, decimal (Bodig and Jayne, 1982).

Among E_L, E_R and E_T, the value of E_L is far larger than that of radial stiffness E_R and tangential stiffness E_T. For example, in spruce, E_L is up to 16.55 GPa, whereas E_R and E_T are only 0.85 GPa and 0.68 GPa respectively; in Douglas-fir, E_L is 15.71 GPa with E_R 1.06 GPa and E_T 0.77 GPa (Bodig and Goodman, 1973; Hearmon, 1948). In the construction industry, the longitudinal direction is designed to sustain major loads and the longitudinal stiffness is usually the most crucial in design codes. Therefore, the present studies have focused on the investigation of the longitudinal stiffness. In what follows, stiffness always refers longitudinal stiffness unless stated otherwise.

3.3. MATERIALS

After the study of the volume (see Chapter 2), all 239 logs were live-sawn to give 1,988 structural timber specimens with dimensions 90 × 35 × 4,200 mm for investigating the stiffness and stiffness gradient in this study. This section describes the preparation of these timber specimens, which included sawing, drying, dressing and machine stress grading. Throughout the process, the identities of individual logs and boards were retained by tagging, and the location of every board relative to the pith was confirmed by reassembling each log after the machine stress grading.

3.3.1. Sawing of boards

Every log was live-sawn to give a 100 mm thick central cant and a series of 40 mm thick flitches. Further sawing involved cutting 100 × 40 mm boards from the cants and flitches as shown in Fig. 3.2. The thickness of saw blade was 5 mm. Boards that are labelled with P1 were "boxed-pith". The pith in most logs was found in two or even three boards due to the pith wander.

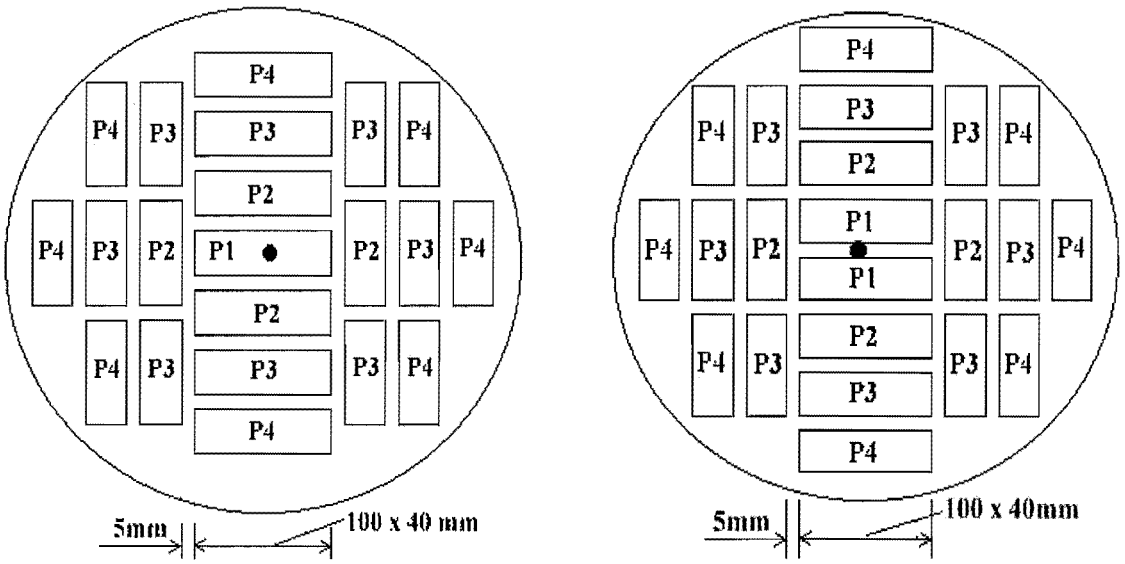

Fig. 3.2. Two sawing patterns used in this study. The numbering of the boards indicates their relative distance from the pith.

3.3.2. Drying of boards

In the sawmill of TITC (Timber Industrial Training Centre), all boards were kiln-dried under 90^0C dry-bulb and 70^0 wet-bulb temperatures with 18 mm stickers on 300 mm spacings. When an average 15% moisture content was reached, the boards were steamed for four hours (reconditioning). After kiln-drying, the boards were stored one month at the Timber Industrial Training Centre. Then every board was dressed to 90 × 35 × 4200 mm (width × depth × length) prior to machine stress grading at a sawmill to measure bending stiffness.

3.4. METHODS

All studied boards were machine stress graded in the sawmill according to the normal mill procedures using a MPC Computermatic stress grader (MK5 system) that was manufactured by "Measuring and Process Control Ltd" Essex, England (Fig. 3.3). In the first section the natural bow of the board is measured using a transducer on the infeed outrigger arm: no load is applied. Immediately afterwards the board enters the testing section where it is flexed between two rollers 0.914 m apart by applying a small constant force at mid-span and measuring the deflection. The measured deflection under load is adjusted for the natural bow in the unloaded board to determine the true deflection. The true deflection is then used to calculate the modulus of elasticity knowing also the applied force and the sectional dimensions of the board. The applied load in this study is 900 N and the sectional dimensions of the timber specimen is 90 × 35 × 4200 mm (width × depth × length).

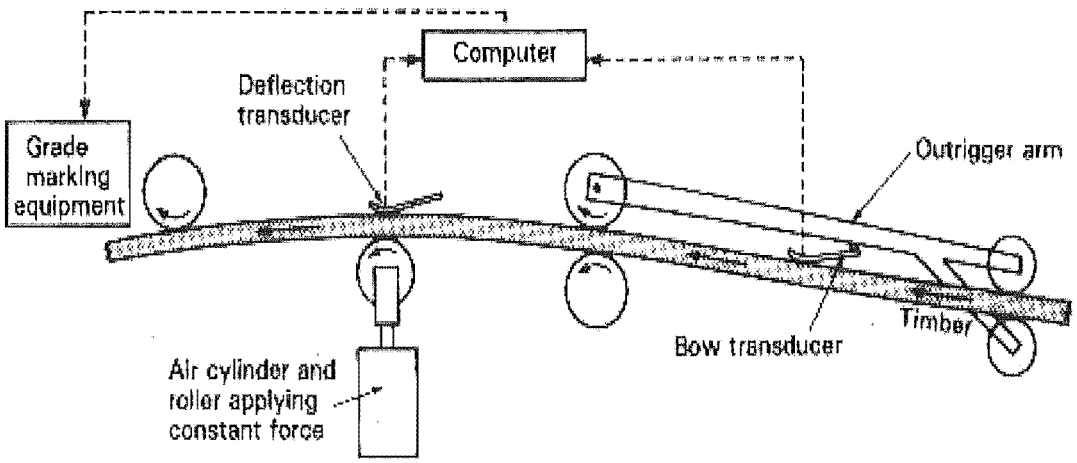

Fig. 3.3. Diagram of the MPC Computermatic stress grader (*after* Fewell, 1984).

After calibrating the machine stress grader, the boards were fed through in a random sequence during a single shift. As each board passed through the stress grader the modulus of elasticity was continuously redetermined at 152mm intervals. The first 0.65 m and the last 0.65 m of each board could not been machine stress graded due to the distance between the supporting rollers. Allowing for the 0.65m ungraded ends, there were typically 19 graded "footprints" on a board ($2\times0.65 + 19\times0.152 \approx 4.2$ metres).

The 19 local stiffness grades were marked along the board by the automatic application of coloured sprays, while the actual experimentally stiffness value of each "footprint" was recorded on the computer (Fig. 3.4). According to the principle of the machine stress grading, the lowest stiffness grade (or colour marking) along each board determines the F-grade (stiffness grade) of this piece, which will be introduced in Chapter 5. In this chapter, the actual experimentally stiffness value of each "footprint" in each board is used to analyse the stiffness gradient, and the colour marks along the board are just used to clarify the length orientation of the board.

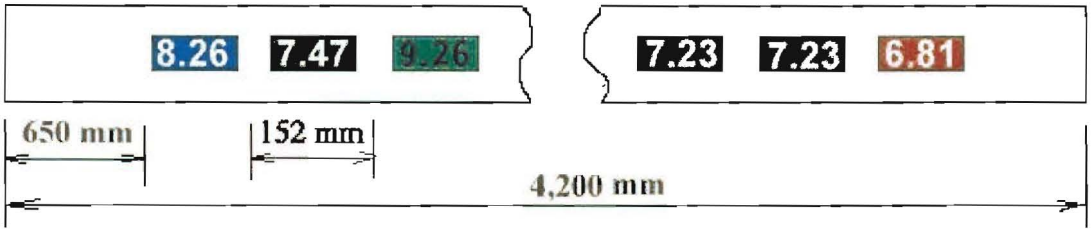

Fig. 3.4. The top view of machine stress graded board.

3.5. RESULTS AND DISCUSSION

This section displays the experimental results, which include the variation of the mean stiffness within log types according to radial distance; and gradient of the local average stiffness in the stems. The discussion of the experimental results and some suggestions based on the experimental results also are presented in this section.

3.5.1. Log mean stiffness variations according to radial distance

This section gives a mean stiffness profile in the four log types (butt, middle, top and upper top) on moving from the pith to cambium (Positions P1, P2, P3...) (Table 3.1). The purpose is to provide a general impression of log quality in terms of the stiffness from the unpruned stand.

A single stiffness value was first obtained from every board, which was the average MOE value for the 19 footprints along the piece. Then the boards were grouped according to their locations, i.e. position (P1, P2, P3...) and log type, so that a mean of

the average stiffness could be obtained. This study had a large enough sample size for the analysis. Typically there were at least 100 boards in each category, except in the outermost positions. Table 3.1 summaries the mean stiffness variations within the stems.

Table 3.1. The mean stiffness (GPa) of logs in the sixty-two radiata pine stems

Location from the pith		P1	P2	P3	P4	P5
Upper-top logs	mean	6.09	7.85	8.42		
	stdev	0.69	1.17	1.23		
	board No.	91	141	32		
Top logs	mean	6.03	7.87	8.51		
	stdev	0.94	1.45	1.51		
	board No.	107	209	113		
Middle logs	mean	6.10	7.98	8.56	8.69	
	stdev	0.99	1.55	1.84	1.89	
	board No.	122	234	182	47	
Bottom logs	mean	5.59	7.29	7.84	8.18	8.56
	stdev	1.37	1.79	1.79	1.69	1.63
	board No.	128	237	219	94	32

As expected, there is a radial increase in stiffness on moving from pith to bark with the greatest rate of change occurring near the pith. The surprising feature in Table 3.1 is that the stiffness of the wood at each position is essentially the same whether in the middle, top or upper top log. However in the butt wood the averaged stiffness values are inferior to those found elsewhere. In all four log types, the butt logs display the lowest average stiffness and middle logs give the highest one. This is a surprise as the butt log is considered the most valuable part of the tree. This study therefore examined the gradient of the local average stiffness along the stems

3.5.2. The gradient of the local average stiffness over stems

This section shows in detail the local average stiffness variations along the length of boards, for each log type according to radial distance from the pith.

Along the length of board, the individual values for the 19 "footprints" are averaged by considering the stiffness at each point (footprint) taken from a particular position (P1,

P2, P3...) and log type (butt, middle, top and upper top). This provides a gradient of the local averaged stiffness map for the entire stem (Fig. 3.5).

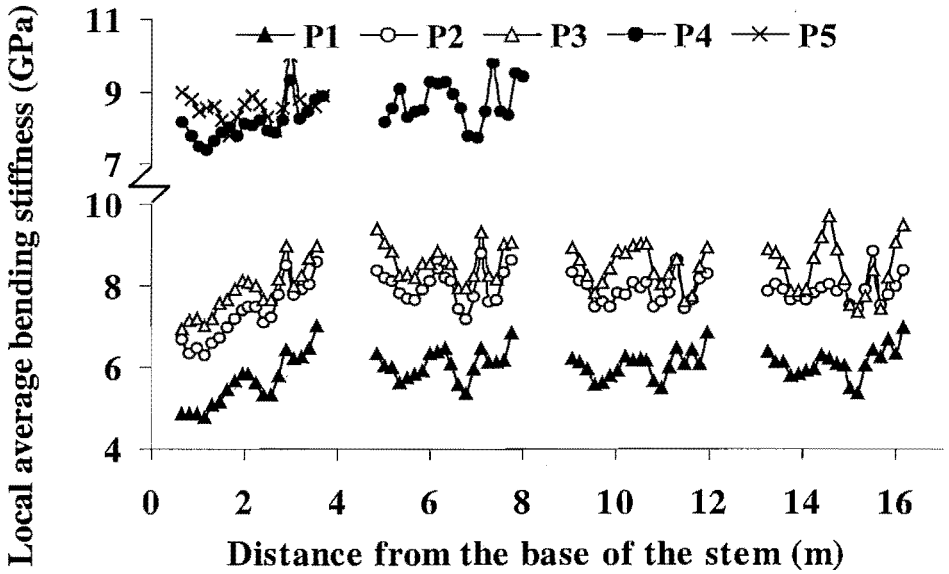

Fig. 3.5. Local average stiffness values (GPa) at 152mm intervals within the unpruned stem. The "missing" data (gaps) corresponds to the 0.65m at either end of the boards that cannot be machine stress graded.

There are two new features in Fig. 3.5 compared to the data in Table 3.1. First, the wood at the base of the tree displays exceptionally low local average stiffness, with evidence of a very low stiffness cone rising to a height of about 3 metres. Secondly, the fluctuating recorded stiffness values suggest vibrational perturbations. For example the local average stiffness is always abnormally low at the seventh footprint from the right-hand end of all the boards.

The issue of perturbations has to be addressed before one can interpret the local average stiffness behaviour in the butt log. Fewell (1984) observed with regard to the MPC Computermatic (Fig. 3.3) that *there are difficulties in trying to maintain a constant bending force on a fast moving variable stiffness material...and this method of operation does result in some inaccuracies. Nonetheless the machine is acceptable and gives an adequate performance.* A more likely interpretation considers the fact that the

leading end of each board must hit the final support roll before it can flex sufficiently to pass on through. Either way, the fluctuating averaged stiffnesses shown for all footprints in all logs cannot be due to local variations in wood stiffness or the presence of knots as these have been averaged out. They have to be systematic effects arising from machine characteristics. The fluctuations appear to be stronger in the outerwood than in the corewood, which is likely to reflect the increased stiffness of the outerwood and the greater difficulty in passing on through the machine stress grader.

The mean stiffnesses in the various positions (P1, P2, P3...) are essentially the same for the middle, top and upper top logs (Table 3.1), so the true averaged stiffnesses for the 19 individual footprints are presumed to have this same value (taken from Table 3.1). Therefore the machine-induced stiffness perturbations at each footprint becomes the difference between the mean stiffness (Table 3.1) and the experimental local average value. With the butt log a linear regression is first applied to the experimental data to estimate the trends of averaged stiffness for the 19 footprints in the averaged board at the various positions (P1, P2, P3...). In the butt log the stiffness perturbations for each footprint hence becomes the difference between the regression-derived averaged stiffness and the experimentally averaged value. In a second iteration of the above procedure, a refined stiffness perturbation for each particular footprint (1, ..., 19) at each position (P1, P2, P3...) is taken to be the average of the four values (perturbations) from the four log types. These refined local averaged perturbations are then subtracted from the local averaged experimental values to give the data points shown in Fig. 3.6. Finally, a best fit line through these data points estimates the true curvilinear stiffness changes in the butt log (Fig. 3.6). In this analysis the positions (P1, P2, P3...) are treated as separate data sets as the intensity of the machine vibrations are clearly greater as one moves out from the pith (Fig. 3.5).

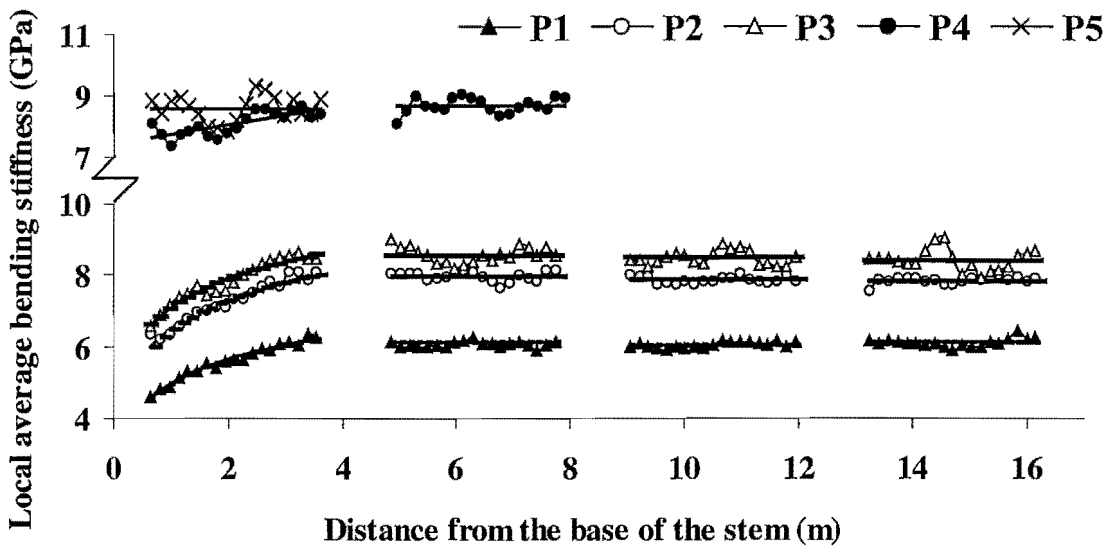

Fig. 3.6. Estimate of the true local averaged bending stiffness after adjusting for machine vibrations.

Thus one deduces that the average stiffness in the middle, top and upper top logs for with-pith lumber (position P1) is 6.1 GPa, but that this drops to only 4 GPa at the groundline. Similarly, at position P2 the average value is about 8 GPa but this falls to about 5 GPa at the groundline. These gradients of local average stiffness could be due to the high microfibril angles found near the base of a tree, because the microfibril angle has a dominant negative effect on wood stiffness according to the previous researches (Hirakawa and Fujisawa, 1996; Walker and Butterfield, 1995; Bendtsen and Senft, 1986; Cave, 1968; Cowdrey and Presfon, 1966). However, the very low stiffness values at the groundline are rarely recognised within the industry.

3.5.3. Variations of local average stiffness with respect to the mean stiffness of the stem for positions P1, P2 and P3

The purpose of this analysis is to find the point where the value of local averaged stiffness in butt log can reach the mean stiffness of the stem. In other words, this indicates how much wood in butt logs should be used for other end-uses due to poor stiffness. The differences between the local average stiffnesses and the mean stiffness of the stem for position P1, P2 and P3 are shown in Figure 3.7. This analysis excludes the boards in the outerwood (P4 and P5), because the sample size in the outerwood is

quite small and the outerwood clearly has adequate stiffness so there appears to be little advantage in considering the stiffness behaviour in these material any further.

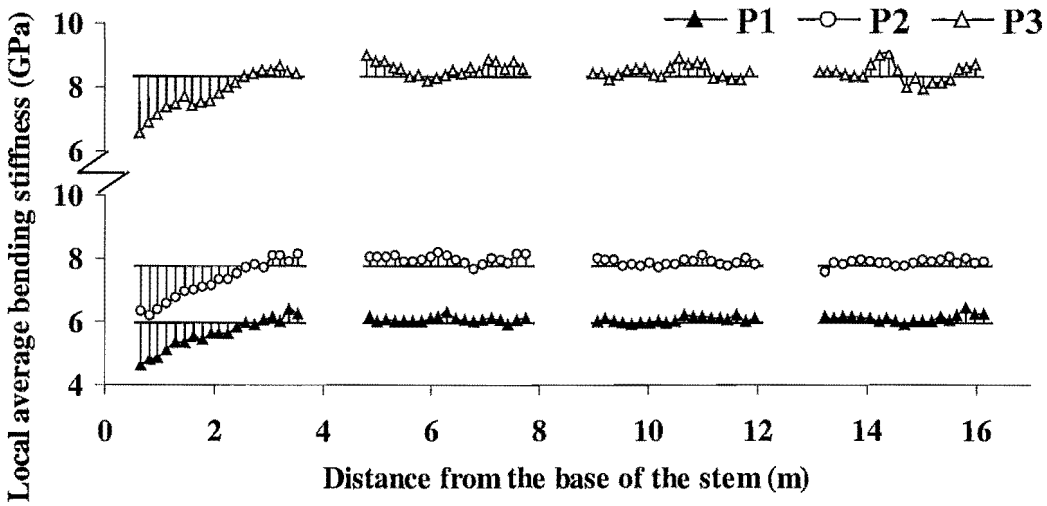

Fig. 3.7. Variations of local average stiffness with respect to the mean stiffness of the stem in positions P1, P2 and P3.

The results of the analysis show that the local average stiffnesses in the base of the stems are much lower than the mean stiffness of the stems until 2.4 m. At 2.7 m of the stem, the local average stiffness reaches the mean value of the stiffness of the stem. This means that if a new standard butt-log length can be cut at 2.4 or 2.7 m, then the value of radiata pine stem could be upgraded by using the base 2.4 m or 2.7 m for other end uses instead of for construction.

Perstorper (1996) reported a similar observation in Norway spruce. In that instance only the lowest 1.0 metre of the butt wood suffered at most a modest 15% loss in stiffness. This is considered to be the same feature as in radiata pine but the volume of the low stiffness cone is insignificant due to the slow growth rate of Norway spruce in Sweden. Consequently we conclude that this phenomenon is important only in fast-grown species.

3.5.4. Log sorting: consideration of the least-stiff logs

This section shows the benefits of log sorting by isolating the least-stiff 20% of logs in the four log types. Figure 3.8 (a) indicates the distributions of local average stiffness in

the least-stiff 20% logs for four log groups, i.e. butt, middle, top and upper top logs. Figure 3.8 (b) shows the variations of local average stiffness in the remaining 50 logs for four log types after isolating the least-stiff 20%. Boards at P4 and P5 locations were not evaluated due to the small sampling size. Further, only two boards cut from P3 would represent the least-stiff 20% upper top log. In order to keep reasonable sampling size, the boards in P3 for upper top logs therefore were excluded from this analysis. By isolating the least-stiff 20%, the mean stiffness of the remaining log is enhanced shown in Fig. 3.8 (b). From Figure 3.8 (b), one can conclude that the boxed-pith board is unsuited for structural purpose, because the highest average stiffness value of P1 for all log types is still lower than the boundary stiffness value for F5 structural grade (6.9 GPa), even if the least-stiff 20% of logs has been isolated.

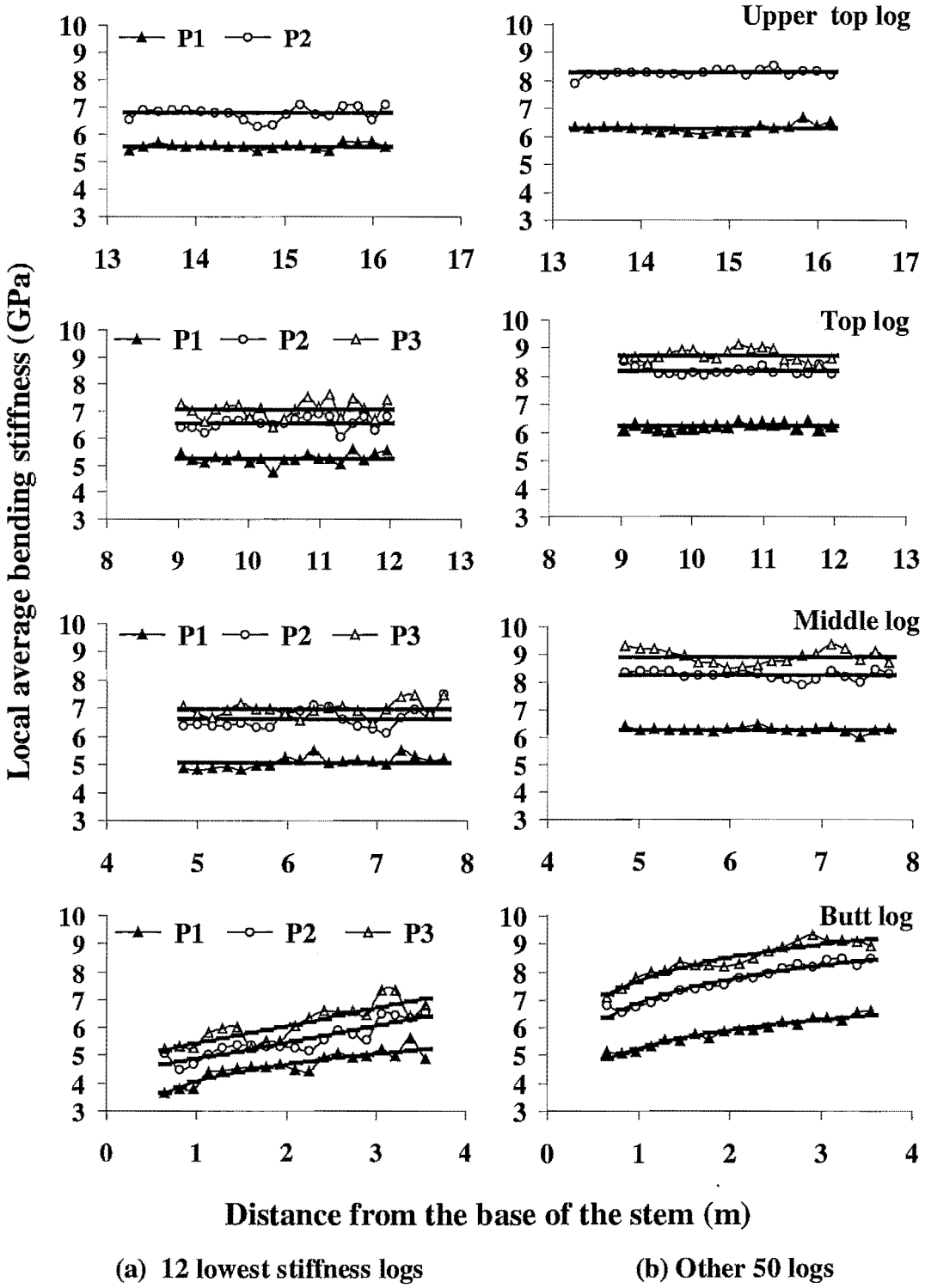

Fig. 3.8. Comparison of the true local average bending stiffness in the 12 least-stiff logs with those values for all other 50 logs in different log types.

3.5.5. The relationship between log volume and log average stiffness

This section gives the analysis about the influence of the log volume on the log average stiffness. When logs ranked in ascending order of volume, the average stiffness in the corresponding logs remains roughly level (Fig. 3.9). The lack of any correlation between the log volume and the log average stiffness further reveals that the log volume is not a potential indicator of the log average stiffness (Fig. 3.10).

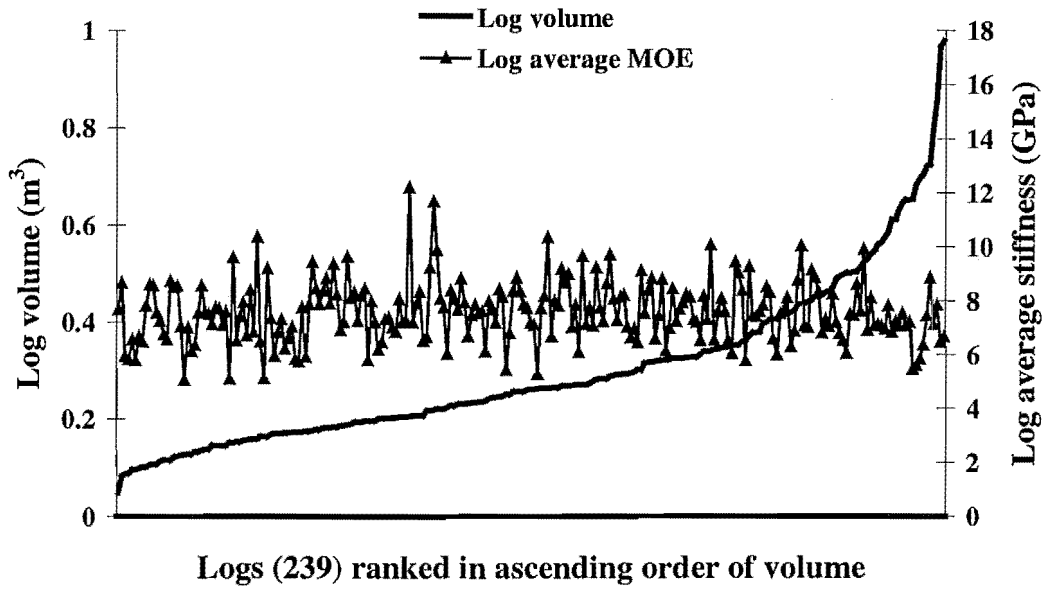

Fig. 3.9. The variations of log volume and log average stiffness.

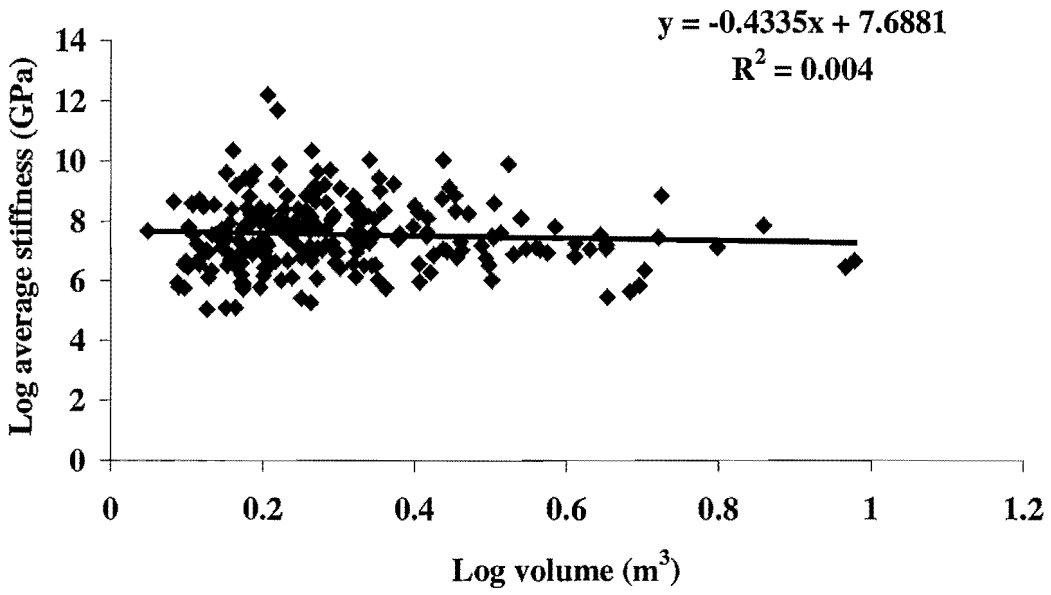

Fig. 3.10. The correlation between log volume and log average stiffness.

3.6. SUMMARY

The stiffness of radiata pine increases with radial distance from the pith. In the vertical direction, the stiffness rises from the groundline and reaches the mean stiffness of the stem at about 2.7 m from the bottom. Thereafter, the variation of stiffness in vertical direction is insignificant. This study shows that the stiffness in the butt logs is generally lower, especially from base up to 2.4 m or 2.7 m. These very low local average stiffnesses should be due to the high microfibril angles found around the base of a tree, because the microfibril angle has a dominant negative effect on wood stiffness according to the previous researches (Hirakawa and Fujisawa, 1996; Walker and Butterfield, 1995; Bendtsen and Senft, 1986; Cave, 1968; Cowdrey and Preston, 1966). Larger microfibril angles inclining to the axial direction lead to the cells being more flexible to longitudinal extension i.e. lower stiffness.

The analysis of this study reveals that the log volume is not a reliable indicator of stiffness. Previous researches show that the fast growing species were often associated with poor wood quality due to higher proportion of corewood, and slow growing species were generally denser and stiffer (Matheson *et al.,* 1997; Bendtsen and Senft, 1986; Cown and McConchie, 1983; Harris, 1965). An interesting question is whether higher stiffness is related to slower growth rate after isolating the influences of species, harvesting age and growth environment. Such speculation that the logs with less yield volume (i.e. slower growing) at the same stand may be stiffer is proved not true in radiata pine species as shown in Figures 3.9 and 3.10. In other words, the log stiffness is irrelevant to log volume in radiata pine under the same yield age (i.e. same proportion of corewood) and growth conditions. This encourages the selection of fast growing genes.

The experimental results reported in this chapter show that most of the corewood (boxed-pith boards) is unsuitable for structural timber, because the highest average stiffness of these boards is less than the minimum value of F5 structural grade (6.9 GPa), even after isolating the least-stiff 20% (Fig. 3.8). Apart from the corewood, this study suggests cutting the stem at about 2.7 m above groundline and using this short butt log for other end uses. Then values of the stem can be upgraded (Fig. 3.6, 3.7). Sorting and isolating the least-stiff 20% of logs may be another approach to upgrade the

value of the logs. The value of the individual boards is determined by the lowest stiffness value along each board.

Chapter 4

TENSILE STRENGTH IN RADIATA PINE STEMS

4.1. INTRODUCTION

As an important quality criterion of wood and timber, strength (i.e. the failure stress) has been studied for years (Addis, 1995; Addis *et al.*, 1995; Walker, 1993; Madsen, 1992; Buchanan, 1990; Grant and Anton, 1984; Bodig and Jayne, 1982; Bier, 1983; Walford, 1982; Pearson *et al.*, 1966; Hinds and Reid, 1957). The failure stress of wood or timber is related to the manner of loading. Hence, strength of wood or timber is further divided into tensile (or tension), compression (or crush), bending and shear strength. This study focuses on the investigation of ultimate tensile strength (UTS) in radiata pine structural timber due to following reasons.

- **Structural applications**

  Breyer (1980) reported that there are a number of structural applications for timbers being stressed in tension. For example, trusses have numerous axial-force members, and roughly half of these are in tension. Axial tension members also occur in the chords of horizontal and vertical diaphragms.

- **Tensile strength can meet interest of the construction industry**

  Madsen (1992) pointed out that the construction industry wants to know how weak the board might be and where the weakest point occurs rather than knowing how strong the board is. The tensile strength rather than bending strength can meet these requests of the construction industry. When a board is in tension, the centre cross section of the board is subject to same tensile forces along the length of board and the failure occurs at the weakest point. The tensile testing therefore indicates the strength at the weakest point in the board. Conversely, the bending test is more sensitive to the precise testing procedure. The bending moment varies along the length of board and board in bending usually fails close to the point of maximum

bending moment regardless of whether the "worst" defect (knot) is in that region. For example, under a central load, the board fails near the middle of the span due to the maximum bending moment there no matter whether the weakest point is there. In other words, if one seeks the strength at the weakest point within a full length of member, then tensile testing is more reliable than the bending test.

- **Tensile test can provide more information for investigation of the strength**

When a board fails in bending, the failure is usually a tensile failure on the tension side of the board. In other words, in the bending test, only half of the cross-section is subjected to tensile stress. However, a tensile test can provide more information for the investigation of the strength because the whole cross-section is subjected to tensile stress.

- **Some advantages for further research**

After tensile testing, the fracture of board is clearer than that after bending or compression testing, which allows for well-characterised samples to be collected from the broken boards for future studies after tensile testing. This is an advantage for our future work because the characteristics at the weakest zone, such as density, microfibril angle, spiral grain and natural defects, are important information giving an insight for breeding and genetic selection.

Therefore, this chapter presents the investigation for the ultimate tensile strength. In what follows, strength always refers ultimate tensile strength unless stated otherwise.

Civil engineers are interested in both the strength of each board, and the distribution of the strength amongst all boards in a stack or population of lumber. Compared to small clear wood, the strength of structural timber is far more complicated because of the morphological features, such as knot, splits, spiral grain, compression wood, injuries due to biological agents (fungi and insects) and non-biological agents (fire and wind), especially in radiata pine structural timber that has larger knots than other species.

Addis (1995) may be among the first to propose a tensile strength map for structural timber in New Zealand radiata pine stems. In 1995, he reported data for the stiffness and the tensile strength of 915 structure timber specimens from a 25-year old unpruned radiata pine plantation on the Canterbury Plains. However, Addis' (1995) tensile strengths are surprisingly high compared to the values given by timber structural standards (AS 1720.1-1997; NZS 3603: 1993). According to NZS 3603, for radiata pine structural timber, the corresponding tensile strength is between 10.6 MPa and 18.2 MPa when the stiffness falls in range 8.0 to 12 GPa (F-grade from F6 to F11). Australian standard (AS 1720.1-1997) gives the relationships of stiffness and strength over all F-grades in softwood. The tensile strengths are 13 MPa and 17 MPa when the stiffnesses are 9.1 GPa (F-grade 8) and 10.5 GPa (F-grade 11), respectively (Appendix 2). However, in Addis' publication (1995), the tensile strength for F-grade 8 was 24.2 MPa and the tensile strength for F-grade 11 was 34.6 MPa, almost doubling the values in the standards. For an unpruned radiata pine species, the average strength that Addis reported (1995) is unusually high.

A reliable strength map in radiata pine stem would provide useful information for structural design and for forestry breeding in New Zealand. Hence, an investigation on tensile strength of radiata pine was undertaken to carefully examine the average strength values and trends within stems. 1,919 graded structural boards with the dimensions 90 $\times$ 35 $\times$ 4,200 mm were employed in this study. Both the variations of the log average strength in the stems and the distributions of the average strength of boards within log types according to the radial distance from the pith are presented in this chapter. The experimental results question the key position of wood density for indicating the strength of structural timber.

The principles and the governing equations of the strength are reviewed in Section 4.2. The experimental materials and methods of this study are listed in Section 4.3. Section 4.4 presents the experimental results. Section 4.5 is a summary.

4.2. PRINCIPLES AND GOVERNING FORMULAS FOR STRENGTH

Strength is the ability of a material to sustain a load or force. For all materials, there is a critical load or critical force. When the load or force that acts on the material is smaller than the critical load or force, the material will just simply be stretched, compressed or bent. Material fails once the load or force reaches its critical value. Hence, strength is defined in terms of failure stress, i.e. stress is the force per unit area (ASTM, 1995; Walker, 1993).

The test loads for determining the strength can be applied in tension, in compression, or in bending. Hence, the corresponding strengths are categorized as tension (or tensile) strength, compressive (or crushing, or column) strength and bending strength (or modulus of rupture) (Hibbeler; 1999; Walker, 1993; Bodig and Jayne, 1982; Breyer, 1980; Gordon, 1978; Benham and Warnock; 1973). The illustrations and the governing equations are shown below.

1) Tensile strength

The tensile load parallel to grain is illustrated in Figure 4.1. The tensile strength (or tension strength) of board can be calculated using the formula:

$$UTS = P/bd \qquad (4.1)$$

where

UTS = ultimate tension strength, MPa;

P = tensile force causing failure, N;

b = the specimen width, mm;

d = the specimen depth, mm.

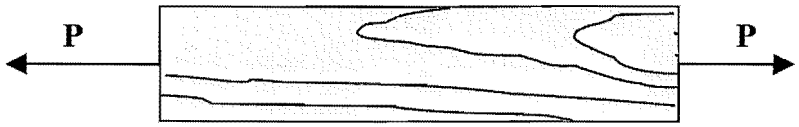

Fig. 4.1. Timber specimen in tension parallel to grain (P is test load).

2) Compressive strength

Board tested in compression is shown in Fig. 4.2. The compressive strength (or crushing strength; or column strength) of board can be calculated from following formula:

$$MCS = P/bd \quad (4.2)$$

where

MCS (Maximum Compressive Stress) = compressive strength, MPa;

P = force or load causing failure, N;

b = specimen width, mm;

d = specimen depth, mm.

Fig. 4.2. Timber specimen in compression parallel to grain (P is test load).

3) Bending strength

The calculation of bending strength of board is more complex than that of tensile and compressive strength, because of following reasons.

- The bending strength relates to the bending moments that vary with the location of the load and the number of loads applied on the beam.

- The bending moments are determined by compressive stress above the neutral surface and the tensile stress below the neutral surface of the beam as shown in Fig 4.3 and Fig. 4.4.
- In addition, there is also shearing action in the vicinity of the neutral surface of the beam when the ratio of the length to the depth of a tested sample is less than 12:1. The shearing force is usually ignored when the ratio of the length to the depth is larger than 12:1 (ASTM, 1995; Bodig and Jayne, 1982; Beijing Forestry University, 1982; Benham and Warnock, 1973).

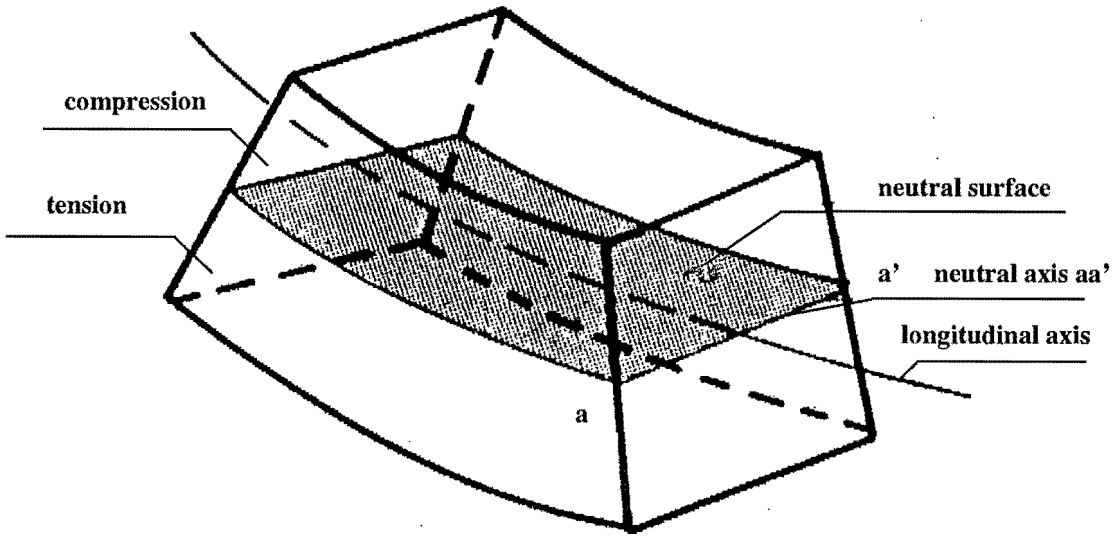

Fig. 4.3. Section of the deformed beam (after Bodig and Jayne, 1982).

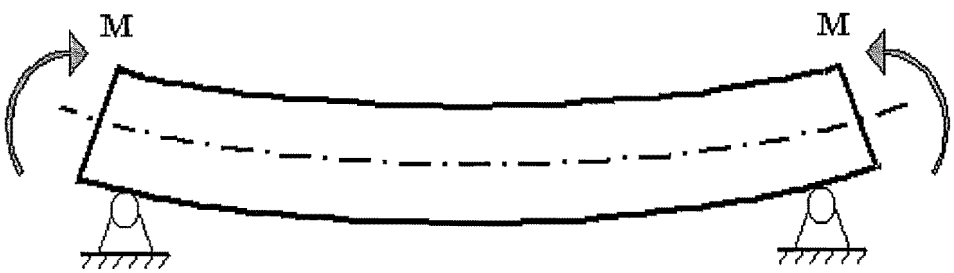

Fig. 4.4. Deformed beam (after Bodig and Jayne, 1982).

Here, a simple bending test with single load acting at the middle of the beam as shown in Fig. 4.5 is described. Under a central load, the bending strength (or modulus of rupture, or MOR) can be calculated by following formula (4.3), and the maximum shear stress can be calculated according to equation 4.4 (Bodig and Jayne, 1982; Beijing Forestry University, 1982; Benham and Warnock, 1973):

$$MOR = \frac{3PL}{2bh^2} \tag{4.3}$$

where

MOR is bending strength (or modulus of rupture, or MOR), MPa;

P is the load causing bending failure, N;

L is the length of span, mm;

b is the specimen width, mm;

and h is the specimen depth, mm.

$$\tau_m = \frac{3P}{4bh} \tag{4.4}$$

where

τ_m = shear strength in the beam, MPa;

P = central load acting on the beam, N;

b = specimen width, mm;

h = specimen depth, mm.

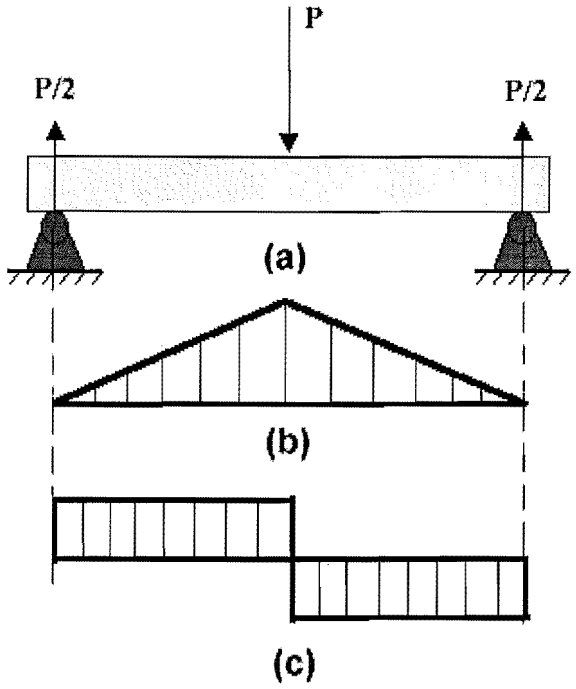

Fig. 4.5. Timber specimen in bending: (a) simple beam under a concentrated central load P; (b) bending moment diagram; (c) shearing force diagram (after Pearson *et al.*, 1966).

4.3. MATERIALS AND METHODS

Among the total 1,988 graded boards, 69 were broken during the machine stress grading due to big knots. Only 1,919 graded boards (90 × 35 × 4,200 mm) were used for strength tests.

Determination of strength is related to the measurements of the tensile failure load and the failure cross-sectional area in board as shown in Equation (4.1). The tensile failure load was measured using a horizontal tensile test machine (Fig. 4.6) located at the Wood Technology Laboratory in the School of Forestry, University of Canterbury. The net span of the tensile test machine between the two grips was set at 3.3 m. The hydraulically operated grips that were 0.45 m long applied the gripping force to hold test specimen. A 200 kN capacity hydraulic ram provided the axial tensile force to the board. A load cell, which was connected in line with the tensile machine and the ram, measured the tensile load continuously and transferred the data to a computer during tensile test. When the board failed, the tensile failure load was recorded by the computer

system. After the board broke, the dimensions of the cross-area at the failure zone were measured immediately and the strength of each board calculated using formula (4.1).

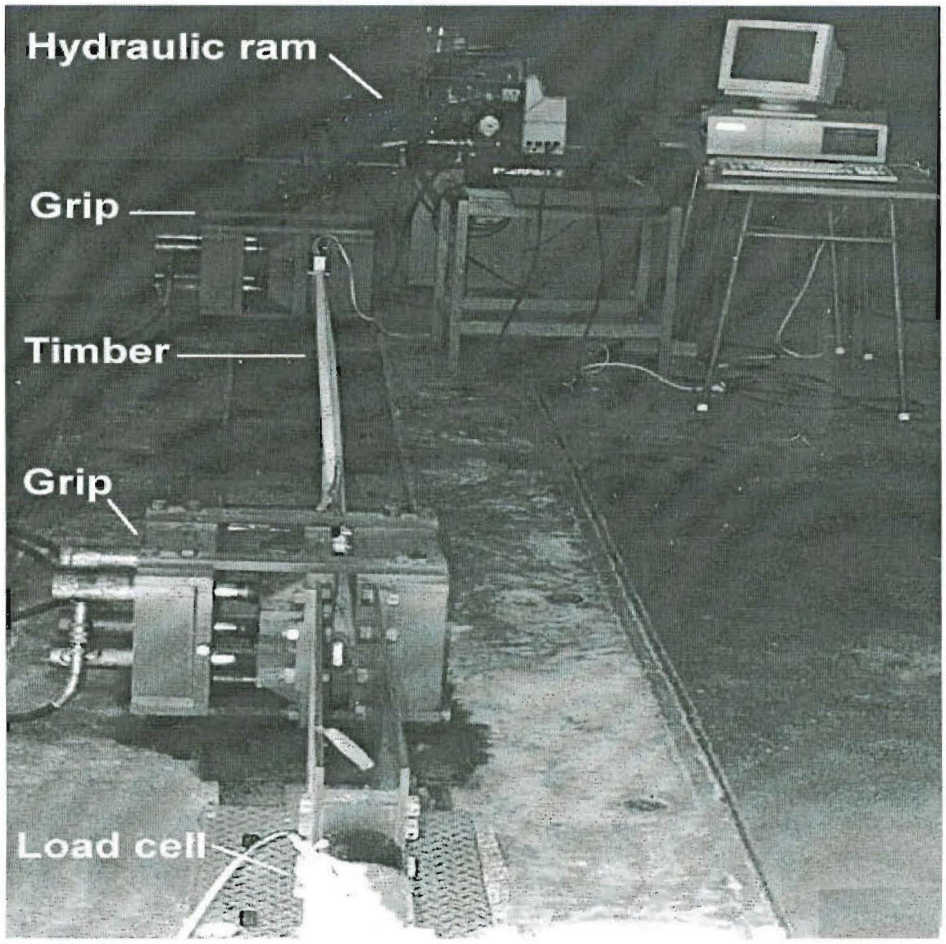

Fig. 4.6. The tensile testing machine.

4.4. EXPERIMENTAL RESULTS AND DISCUSSION

This section presents the experimental results, which include the variations of log average strength in the stems and the variations of the average strength of boards within log types according to the radial distance from the pith.

Figure 4.7 (a) shows the variation of log average strength in the stems. In the vertical direction, the middle logs rather than butt logs display the highest average strength. Log

average strength increases from the base to the middle, and then decreases from thereafter.

Figure 4.7 (b) lists the variations of average strength of boards within log types according to the radial distance from the pith. In the cross–section, the average strength of board increases from the pith. However, there is a decline in the wood zone adjacent to bark in the top and upper top logs.

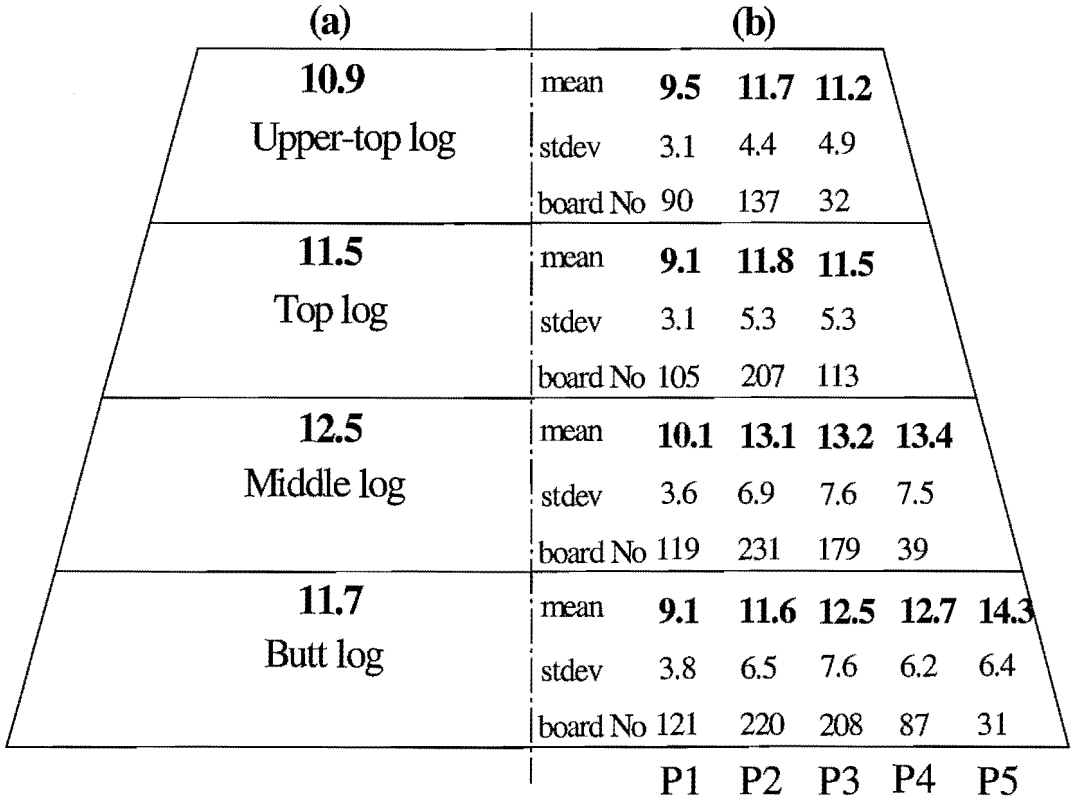

Fig. 4.7. Tensile strength (UTS) map in sixty-two radiata pine stems: (a) variations of log average strength (MPa) in the stems; (b) variations of average strength (MPa) of boards within log types according to radial distance from the pith.

Compared to stiffness, the variation of strength in the stem is more complex and less regular. Scientists have been long interested in seeking a predictor of the strength. Wood density was traditionally considered as a "good index" for the strength in clear wood (Walford, 1991; Zobel & Van Buijtenen, 1989; Bamber & Burley, 1983; Cown

and McConchie, 1983; Bunn, 1981; Summitt & Sliker, 1980). The following exponential function (4.5) and linear equation (4.6) were generally recommended for clear wood:

$$S = \alpha D^{\beta} \quad (4.5)$$

where
S = predicted value for a particular mechanical property;
D = wood density;
α = constant;
β = constant (U.S. Forest Products Laboratory 1974).

$$S = a + bD \quad (4.6)$$

where
S = predicted value for a particular mechanical property;
D = density;
a = constant;
b = constant (Liska, 1965; Forest Products Laboratory, 1987).

However, these relationships may be invalid for structural timber. The mean wood density increases with radial distance from the pith and decreases with the height from the base as shown in Figure 4.8 and Table. 4.1 (McConchie and Metcalfe, 1999; Cown *et al.*, 1991a). If the wood density itself were a good indicator of the strength of the structural timber, the butt logs should be the strongest logs and the average strength should increase with the radial distance from the pith. However, the experimental results of this study reveals that the butt logs are not the strongest and the average strength does not always increase with the radial distance. For example, the average strength decreases from P2 to P3 in the top and upper top logs [Fig. 4.7 (b)].

Therefore, the investigation of the relationship between the wood density and the strength in structural timber is proposed for further research. In this study, the small

clear wood samples have been cut from adjacent zone to the failure point in each board for later research.

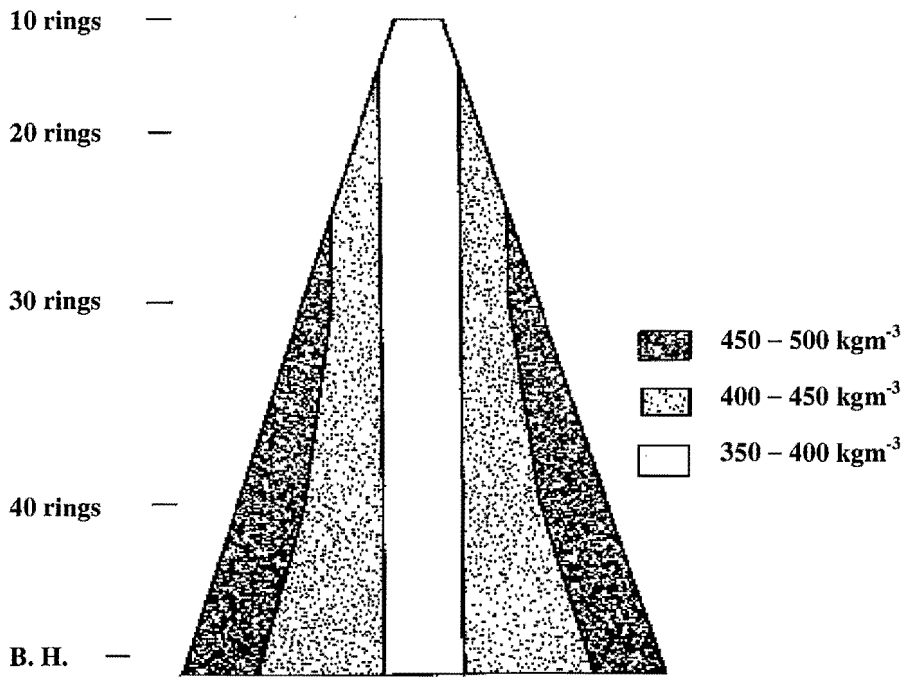

Fig. 4.8. Distribution of mean basic density within-tree (after Cown *et al.*, 1991).

Table. 4.1. Predicting wood density for tree and components using MARVL system (after McConchie and Metcalfe, 1999).

Tree age	10	15	20	25	30	35	40
Odbh	306	346	369	381	388	392	394
butt log	322	354	372	382	388	391	393
2nd log	0	340	357	367	372	375	377
3rd log	N/A	N/A	351	360	365	368	370
4th log	N/A	N/A	345	353	357	359	361
whole tree	313	344	361	371	376	379	381
sawlog	311	345	363	373	379	382	384
pulplog	300	326	341	349	354	357	358

Note: 1) odbh means outerwood density at breast height. 2) MARVL means a Method for Assessment of Recoverable Volume by Log-type.

4.5. SUMMARY

This study measured the strength of structural timber specimens using tensile test, in order to give an average strength map in radiata pine stem. The experimental observations are as follows:

- In vertical direction, the middle logs display the highest strength value in each wood zone, whereas the butt logs had the lowest strength value at the two wood zones, containing the pith (position 1) and adjacent to the pith (position 2).

- In cross section, the average strengths of the boards do not always increase with the radial distance from the pith.

- Wood density in radiata pine increases with the radial distance from the pith and decreases with the height up the stem, which does not match the map of the average strength obtained during this study. Hence, it is suspected that wood density may not be a good indicator of the strength of structural timber. Further investigation about that is proposed for the future.

Chapter 5

ESTIMATING TENSILE FAILURE STRENGTH IN RADIATA PINE STRUCTURAL TIMBER

5.1. INTRODUCTION

A non-destructive estimate of the failure strength in a piece of timber (i.e. the strength of the weakest point in a board) has been an important challenge for forestry and civil engineering scientists, since customers wish to know this essential information to prevent catastrophic disaster without damaging the timber.

The local strength is the strength in a location of the timber. Owing to the random distribution of the nature defects, the local strength of a board varies along its length. Thus failure strength is defined as the local strength at the weakest point of board in this study. The next weakest point (which did not fail) may be only slightly stronger or much stronger than the point that failed. In considering strength, engineers need to estimate how weak the board might be and where the weakest zone is likely to occur rather than how strong the board is. This is because the effect of the failure strength is catastrophic if the beam breaks (Walker, 1998; Simperingham, 1997; Madsen, 1992). This study thus targeted two aspects: estimating the likely failure strength and identifying the likely weakest zone within each piece of timber. The later study is presented in the next chapter (Chapter 6).

Previous approaches for estimating the failure strength of structural timber include: estimating failure strength by average stiffness, F-grade and the maximum KAR of timber (Addis *et al.*, 1998, 1996; Zhou, 1991; Bier and Collins, 1985; Grant and Anton, 1984; Kunesh and Johnson, 1972). Also, estimation of the strength in bending (MOR, modulus of rupture) from the local failure stiffness (bending stiffness in the failure zone) is found in a few publications (Bier and Collins, 1985; Grant *et al.*, 1984). However, there are some shortcomings in these previous approaches – either difficult to estimate the value of the failure strength or hard to identify the weakest point of the board, which are described in literature review (Section 5.2). Hence this study considers

estimating failure strength of board in tension by local failure stiffness. The main reason for using tensile strength instead of bending strength or compressive strength is that measured failure strength in tension indicates the strength of the weakest section of the board, as stated in the Chapter 4. Thus the correlation between the failure strength and the local failure stiffness is a legitimate and valid method to test whether the local failure stiffness can be treated as an indicator of the failure strength value at the weakest point in the board.

This study first explored the correlation between the failure strength in tension and the local failure stiffness in timber. Also, this study examines carefully other suggested indicators of failure strength, such as average stiffness in bending, average stiffness in tension, F-grade mark, the maximum KAR, to compare with the method first introduced in this study, i.e. estimating the failure strength of board in tension with respect to local failure stiffness.

The experimental results of this study show that the local failure stiffness is the best indicator of the failure strength for structural timber, due to its strong correlation (R^2 = 0.54), while the average stiffness (both the average in bending and in tension) and the maximum KAR cannot be considered such useful indicators of the failure strength due to their lower correlation coefficients (R^2 = 0.35, R^2 = 0.45, R^2 = 0.21 respectively). The "*lowest F-grade mark*" in board may give the failure strength value. However, using "*lowest F-grade mark*" is hard to identify the failure point of board. Indeed, the current experimental results reported here reveal that there is only 38% confidence to identify the failure zone by using "*lowest F-grade mark*" of board.

Combining an accurate prediction of the weakest point in board with the local stiffness there (the best indicator of the failure strength value) would give a useful non-destructively estimation model for the failure strength of structural timber. A further investigation regarding the failure features of the weakest zone is presented in the succeeding chapter. In this chapter, Section 5.2 gives a literature review. Section 5.3 describes the materials used in this study. Terms, definitions and experimental methods are introduced in Section 5.4. Section 5.5 presents the results of this investigation. Finally, there is a summary and discussion in Section 5.6.

5.2. LITERATURE REVIEW

This section reviews previous approaches for estimating the failure strength of structural timber, which include: estimating failure strength from average stiffness, F-grade, maximum KAR and estimating failure bending strength from the local failure stiffness.

5.2.1. Estimating the failure strength from the average stiffness of boards

In the longitudinal direction, the average stiffness of a board can be obtained either by bending test or by tensile test. Correspondingly, the resultant average stiffness is called the average stiffness in bending or the average stiffness in tension. Machine stress grading measures the local bending stiffness of a board at each 152 mm intervals along the length (Chapter 3). The mean of all local bending stiffnesses then gives the averaged stiffness of the board in bending. In tension, a tensile load is applied in the longitudinal direction. The average stiffness in tension is the tensile stress (i.e. tensile load divided by the area of cross-section) divided by the tensile strain (i.e., axial dimensional increment divided by the original axial dimension) in the elastic region (Bodig and Jayne, 1982).

Addis *et al.* (1996, 1998) investigated the correlation between the average stiffness in tension and the failure strength (ultimate tensile strength) in 915 (90 × 36 × 3,600 mm) and in 1,333 (90 × 35 × 4,200 mm) radiata pine boards. Their experimental results showed that there was no strong correlation between the failure strength and the average stiffness, $R^2 = 0.32$ was given in the first publication and $R^2 = 0.46$ was shown in their later investigation.

It is understandable that there is not a strong correlation between the average stiffness and the failure strength of the board because of the variation of the natural defect along the length. Therefore, the average stiffness of a board theoretically does not reveal the features of the weakest zone; and practically is not expected to provide a strong correlation.

5.2.2. Estimating the failure strength from F-grade of board

F-grade is a machine stress grade of timber that is generally used for building construction (eg, wall framing, trusses, joists) and pallets (AS 1720.1, 1997; Ministry of Forestry, New Zealand, 1995; AS/NZS 4063: 1992). Normally, there are several local F-grade marks along the length of the board, but the lowest local F-grade mark determines the F-grade of the board. The local F-grade values are measured by machine stress grading (AS/NZS 4063: 1992; NZS 3618: 1984; AS 1748: 1978, AS 1749: 1978). During machine stress grading, local F-grades are marked on the board surface by spraying a colours according to the stress grade colour code (AS 1748: 1978) (Appendix 1).

According to Australian Standard (AS 1720.1-1997), each local F-grade corresponds a certain local bending stiffness range and a suite of local strength characteristics (Appendix 2). For softwoods, grade "F 7" means the local bending stiffness in the range of 7.9 GPa ≤ MOE < 9.1 GPa; corresponding to local bending, tensile, compression and shear strengths 20, 10, 15 and 2.1 MPa, respectively. The details of the grade standard are listed in Appendix 2.

Estimating the failure strength by F-grade of a board is based on the relationship between the local stiffness and local strength. By assuming the lowest local F-grade mark on a board indicates a likely weakest zone of this board, the failure strength of the board thus is estimated according to machine stress grading standard showed in Appendix 2. However, one must remember that a local F-grade mark corresponds a local bending stiffness range rather then a local bending stiffness value according to F-grade rules. In other words, each individual board may have several *"lowest* local F-grade marks" along its length, as long as the stiffnesses at these locations all fall in the same range. Figure 5.1 shows a real experimental example, there are five red colour marks (6.1GPa <= MOE < 6.9 GPa) corresponding to "the *lowest* local F-grade" of this board. In this case, F-grade is not strictly applicable to indicate the weakest zone, because the failure may not always occur at the lowest local stiffness point even though the board breaks at one of the zones with the *lowest* local F-grade mark. In addition, board may break unexpectedly at a higher local F-grade mark.

Fig. 5.1. Illustration of the local F-grade marks on board.

Therefore, an investigation for the probabilities of failure occurring at the lowest stiffness point, or at one of the lowest recorded grade marks, or at a higher stiffness grade mark was conducted in this study. The results of this study show that there was only 38% confidence in predicating the failure zone by using F-grade marks on the board.

5.2.3. Estimating failure bending strength from the local failure stiffness

The local failure stiffness is the local bending stiffness in the actual failure zone of board. Compared with the F-grade, the local failure stiffness is expected to be a better indicator for the failure strength of board because this stiffness is unique to the failure zone for each board. In addition, the advantage of investigating the local failure stiffness is obvious where the failure strength of the board does not match that designated by the F-grade.

Some previous researches focused on the correlation between the local failure stiffness and the failure strength in bending (or modulus of rupture, i.e. MOR) of timber. The failure strength in bending was found to be reasonably correlated to the local failure stiffness (R^2 from 0.36 to 0.72) of timber (Walker, 1993; Bier and Collins, 1985; Walker, 1975). However, the failure strength in bending (MOR) may not be the failure strength in the weakest zone of a full-length member because the bending moment varies along the length of a board and often leads to failure in the maximum bending moment zone instead of in the weakest zone. In other words, the failure strength in bending usually indicates the local failure strength in the maximum bending moment zone rather than the failure strength in the weakest zone of board. This means that the failure strength in bending does not serve the major concern of forestry industry, namely how weak the board is. Some previous researches have showed that the detrimental effect of natural defects is more severe and more sensitive in tension than in bending

(Phillips *et al.*, 1981; Doyle and Markwardt, 1967). Therefore, research to investigate the relationship between the failure strength in tension and the local failure stiffness was considered in this study in order to find the best indicator of the failure strength in structural timber. The experimental result in this study will show that the failure strength in tension is well correlated to the local failure stiffness (R^2 = 0.54) of board. Compared with average stiffness and F-grade, the local failure stiffness is a better indicator of failure strength in structural timber.

5.2.4. Estimating failure strength by maximum KAR of board

Knottiness has been considered as a harmful factor on the failure strength of timber (Zhang *et al.*, 1997; Barrette and Kellogg, 1991, 1986; Middleton and Munro, 1989; Pellicane *et al.*, 1987; Tustin and Wilcox, 1978). The knottiness is generally described by Knot Area Ratio (KAR) in visual grading systems. Visual grading standards define Knot Area Ratio (KAR) as the ratio of the sum of projected cross-sectional areas of the knots to the cross-sectional area of the piece (BS 4978: 1988; AS 2858: 1986). For each individual board, the largest knot area ratio at any point along the board is defined as the maximum KAR for this board.

Based on the permissible maximum KAR and other defects, such as grain slope, checks, drying defects, the standards of visual stress grading denote five structural grades, which are range from structural grade No.1 to No.5. According to Australian and New Zealand standards, each structural grade fits a certain F-grade (AS/NZS 4063: 1992). The Australian standard (AS 2858: 1986) shows the relationships of structural grades, permissible KAR, and corresponding F-grades (Appendix 3). Failure strength can be estimated from these quantitative relationships. For example, if the KAR of a board for face knot, edge knot and other knots are 25%, 50% and 15% respectively, the structural grade and the F-grade of this board would match No.3 and F8, respectively (Appendix 3). Then the failure tensile strength is estimated as 13 MPa according to the quantitative relationship of strength characteristic between structural grade and the F-grade (Appendix 2). The Australian standard (AS 2858: 1986) states these relationships both with regard to Australian radiata pine and New Zealand radiata pine.

Compared with machine stress grading, visual stress grading is more subjective and less accurate (Zhang, 1997; Ministry of Forestry, New Zealand, 1995; Kennedy, 1995; Walker, 1993; 1975; Williamson, 1982). The coefficient of determination (R^2) between the maximum KAR and the failure strength in bending is around 0.09 ~ 0.16, which is much lower than the R^2 (0.25 ~ 0.72) between the local failure stiffness and the failure strength in bending (Walker, 1993, 1975).

Little information is available for estimating the failure strength in tension by the maximum KAR of radiata pine timber. Hence, this study investigated the correlation between the maximum KAR and the failure strength in tension to evaluate the influence of the maximum KAR on the failure strength of board. The experimental results from this study will show that the maximum KAR alone is not a good indicator of the failure strength of timber due to the poor coefficient of determination (R^2 = 0.21). Further investigations regarding features of knots in the failure zone are presented in next chapter.

5.3. MATERIALS

1,589 boards with dimensions 90 × 35 × 4,200 mm were used to evaluate various possible indicators of failure strength in this study. The number of boards used in the analysis of this study was less than total number of the tensile tested boards (1,919) due to "end failures" in some boards. As described in Chapter 3, the first 650 mm and the last 650 mm of each board had not been machine stress graded due to the distance between the supporting rollers. This means that a value for the local failure stiffness could not be obtained where failure occurred in the ends of the board. Therefore, the "end failure" tests were excluded from the analysis. In order to keep same sampling size, all other analyses in this chapter are also based on data from the same 1589 boards among all 1919 samples.

The pre-processing of timber specimens, such as log cutting, board sawing, drying, dressing, grading, and determination of board positions in the logs, are presented in detail in Chapter 2 and Chapter 3.

5.4. TERMS, DEFINITIONS AND EXPERIMENTAL METHODS

This section describes all terms, definitions and experimental methods that were used in this investigation.

5.4.1. Terms, definitions of knots and measurement of KAR

A knot is the base of a branch embedded in the stem or a large branch; the remains of a branch present in boards are also termed as knots (Ministry of Forestry, New Zealand, 1995; Pellicane and Franco, 1994; Samson, 1993; Philips *et al.,* 1981).

A knot is generally classified as an intergrown, an encased or a group knot. An intergrown knot is wholly intergrown with continuity between the fibres of the surrounding wood; the wood of a bark-encased knot is not intergrown with those of the surrounding wood being separated by a layer of bark; and a group knot is two or more single knots grouped together. A living branch forms an intergrown (tight or red) knot, and a dead branch forms an encased (or bark) knot. A group-knot results from clustered branches (ASTM D9-87, 1995; Ministry of Forestry, New Zealand, 1995).

Referring to the position of knots within the board section, the Australian standard (AS 2858 -1986) and the New Zealand standard (NZS 3631: 1988) divide the cross-section into a central and margin portions (Fig. 5.2). The central face area is the central-located designated proportion in the width of the piece of timber, and this defines and restricts the size of a central face knot. The margin regions lie on both sides of the designated central region of the face. Each margin region equals one-quarter of the total cross-sectional area, based on actual dimensions of the piece (Ministry of Forestry, New Zealand, 1995; NZS 3631: 1988; BS 4978: 1988). Arris is defined as the sharp intersection of two surfaces, for example the face and edge of a piece of timber.

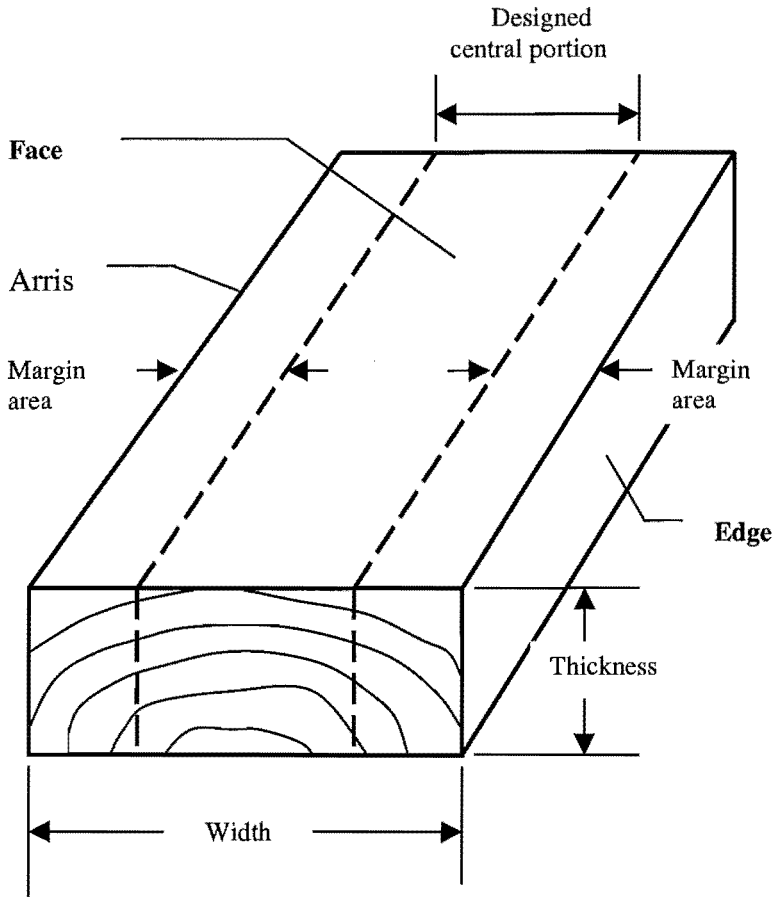

Fig. 5.2. Illustration of the terms arris, designated central portion, edge, face, margin areas, thickness (T) and width (W) (after AS 2858-1986).

According to the position within the cross-section, knots are classified as face knots, margin knots, edge knots and arris knots. Compared with American standard (ASTM D9-87, 1995) and British standard (BS 4978, 1988), the Australian standard and the New Zealand standard (AS 2858, 1986; NZS 3631: 1988) give a more detailed description for the types of knots. The Australian and New Zealand standards thus are used in identifying knot types in this study.

Regarding the calculation of KAR, this study followed the regulations of Australian and New Zealand standards (AS 2858, 1986; NZS 3631: 1988). The KAR of different knot types in each board was measured, calculated and compared to obtain the maximum KAR in each board. In order to study the failure features of board, the KAR at the actual failure zone was also investigated in each board, which is shown in Chapter 6. British standard (BS 4978, 1988) gives a specific knot area ratio, known as the "margin knot

area ratio" (MKAR), to describe the knot size in the margin. In New Zealand standard (NZS 3631, 1988), MKAR is referred in the engineering grade, but the definition of MKAR is not given. According to British standard (BS 4978, 1988), MKAR is the "ratio of the sum of the projected cross-sectional areas of all knots or portions of knots in a margin intersected at any cross section, to the cross-sectional area of the margin". In this study, MKAR is excluded to reduce the workload to a manageable size. From the definitions of knot types, the locations of face, margin, edge and arris knots are clearly distinguished, but the location of group knots may be anywhere in the cross-section. However the frequency of failed group knots is far less than the rest of knot types in outerwood as shown in table 6.1. In this study, the knot type, the maximum KAR, and the KAR of the failed knot are considered as more important features than MKAR in terms of indicating the failure strength. The effects of MKAR and grain distortion on strength are left to future studies.

According to Australian standard and New Zealand standard (AS 2858, 1986; NZS 3631: 1988), the definitions of knot types and the calculations of the KAR are illustrated below.

A **face knot** is confined entirely within the designated central portion of the face or cross-sectional area of the piece (Fig.5.3). The KAR, the area of the projection of the projection trapezium divided by the cross-section area, is expressed as

$$KAR = [H(D1+D2)/2] \div TW = (D1+D2)/2W$$

where D1 and D2 are the lengths of the parallel sides of the projection trapezium, W and T are the width and thickness of the board (T = H)

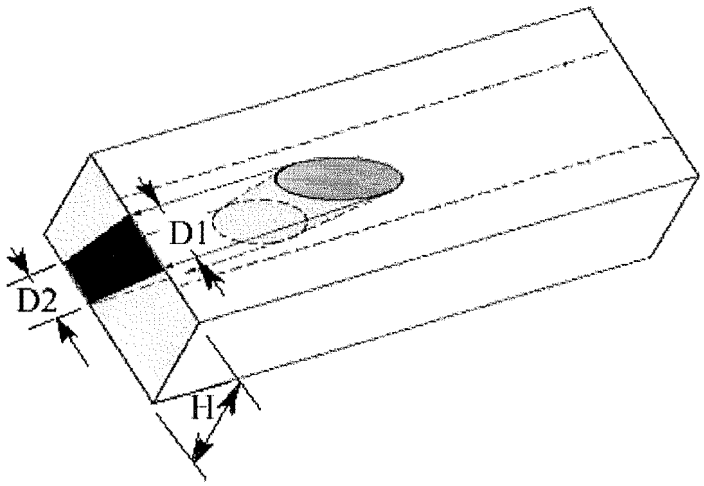

Fig. 5.3. Face knot and its projected cross-sectional area.

An **arris knot** appears only on the adjoining face and edge of a piece and contains the intersection of these surfaces (Fig. 5.4). The KAR can be calculated by

$$KAR = DH/2WT$$

where D and H are the length of the base and the height of the projection triangle, W and T are the width and thickness of the board.

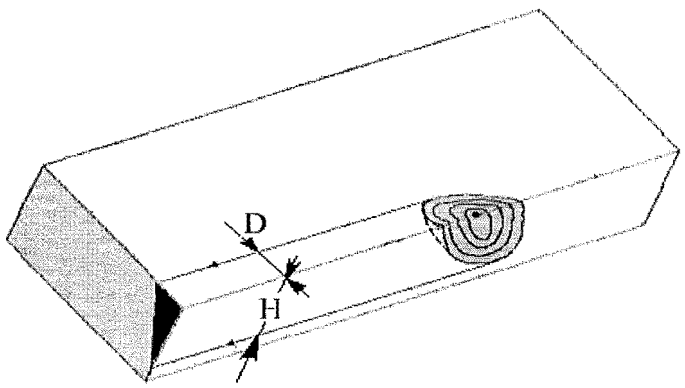

Fig. 5.4. Arris knot and its projected cross-sectional area.

A **through knot** matches one of the following two conditions:

a) it appears on both the edge and face of the piece, but does not contain the intersection of these surfaces (Fig. 5.5);

b) it appears on both the adjoining face and edge of a piece containing the intersection of these surfaces and on the opposite face, edge or arris (Fig. 5.6).

In the second case, a through knot is actually an arris knot passing through the piece. This study calls this type of through knot as a "through arris knot" in order to distinguish the two types of through knots (Fig. 5.6).

The projection of the first type of through knots is a larger triangle taking away a smaller triangle (Fig. 5.5). The corresponding KAR is

$$KAR = (DH - dh)/2WT$$

where D and H are the length of the base and the height of the larger triangle, d and h are the lengths of the base and the height of the smaller triangle, W and T are the width and thickness of the board.

The projection of a "through arris knot" is a trapezium subtracted by a triangle (Fig. 5.6). The KAR can be expressed by

$$KAR = [(D1 + D2)H - d2*h]/2WT$$

where D1 and D2 are the lengths of parallel sides of the trapezium, H is the height of the trapezium, d2 and h are the lengths of the base and the height of the triangle, W and T are the width and thickness of the board.

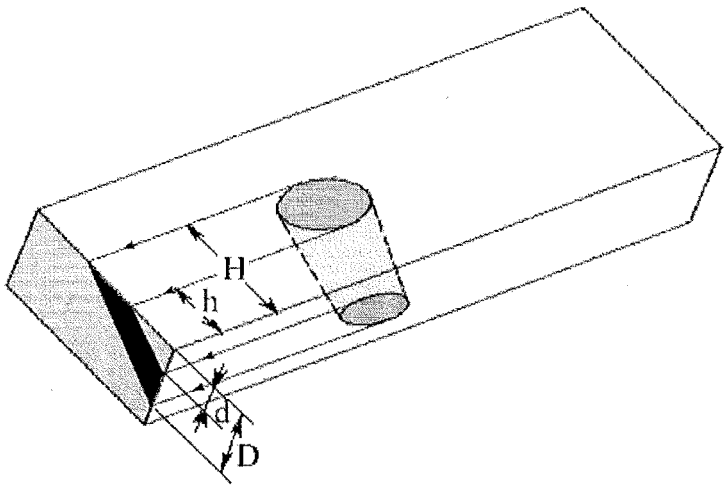

Fig. 5.5. Through knot and its projected cross-sectional area.

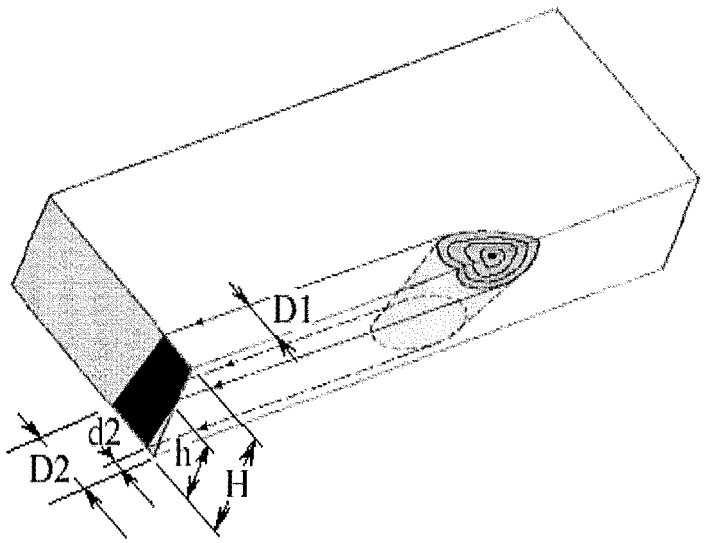

Fig. 5.6. Through arris knot and the projected cross-sectional area.

A **margin knot** appears outside or partially outside of the designated central portion of the face of the piece (Fig. 5.7 and Fig. 5.8). The projection trapezium divided by the cross-section area can be expressed as

$$KAR = (D1 + D2)/2W$$

where D1 and D2 are the lengths of the parallel sides of the projection trapezium, W is the width of the board.

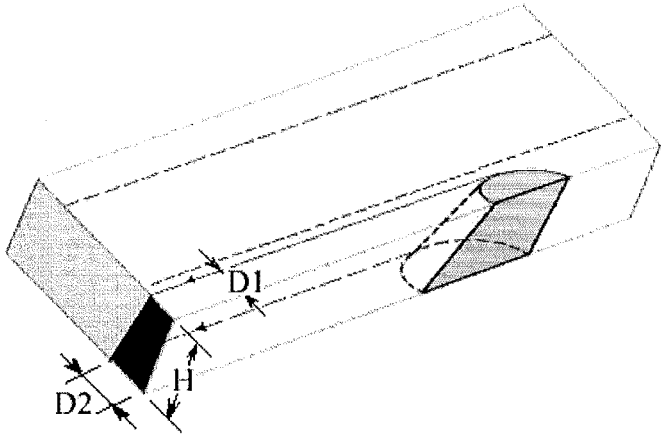

Fig. 5.7. Margin knot one and its projected cross-sectional area.

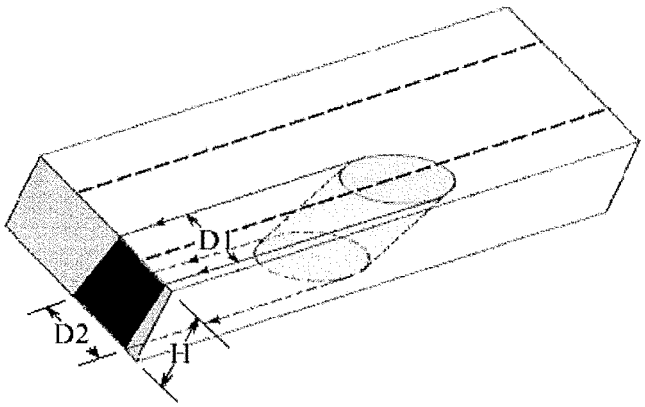

Fig. 5.8. Margin knot two and the projected cross-sectional area.

An **edge knot** appears on one or both edges of the piece (Fig. 5.9; Fig. 5.10; Fig. 5.11). New Zealand standard defines the edge knot that only appears on one edge of the piece as a spike knot (Ministry of Forestry, New Zealand, 1995). The projection areas of the edge knots could be a triangle (Fig.5.9 and 5.10) or a trapezium (Fig. 5.11). For triangular and trapezium projections, we have

KAR = DH/2WT (triangular projection)

KAR = (D1 + D2)/2T (trapezium projection)

where D and H are the lengths of the base and the height of the projection triangle, D1 and D2 are the lengths of the parallel sides of the projection trapezium, W and T are the width and thickness of the board.

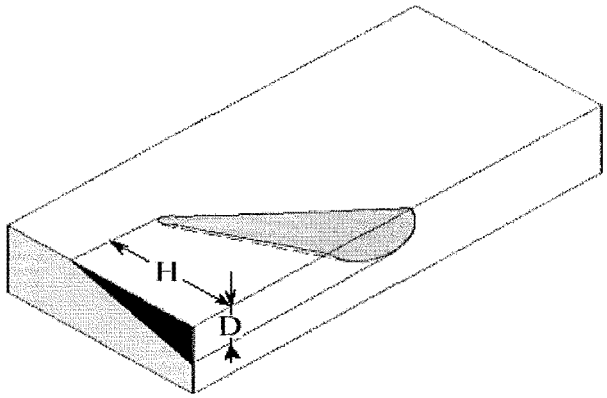

Fig. 5.9. Edge knot one (spike knot one) and the projected cross-sectional area.

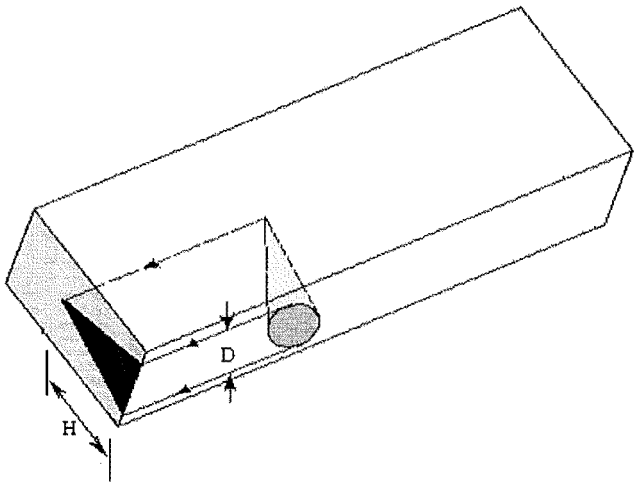

Fig. 5.10. Edge knot two (spike knot two) and the projected cross-sectional area.

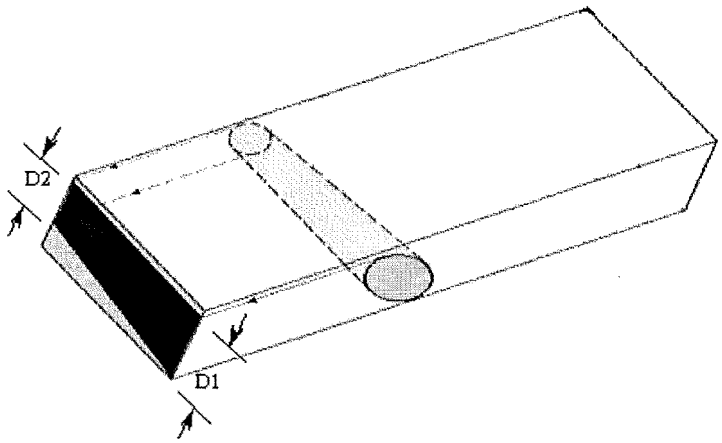

Fig. 5.11. Edge knot three and its projected cross-sectional area.

Group knots: Two or more single knots grouped together form a group knot. The knots that form a group knot can be face, arris, margin, through and edge knot. Fig. 5.12 shows an example of the group knot.

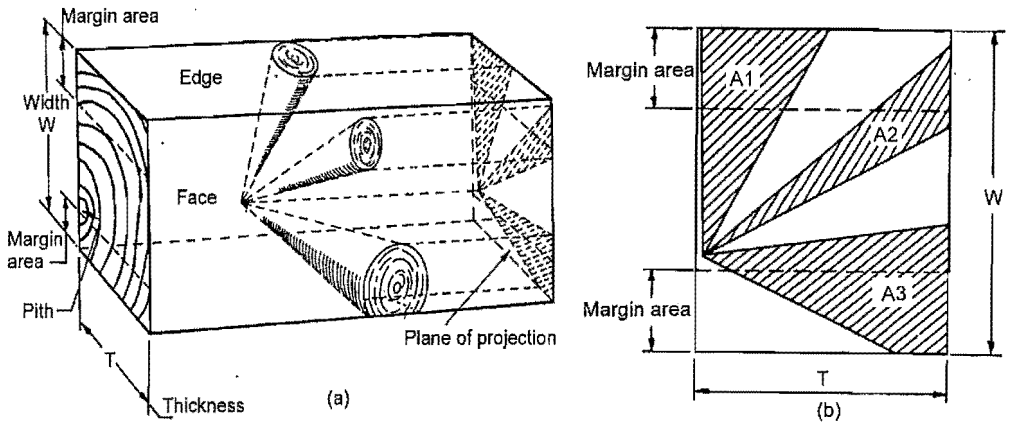

Fig. 5.12. A group knot: (a) the axonometric view of a group of knots in a piece, (b) the front view of the projection plane (KAR = A1 + A2+ A3 i.e. the sum of the hatched areas) (after AS 2858:1986).

In this study, before destructive testing, all surfaces of each board were checked carefully. The diameters of the maximum knots for each type were measured and recorded to calculate the maximum KAR for each board. Then the likely failure zone of

the board was determined according to Australian standard (AS 2858: 1986) (Appendix 3).

5.4.2. Measurements of average stiffness, F-grade, failure strength and local failure stiffness

1) Measuring average stiffness in bending

In this study, each piece of timber was machine stress graded in the sawmill. The procedure of machine stress grading has been introduced in proceeding chapter. The average stiffness of board in bending is calculated from the mean of local bending stiffnesses along each board.

2) Determining F-grade of board

During machine stress grading, the local F-grade marks were sprayed on the board surface according to the corresponding local bending stiffness range at each particular point. The lowest F-grade mark along the length of each board is the F-grade of the board.

3) Measuring average stiffness in tension

The average stiffness in tension was measured using a horizontal tensile test machine shown in Figure 4.6. The operation of the machine is described in Chapter 4. During the tensile test, a 200 kN capacity hydraulic ram provided an axial tensile force to the board. The longitudinal dimension of each piece increased with the increase of this axial load. This was measured by a displacement potentiometer. Then the average stiffness in tension was obtained from following calculation:

$$\text{Average stiffness in tension} = \frac{Stress}{Strain} = \frac{\Delta F / bd}{\Delta L / L} = \frac{\Delta FL}{\Delta Lbd} \qquad (5.1)$$

where ΔF is change of the axial load (N); ΔL is the increment of the axial dimension of the board (m); L is the length of the span (3.3m); b and d are the width and depth of the board (m).

4) Measuring failure strength of board in tension

The measurement of the failure strength of board in tension is described in detail in Chapter 4.

5) Measuring local failure stiffness of board

As described in Chapter 3, the machine stress grading measured the local bending stiffness along each piece and the corresponding colour mark was sprayed on the surface of the board at each 152 mm interval. After the destructive testing, matching the colour mark at the failure zone, the local stiffness value can be read from the original data for that board obtained at the sawmill.

5.5. EXPERIMENTAL RESULTS

This section sets out all the experimental results, which include the correlation between the failure strength and the average stiffness in bending; the correlation between the failure strength and the average stiffness in tension; the correlation between the failure strength and the maximum KAR and the correlation between the failure strength and the local failure stiffness. This section also sets out two percentages: 1) of the boards that failed in a zone whose local failure stiffness was not the lowest value in the board; 2) of the boards that broke in a zone whose local failure stiffness was higher than the stiffness range indicated by the F-grade of the board.

5.5.1. The correlations between the failure strength (UTS) and the average stiffness

The experimental results show that both the average stiffness in bending and the average stiffness in tension were not good indicators of the failure strength of board due to their lower correlation coefficients. The coefficient of determination (R^2) of the

failure strength and the average stiffness in bending was 0.35 and the R^2 of the failure strength and the average stiffness in tension was 0.45 (Fig. 5.13 and Fig. 5.14).

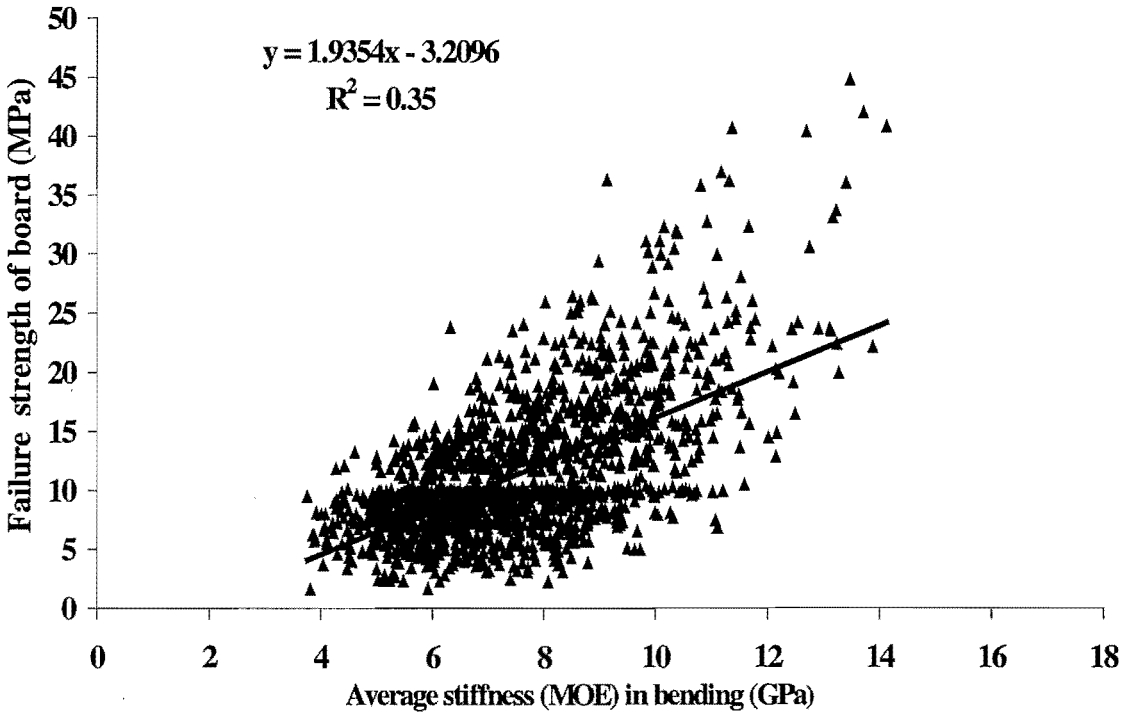

Fig. 5.13. The correlation between failure strength (UTS) and average stiffness in bending.

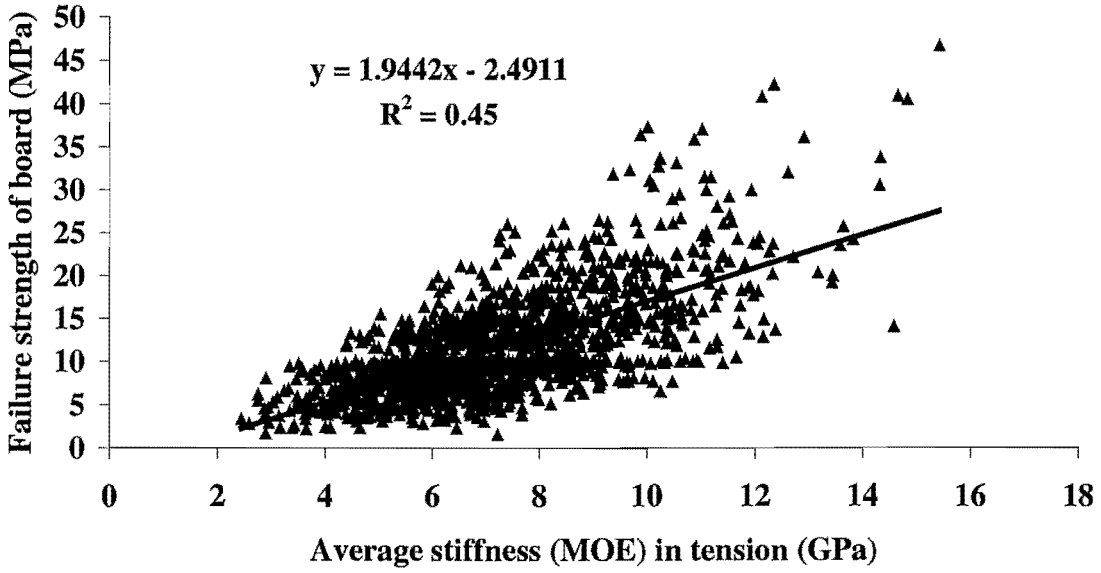

Fig. 5. 14. The correlation between failure strength (UTS) and average stiffness in tension.

5.5.2. *Estimating the failure zone by F-grade of board*

In order to investigate the accuracy of estimating the failure strength by F-grade of the board, this study examined the percentage of local failures that did not occur at a point in the board carrying the lowest F-grade mark. The study showed that: 985 (62%) out of all 1589 boards failed in a zone whose local failure stiffness was not the *lowest* local stiffness point in the board; and in those 985 boards, 1) 532 boards broke at a point displaying the lowest F-grade mark but not at the lowest stiffness point of board; 2) the failure point of 453 boards displayed a higher F-grade mark instead of the *lowest* F-grade mark on the surface of the board (Table 5.1).

The experimental results revealed there was only 38% confidence to predicate the failure zone by using the lowest local stiffness in the "lowest local F-grade mark" zones when there were several "lowest local F-grade marks" along the length of board. In summary, F-grade marks cannot be used to identify the weakest point of the board.

Table. 5.1. Record of failure point in 1589 radiata pine boards.

Failure point	No. of board	Percentage of 1589 boards
Failed at the lowest stiffness point	604	38%
Failed at a point displaying the lowest F-grade mark but not at the lowest stiffness point	532	33.4%
Failed at a point displaying a higher F-grade mark rather than the lowest F-grade mark	453	28.5%

5.5.3. *The correlation of the failure strength (UTS) and the maximum KAR of board*

Before destructive testing, the maximum KAR of each board was measured to see whether the maximum KAR was a good indicator of the failure strength of board. The experimental results indicate that the correlation between the failure strength and the maximum KAR of board is weak ($R^2 = 0.21$) (Fig.5.15).

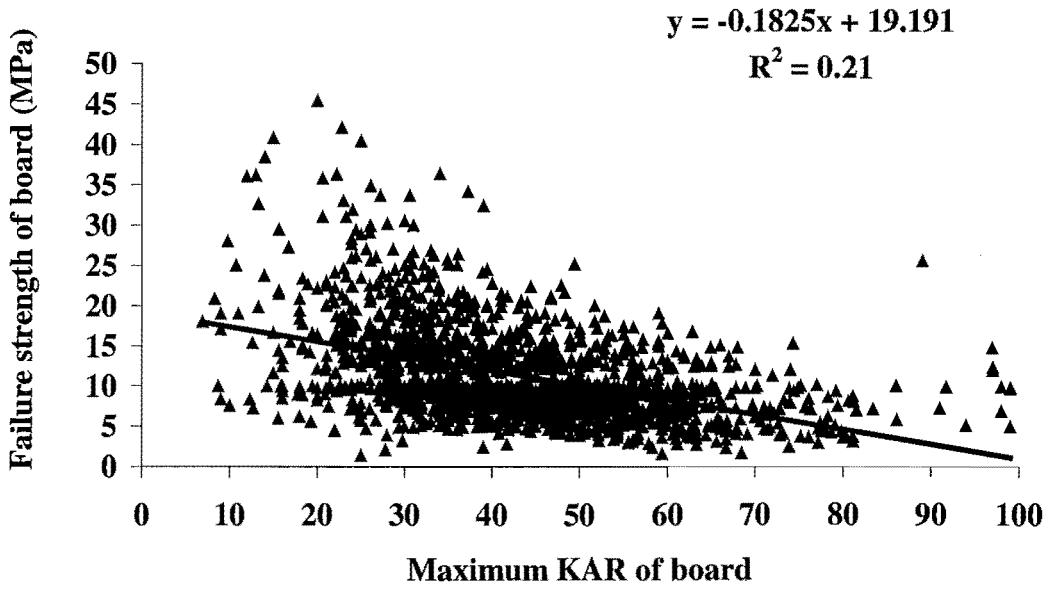

Fig. 5. 15. The correlation between the failure strength and the maximum KAR of board.

5.5.4. The correlation of the failure strength (UTS) and the local failure stiffness of board

The local failure stiffness is better indicator of the failure strength of board due to the strong correlation ($R^2 = 0.54$) between the local failure stiffness and the failure strength of board (Fig. 5.16), compared with the average stiffness in bending, the average stiffness in tension and the maximum KAR.

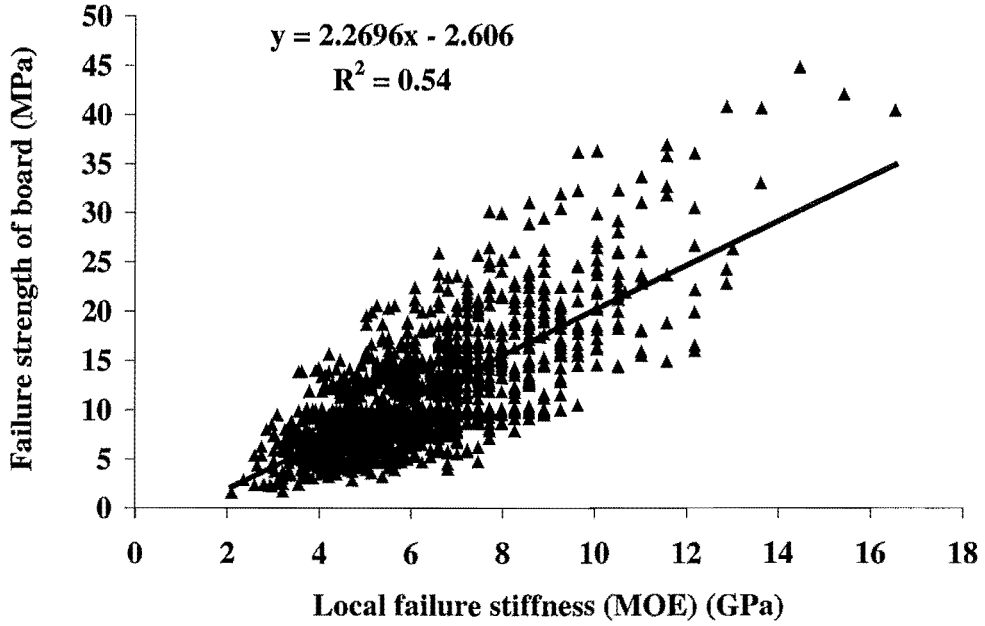

Fig. 5.16. The correlation of the failure strength (UTS) and the local failure stiffness of board.

5.6. SUMMARY

This study targeted the estimation of the weakest zone and the failure strength in tension, which had not been well explored previously. Various suggested indicators of failure strength, such as average stiffness in bending, average stiffness in tension, F-grade mark, the maximum KAR and the local failure stiffness were investigated to compare with the approach first introduced in this study, i.e. estimating the failure strength of board in tension with respect to local failure stiffness.

The conclusions and speculations are summarised as follows:

- The average stiffness of a board is not an acceptable indicator of the failure strength in this board because the stiffness outside the weakest point is irrelevant to the characteristics of this point. The weak correlations between average stiffness and failure strength in both previous and this study prove this.

- The F-grade approach failed to identify the weakest zone. 28% of 1589 boards do not fail at a point along the board's length that corresponded to the lowest F-grade mark. Even when failure occurs at a point carrying the lowest F-grade mark, the point with the lowest local stiffness value is only correctly identified for 38% of all tested boards (Table 5.1).

- The poor correlation (R^2 =0.21) suggests that the maximum knot size alone is not a good indicator of the failure strength value.

- Of all indicators for the failure strength, the local failure stiffness is the best indicator of the failure strength value in structural timber, due to its strong correlation (R^2 = 0.54). Further research regarding the failure features of the weakest zone is displayed in the succeeding chapter. A correct estimation of the weakest zone combined with the local stiffness there would give a successful non-destructive estimate of the failure strength of timber.

Chapter 6

FAILURE FEATURES OF KNOTS IN RADIATA PINE STRUCTURAL TIMBER

6.1. INTRODUCTION

Knot is considered as an important factor weakening the mechanical properties of structural timber, both due to their severe local drying deformation (i.e. distortion and check) and material discontinuity (Walker, 1993; Kinimonth and Whitehouse, 1991; Forest Products Lab., USA., 1989; Kininmonth, 1961). The mechanisms of failure associated with knots have been studied for many years. Regarding the failure caused by knots, three hypotheses have been proposed, including material discontinuity (called hole theory), stress concentrations theory and effects arising from grain deviation.

- The material discontinuity theory (or called hole theory) treats a knot as a hole of the same size in the board. The weakening of board strength is from the reduction of the cross section area (Walker, 1993; Green and Zerna, 1968). If the "hole theory" were true, the maximum KAR (knot area ratio) might be the best indicator of the weakest zone. Unfortunately, this study reveals that more than one third boards do not fail at their maximum KAR zone; and the correlation between the maximum KAR and the strength is weak (Chapter 5). It means that the "hole theory" oversimplifies the nature of knots and is proved unreliable for the prediction of the weakest zone in structural timber.

- The stress concentration theory suggests that a large stress concentration is the failure cause of a knotty zone. A stress concentration is defined as a larger local stress around the tip of the initial cracks in a knotty zone compared to the average stress value where the stresses distributed uniformly. In order to represent the distribution of stress in timber, the stress trajectory approach is employed. When a defect-free board is in tension, all parts of the board are equally stressed and the stress is transferred uniformly from one end of the specimen to the other end, which is

represented by a group of parallel stress trajectories (Figure 6.1 a). If there is an internal or surface crack in the board, which often occurs in the knotty zone, the local stress at the tip of the crack will be much higher than the average value. The stress concentration can be represented by the bending and crowding of stress trajectories around the tip of the crack (Figure 6.1 b, c). The sharper the tip of the crack, the larger the stress concentration is. Once the local stress reaches the critical stress of the material, the failure runs from the tip of the crack across the board (Walker, 1993; Tang, 1984; Cramer and Goodman, 1983; Bodig and Jayne, 1982; Gordon, 1978).

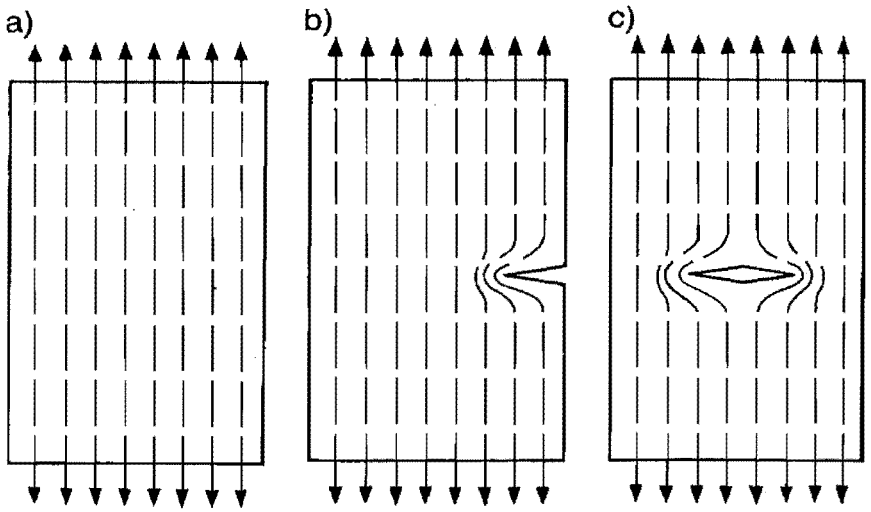

Fig. 6.1 a) b) c). Stress trajectories in a tension member (reproduced from Gordon, 1978).

The stress concentration theory is generally employed to describe the propagation of failure due to an internal or surface check that may result from drying in the knotty zone. If there is not an internal or surface check in the knot zone, this theory assumes the knot itself can be treated as a "blunt crack", thus the stress concentration around the "crack" causes the failure of the board. According to stress concentration theory, the knots that have rounded shapes, such as face, margin and through knots, can be treated as "circular cracks" with a stress concentration factor 3. However, experimental evidence for this assumption has not been found in previous published literatures. In addition, the stress concentration theory generally is hard to apply directly in practice if there is not visible check on the surface of board, or if the wild

grain surrounding a knot is located within one board while the knot itself is confined to an adjacent board.

- The third hypothesis for failure cause of knot is assumed to be due to grain deviation. Severe grain deviations around knots is believed to do even more harm than knots themselves to the strength of timber (Zhang, 1997; Walker, 1993; Samson, 1993; Cramer, *et. al.*, 1988; US Forest Products Laboratory; 1974; Panshin and Dezeeuw, 1970; Wangaard, 1950). The grain around a knot flows around an object. Hence the wood grain has been modelled using fluid mechanics equations, a method which is called the flow grain analogy (Phillips *et al.*, 1981; Dabholkar, 1980; Goodman and Bodig, 1980). On the basis of the flow grain analogy, finite element analysis has been used to predict the stress associated with grain deviation around knots (Fig.6.2) (Pellicane and Franco, 1994; Zandbergs and Smith, 1988; Cramer and Goodman, 1986, 1983; Phillips *et al*, 1981). However, the evaluation of grain deviation is very tricky due to the large variability of grain slope in the region of a knot. It means this theory is hard to validate by any means.

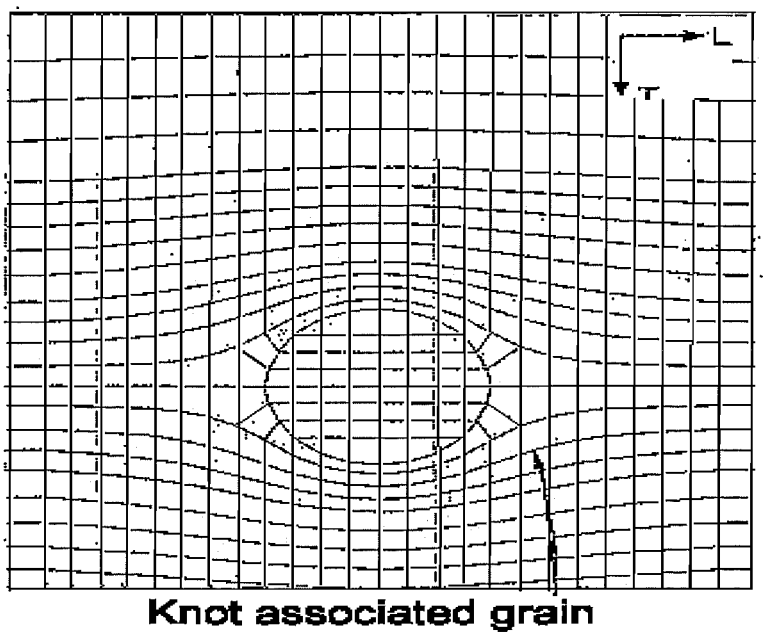

Fig. 6.2. Simulated grain pattern resulting from the flow-grain analogy (after Cramer and Goodman, 1983).

In summarising, the existing three hypotheses for the mechanisms of failure associated with knots have obvious shortcomings -- either inaccurate or lack for experimental

evidence. Therefore, this study seeks experimental evidences to estimate the weakest point, especially those associated with knots. Identifying an efficient method to predict the weakest point of structural timber is also an objective of this study. 1,919 radiata pine boards with dimension 90 × 35 mm in cross- section and 4,200 mm long served for these purposes in this study. The failure features of knots, such as the failure probabilities of different knot types, the influence of KAR on the failure strength in different knot types, failure patterns of knots and the influence of failure angles in different knot types are investigated.

The experimental results of this study show that 1,894 (98.7%) out of 1919 boards broke at a knot zone, which reveals that the knot is the main cause of the failure in structural timber. On the basis of the experimental facts, two basic failure patterns, i.e. the "boundary- broken" (the curved failure surface is along the interface between the knot and stem wood) and the "plane-broken" (the failure plane through the pith of the branch within the knot itself) are first presented in this study. The failure modes of different knot types are identified. In line with the identification of failure patterns, measurement methods were designed to quantify the failure features. The mode of failure angles is thus presented. These results may give an insight for identifying the weakest point in structural timber and provide useful information to forestry industry for cutting and visual grading.

In this chapter, the experimental materials and methods are introduced in Section 6.2. Experimental results are presented in Section 6.3. Discussions are given in Section 6.4.

6.2. MATERIALS AND EXPERIMENTAL METHODS

1,919 boards with dimensions 90 × 35 × 4,200 mm were used in this study. All pre-processing of these boards, such as log cutting, board sawing, drying, dressing, grading, and determination of board positions in the logs, are presented in detail in Chapter 2 and Chapter 3.

Before destructive testing, the potential weakest point in each board was predicted according to the maximum KAR (AS 2858: 1986). The measurement and calculation of

the maximum KAR are introduced in Chapter 5. The potential weakest point was marked on the surface of the board once the point was determined. After tensile testing, the failure features of the actual failure point in each board, such as the type of failure knot; the KAR of the failure knot, the failure pattern at the knot and the failure angle of knot, were measured carefully. The failure pattern and the failure angle of knots are defined as follows.

6.2.1. Boundary-broken pattern around knots

1) The definition of boundary-broken pattern

The author defines the failure pattern as boundary-broken when the broken surface occurs along the interface between the knot and stem wood. This broken pattern generally results from the material discontinuity due to the bark of the encased knot separating the stem wood from the knot wood. The boundary-broken failure may occur in different knot types. The following photos show the boundary-broken pattern in margin, edge and through arris knots (Fig. 6.3 ~ 6.5).

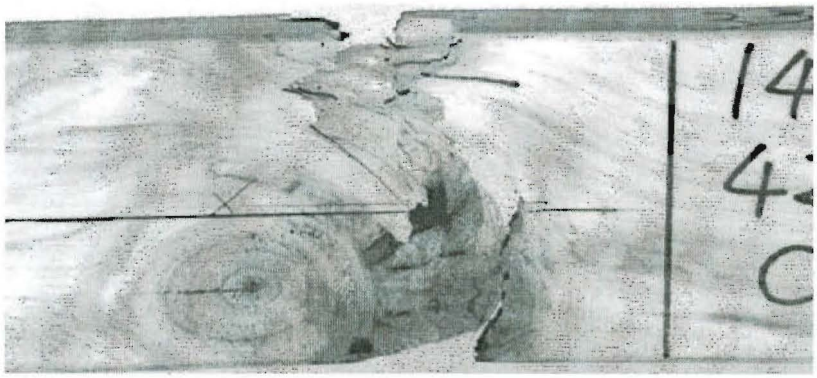

Fig. 6.3. The boundary-broken pattern in a margin knot.

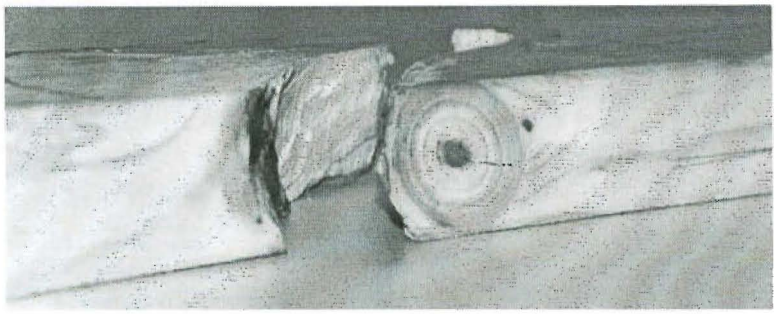

Fig. 6.4. The boundary-broken pattern in an edge knot.

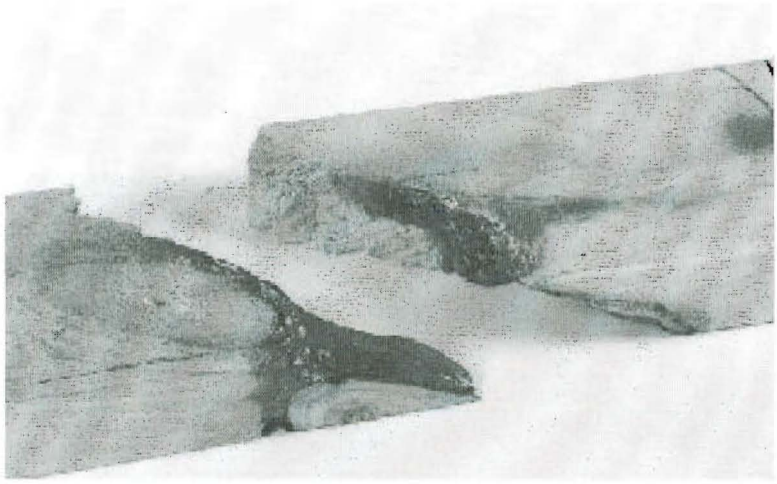

Fig. 6.5. The boundary-broken pattern in a through arris knot.

2) Measuring knot failure angle in the boundary-broken pattern

This study defines failure angle as the angle of the exposed failure surface of the knot. Analogous to KAR measurement, the boundary-broken knots were first projected to the edge or face of the board. The projections form angles with the vertical (or axial) direction of the stem (Fig. 6.6 ~ 6.8).

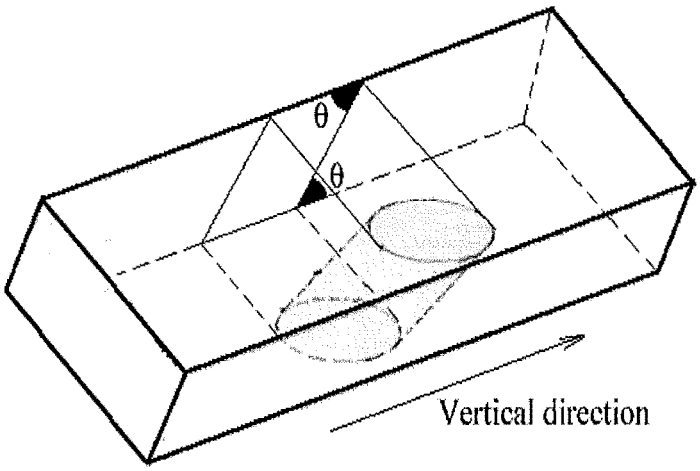

Fig. 6.6. Failure angle in a margin knot.

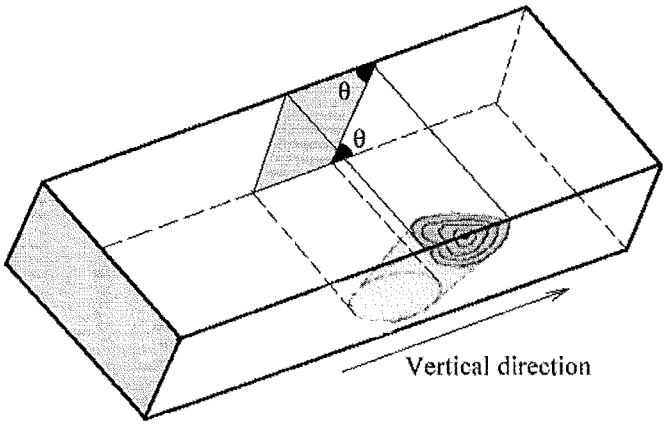

Fig. 6.7. Failure angle in a through arris knot.

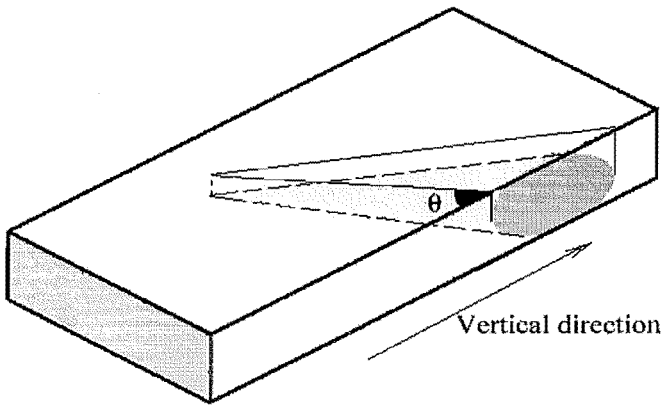

Fig. 6.8. Failure angle in an edge knot.

6.2.2. Plane-broken pattern of knots

1) The definition of the plane-broken pattern of knots

The plane-broken pattern refers the failure along a plane containing the pith of the branch. As with the boundary-broken pattern, the plane-broken pattern also occurs in different knot types. The following photos show the plane-broken pattern in margin, edge and through arris knots (Fig. 6.9 ~ 6.11). Note that the pith of the branch wood is clearly visible in the failure plane.

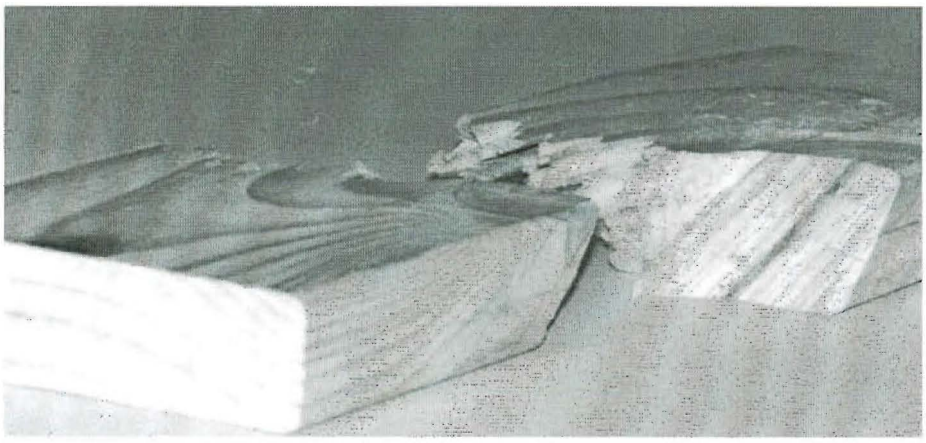

Fig. 6.9. The plane-broken pattern in a margin knot.

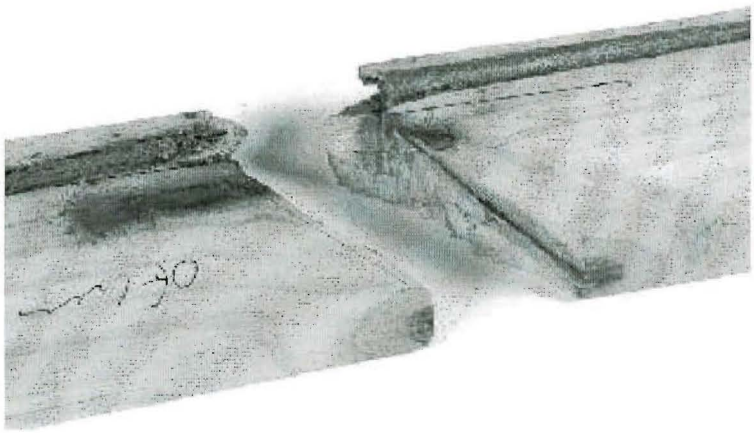

Fig. 6.10. The plane-broken pattern in an edge knot.

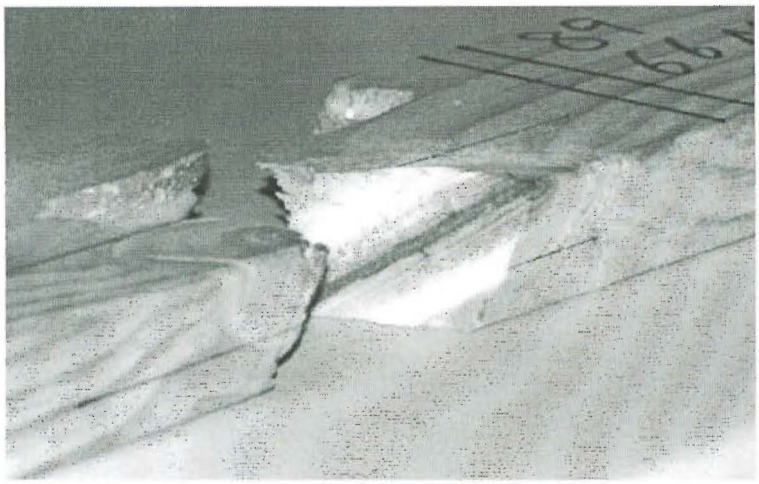

Fig. 6.11. The plane-broken pattern in a through arris knot.

2) Measuring the failure angle in the plane-broken pattern

In the plane-broken pattern, the failure surface is approximately a plane containing the pith of the knot. The failure angle θ, i.e. the angle between the failure plane and the face of the board, is used to determine the inclination of the failure plane of this board.

By convention, an angle between two planes is the largest angle formed by lines on the two planes. The intersection of the face and the failure plane is CD as shown in Fig. 6.12. Lines AD and BD, perpendicular to CD, lie on the failure plane and face respectively. AD and BD form the failure angle θ (∠ ADB).

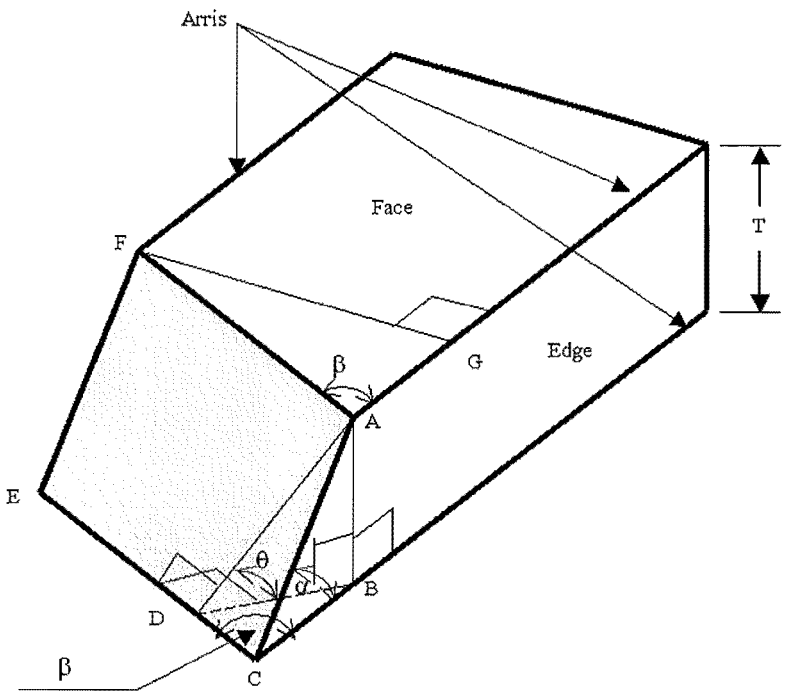

Fig. 6.12. Measuring the failure angle θ in the plane-broken pattern.

The failure angle θ of the plane-broken pattern then can be calculated by the measurement of the angles α and β, where α (∠ ACB) is the angle between BC (an arris) and AC (an intersection of edge plane and failure plane), and β (∠ BCD) is the angle between AG (an arris) and AF (an intersection of face and failure plane). From the right-angled triangle ABC, it is shown that

$$BC = AB / \tan(\angle ACB) = T / \tan\alpha$$

where T is the board thickness, i.e. AB.

In the right-angled triangle BCD, we have

$$BD = BC \times \sin(\angle BCD) = (T / \tan\alpha) \times \sin\beta$$

The tangent of θ (angle of the failure plane and face of the member) in the right-angled triangle ABD is the ratio of AB and BD

$\tan\theta = \tan(\angle ADB) = AB / CD = \tan\alpha / \sin\beta$

The angle of failure plane with the member face can be calculated using the measurements of α and β as

$\theta = \tan^{-1}(\tan\alpha / \sin\beta)$

Notice that $\theta = \alpha$ when $\beta = 90^{\circ}$ ($\sin\beta = 1$).

6.3. EXPERIMENTAL RESULTS

This section shows the experimental results of this study including the variations of the types of failed knots according to radial distance; the relationship between failure strength and KAR at the actual failure point; the failure pattern of knots; the influence of the failure angle for a single knot on the failure strength.

6.3.1. Types of failed knots variations according to radial distance

Table 6.1 shows the failures associated with specific knot type according to radial distance from pith. Regarding the failure probabilities given in Table 6.1, the following facets should be noted:

- 1894 (98.7%) of 1,919 boards broke at a knot zone and only 25 (1.3%) of the 1,919 boards failed in knot-free wood.
- Amongst all types of failed knots, the margin and face knots resulted in the highest and lowest failure frequencies. Margin knots caused nearly half of the failures, whereas the failures related to face knots was insignificant.
- Group knots are mostly associated with failures at P1 (boxed-pith), and the failure frequency significantly declines with the increase of the radial distance from pith. Margin knots are mostly associated with failures at outerwood, and the failure frequency noticeably increases from position 2.

Table 6.1. Distribution of the types of failed knots according to radial distance

Location of failed boards	Margin knot	Group knots	Through arris knot	Edge knot	Through knot	Face knot
P1 (447)	5.1% (23)	73.8% (330)	4.7% (21)	16.4% (73)	0	0
P2 (765)	39.7% (304)	33.5% (256)	14.2% (109)	9.8% (75)	2% (15)	0.8% (6)
P3 (509)	67% (341)	7.9% (40)	16% (81)	6.9% (35)	2.2% (12)	0
P4 (141)	81.7% (115)	4.2% (6)	9.2% (13)	4.9% (7)	0	0
P5 (32)	76.9% (25)	2.6% (1)	12.8% (4)	7.7% (2)	0	0
All (1894)	42.7% (808)	33.4% (633)	12% (228)	10.2% (192)	1.4% (27)	0.3% (6)

Note: the figures in bracket are number of failure boards that broke due to knots

One might argue that the remarkable differences of failure frequency between margin and face knots could reflect the large number of margin knots and a small number of face knots in the tested boards. Fortunately, our sample is long enough (4.2 m) to allow all knot types to be present randomly and the sampling size is large enough to produce a large number of face knots. In addition, our samples were cut from an unpruned forest stand, which contains more branches with an even distribution of knot types than would occur in a pruned sample. In other words, from the experimental result one is able to conclude that the insignificant number of face knot broken was because face knots rarely broke and not because there were only a few face knots present in the samples.

6.3.2. Relationship between failure strength and KAR at actual failure zone

The maximum KAR of the board has been proved to be a poor indicator of the failure strength in Chapter 5. This Chapter further reveals the KAR of the actual failure point is also not good indicator of the failure strength of the board. The relationships between the failure strength and the KAR at the actual failure point are presented in this section according to the different knot types. The analysis concerning face knots and through knots were excluded from this study because only a few of boards failed due to face and through knots. The results show that the failure strength does reduce with the increase of the KAR at the actual failure zone. However, the coefficient of determination (R^2) between the KAR of failed knot and failure strength is weak, especially in group knots and edge knots (Figures 6.13 ~ 6.16). Combined with the results reported in Chapter 5, one can concluded that KAR has difficulty in predicting the failure zone in structural timber.

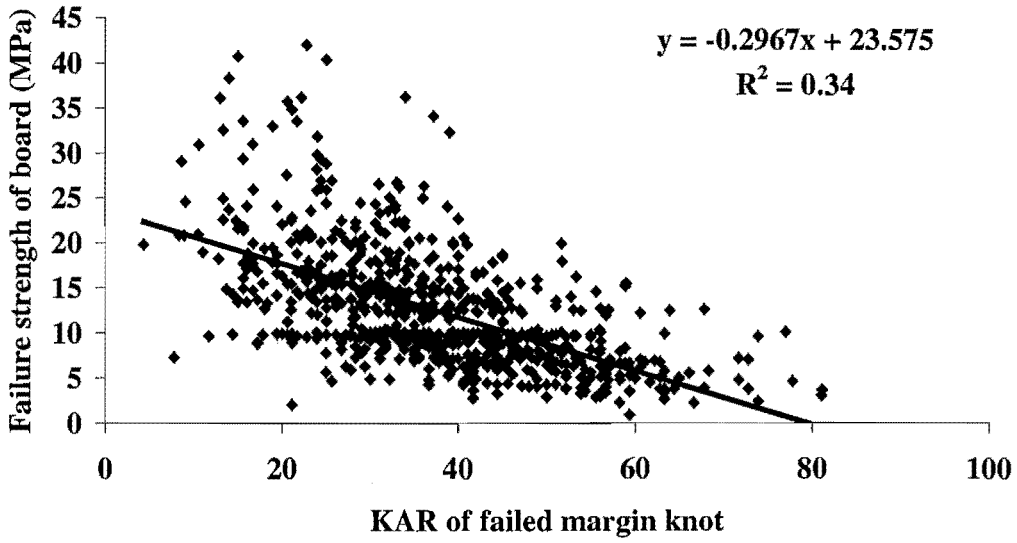

Fig. 6.13. The relationship between the failure strength and KAR of failed margin knots.

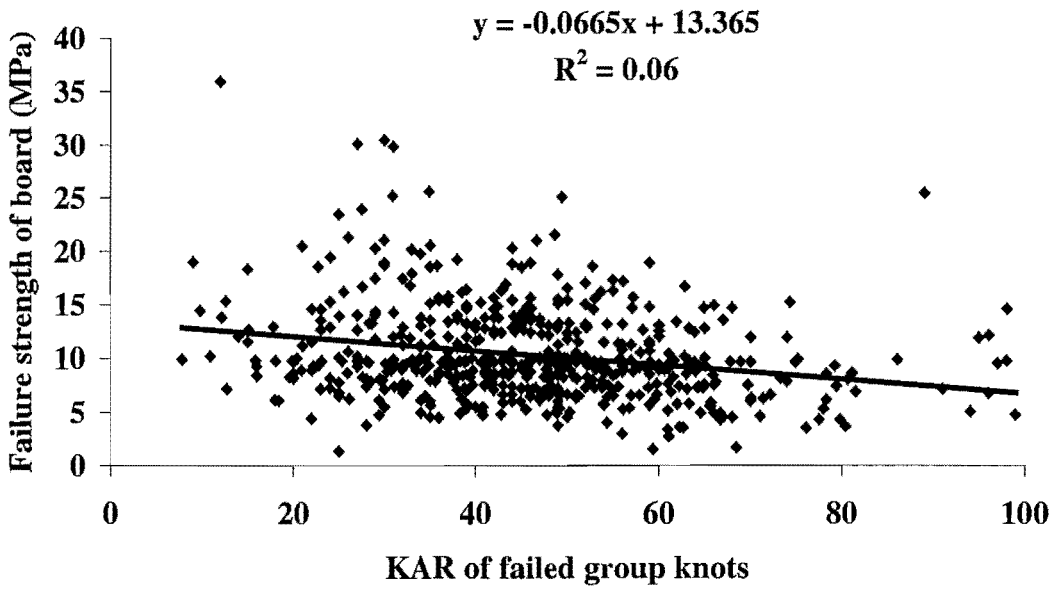

Fig. 6.14. The relationship between the failure strength and KAR of the failed group knots.

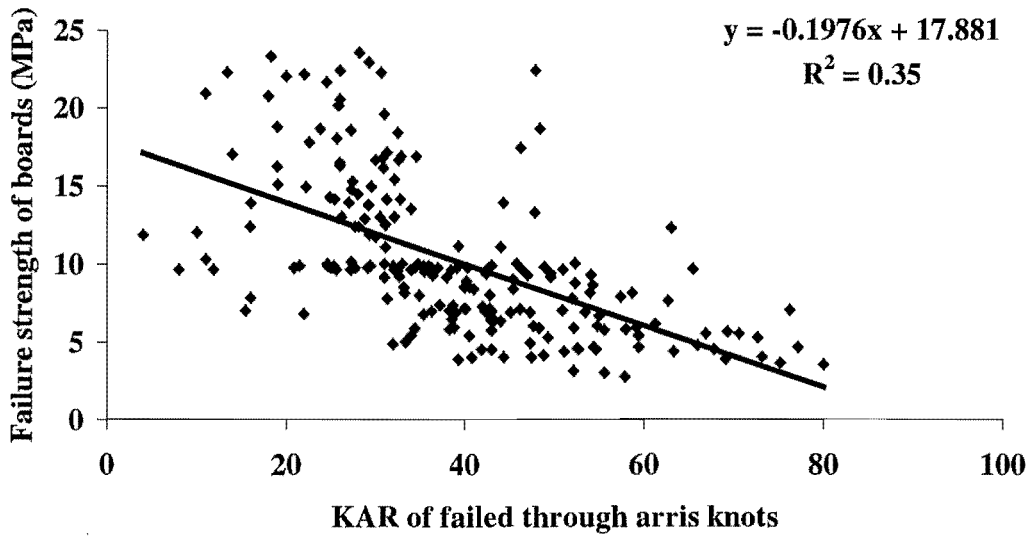

Fig. 6.15. The relationship between the failure strength and KAR of the failed through arris knots.

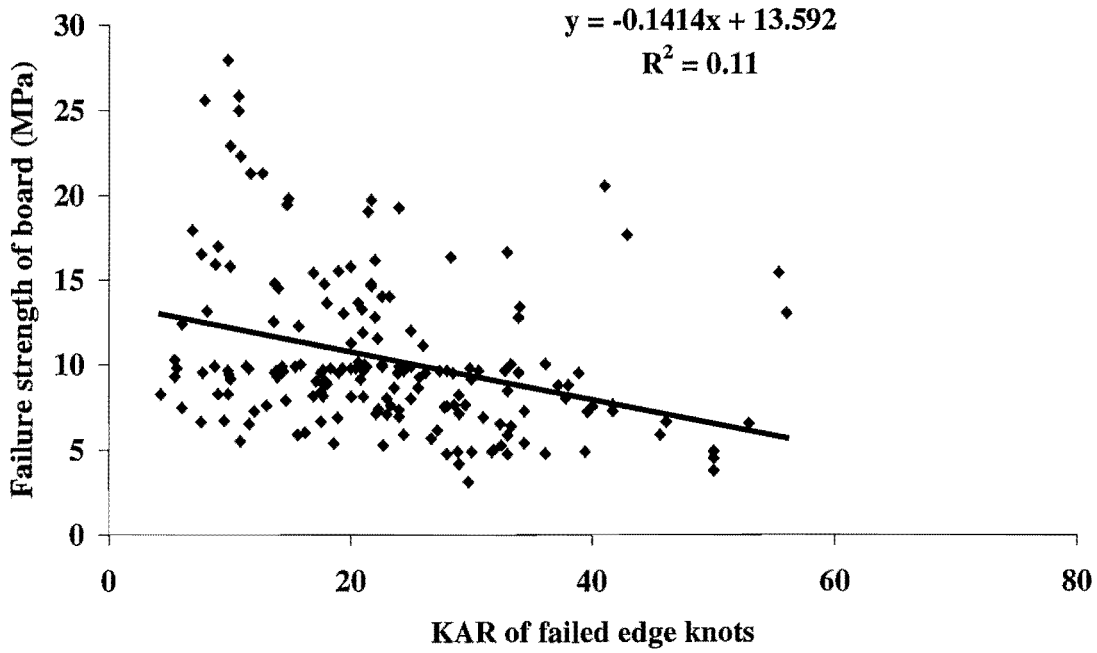

Fig. 6.16. The relationship between the failure strength and KAR of the failed edge knots.

6.3.3. Failure pattern of knots

This study found that the failure initiated at the knot before propagating to the adjacent clear wood when a board failed due to a single knot (Fig. 6.3, 6.4, 6.5, 6.9, 6.10 and Fig. 6.11). When a board failed due to a group of knots, the failure began at a particular knot (called the first broken knot), then the failure spread out to other knots or to adjacent clearwood zone (Fig. 6.17, 6.18).

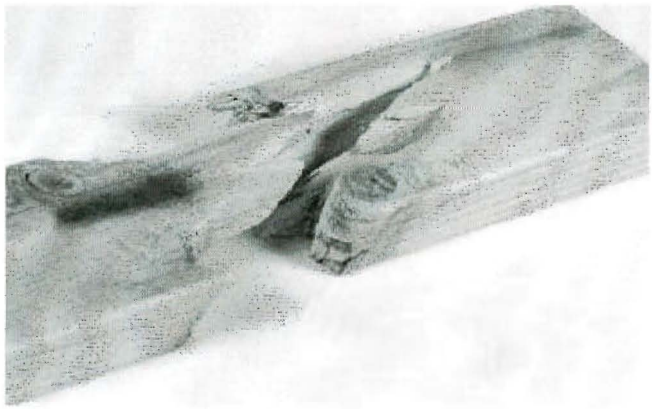

Fig. 6.17. Board failed due to group knots (boundary-broken pattern).

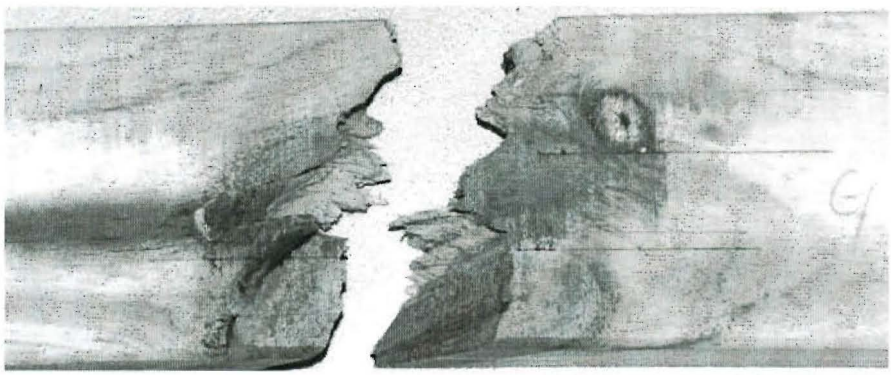

Fig. 6.18. Board failed due to group knots (plane-broken pattern).

Both the single knots and the group knots failed in the two major patterns, i.e. the boundary-broken and plane-broken pattern. Indeed in all 1,894 boards that broke due to knots, 64.5% of failures fitted the boundary-broken pattern; and 27.3% of failures fell

into the plane-broken pattern; only for 8.2% was the failure pattern hard to define (Table 6.2).

Table. 6.2. Frequency of different failure patterns

Knot type	Boundary-broken pattern	Plane-broken pattern	No obvious pattern
Margin knot	29.8% (564)	10.4% (197)	2.5% (47)
Group knot	20% (379)	9.9% (188)	3.5% (66)
Through arris knot	6.4% (122)	4.5% (85)	1.1% (21)
Edge knot	7.2% (136)	2.2% (42)	0.7% (14)
Through knot	1.0% (19)	0.2% (3)	0.3% (5)
Face knot	0.1% (2)	0.1% (2)	0.1% (2)
Total	64.5% (1222)	27.3% (517)	8.2% (155)

Note: the figures in bracket are number of failure boards in different failure patterns.

6.3.4. The influence of failure angle on the failure strength

This section shows the influence of failure angle on the failure strength according to their failure patterns. In the boundary-broken pattern, the failure angles ranging from 40 ~ 50° were observed frequently and were associated with the lowest average failure strength (Figures 6.19 ~ 6.21).

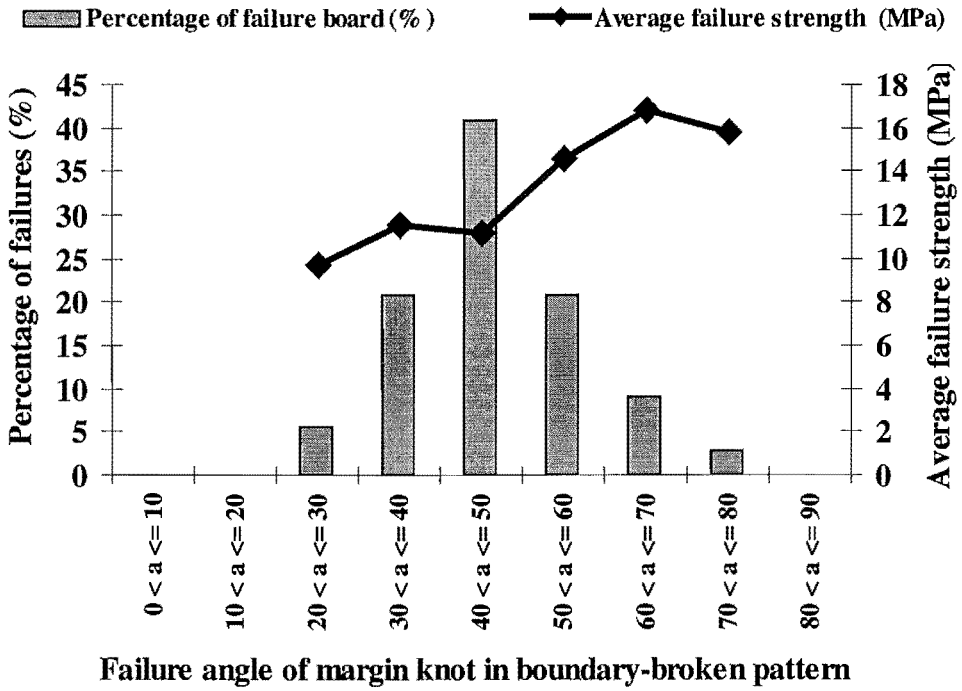

Fig. 6.19. The percentage of failures, the average failure strength, and the failure angle for margin knots in boundary-broken pattern.

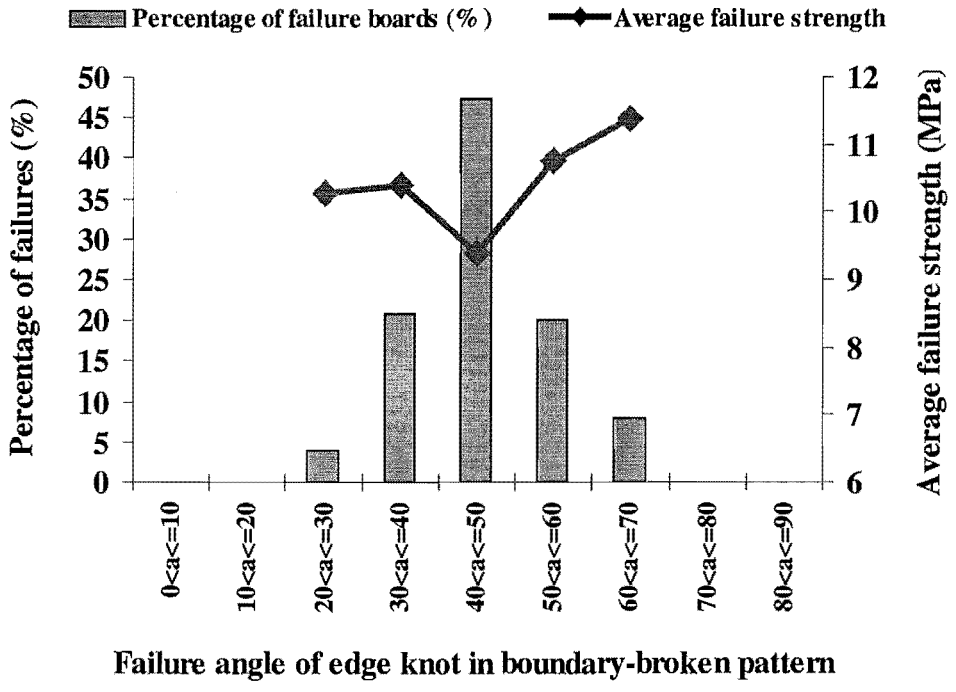

Fig. 6.20. The percentage of failures, the average failure strength, and the failure angle for edge knots in boundary-broken pattern.

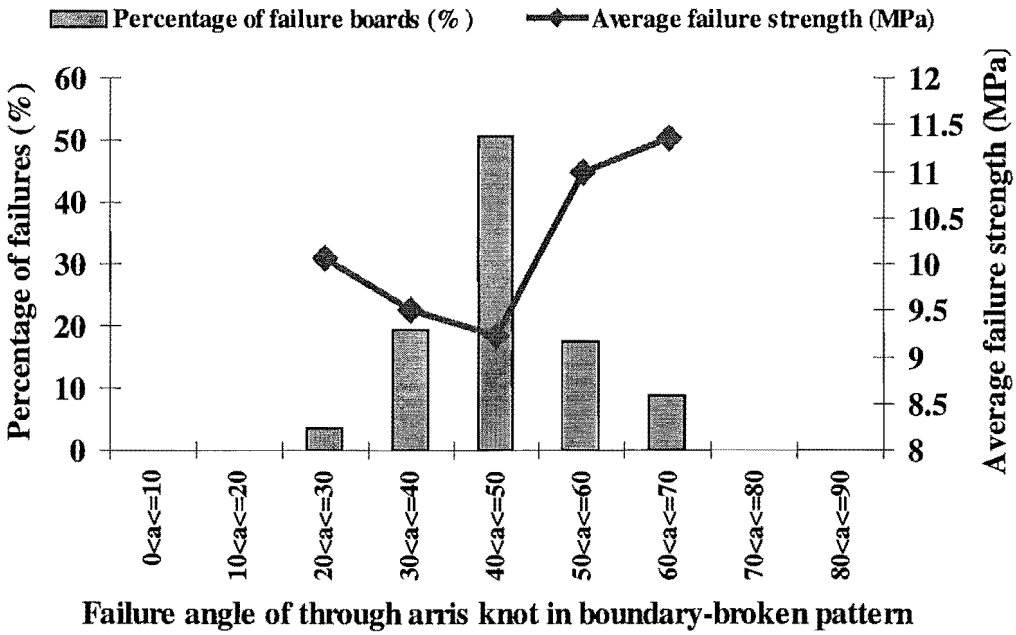

Fig. 6.21. The percentage of failures, the average failure strength, and the failure angle for through arris knots with the boundary-broken pattern.

When a board failed in the plane-broken pattern, the relationship of failure angle and the failure strength varies with the knot types. Most of margin knots broke with failure angles ranging from 40 ~ 50° and this angle range was also associated with the lowest average failure strength (Fig. 6.22). For the through arris knots, the failure angles ranging from 60 ~ 70° appeared frequently with the minimum average failure strength (Fig. 6.23). Among boards broken around edge knots, the weakest ones were associated with failure angles from 80 ~ 90° (Fig. 6.24).

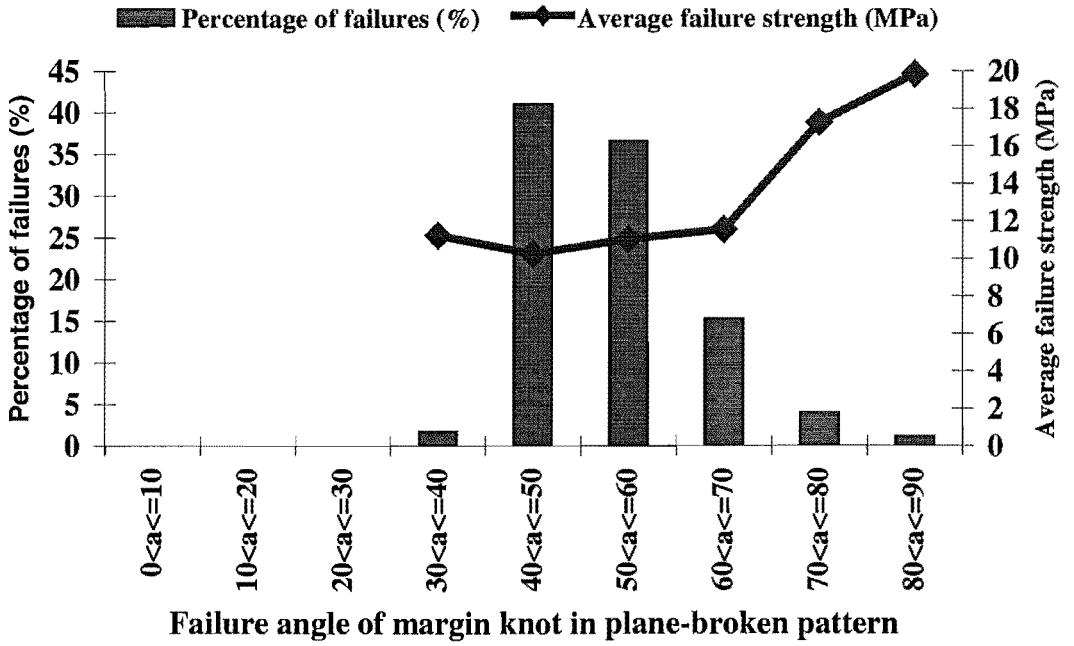

Fig. 6.22. The percentage of failures, the average failure strength, and the failure angle for margin knots with the plane-broken pattern.

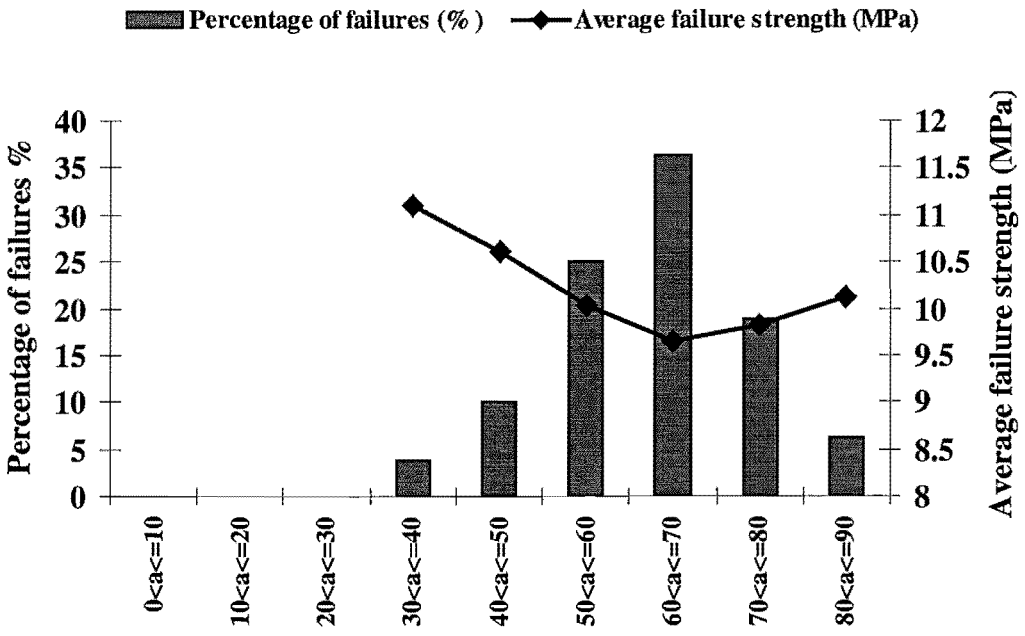

Fig. 6.23. The percentage of failures, the average failure strength, and the failure angle for through arris knots with the plane-broken pattern.

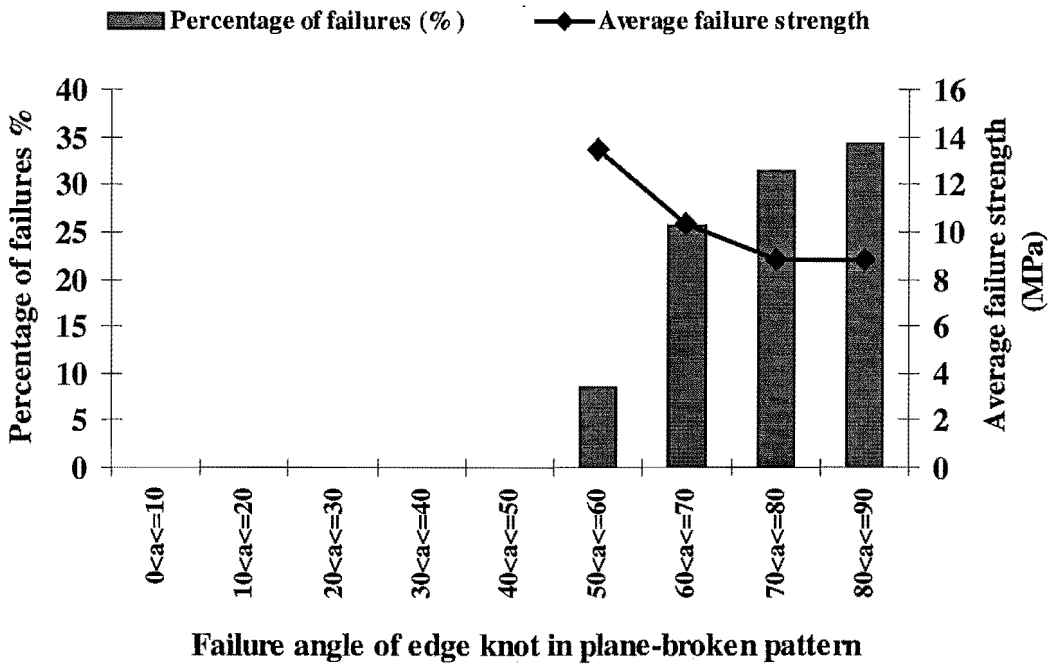

Fig. 6.24. The percentage of failures, the average failure strength, and the failure angle for edge knots with the plane-broken pattern.

6.4. DISCUSSION

Nearly 99% of the boards broke at a knot zone. Among these samples, 92% were categorized as either the boundary- or plane-broken pattern. The boundary-broken (along the interface surface between knot and stem wood) or plane-broken (failure plane containing the pith of the knot) around knots appear to be the two major failure modes of the structural timber in tension. The applicability of this conclusion to other softwoods or hardwoods would be subject to the validation.

A failure following either pattern depends on the stress first exceeding the strength at the boundary or the symmetrical plane of the knot. An encased knot is almost completely separated from the board due to the bark between the knot and the adjacent wood. In other words, the boundary of the encased knot is the weakest site of the knot. Therefore, the failure always propagates along the boundary of the encased knots, which forms the boundary-broken pattern of knot. For an intergrown knot, both boundary-broken and the plane-broken failure may occur. When an intergrown knot appears totally inside the cross-section, the knot itself may be tougher than the discontinuous grain boundary

where there is no severe interior or surface checks in the knot. In this case, the failure may have a boundary-broken patter. If an intergrown knot appears partially outside the cross section of the board, the failure may display a plane-broken pattern.

This study reveals that the plane-broken pattern generally crosses the symmetrical plane of the knot and always contains the pith of the knot. A possible explanation for the plane-broken is that it arises from the propagation of a drying check. Drying checks initiate in knots and very likely occur in the symmetrical planes of knots due to faster drying of knot wood, to far higher casehardening and to stress concentrations (Liu, 1998; Walker, 1993; Kininmonth, 1961). In tension, the failure within the knot itself may spread from the initial check by crossing the pith.

In the boundary-broken pattern, the lowest strength was always related to the failure angles from 40 to 50°. In the plane-broken pattern, the weakest margin knots broke at failure angles ranging from 40 ~ 50°; for the through arris and edge knots, failure angles ranging from 60 ~ 70° and 80 ~ 90° were found to be related to the lowest strength.

Among the 1,894 knot-broken boards, failures associating with face knots are only 0.3%. In this study, the length of boards is long enough to allow equal opportunity for all knot types to be present in boards. The 0.3% of failures at face knots evidently supports the view that the face knot is rarely broken. This provides useful information for visual grading.

Chapter 7

WARP IN RADIATA PINE STRUCTURAL TIMBER

7.1. INTRODUCTION

Wood shrinks during moisture desorption, once the moisture content is below fibre saturation point, i.e. at the point when wood cell walls are saturated with bound water but no free water remains in the cell cavities. The differential drying stresses due to the shrinkage and stiffness gradients lead to distortion (called warp) in timber (Siau, 1995, 1984, 1971; Walker, 1993; Nestic and Miler, 1991; Wiedenbeck *et. al.*, 1990; Forest Products Laboratory, USA. 1989; Talor, 1989; Skaar, 1988, 1972; Price and Koch, 1980; Hsu and Tang, 1975; Harris, 1961).

The characteristics of shrinkage in radiata pine have been well documented in the literature. The tangential, radial and volumetric shrinkage in radiata pine increase from the pith outwards. The longitudinal shrinkage is less than 0.5%, except for the corewood (Cown *et al.*, 1991a). In general, the tangential shrinkage of radiata pine is about twice as much as its radial shrinkage, and both the tangential and the radial shrinkage are much larger than the longitudinal shrinkage (Walker, 1993; Kinimonth and Whitehouse, 1991; Cown *et al.*, 1991a).

The shrinkage-induced warp denotes any deviation of a piece of lumber from a plane surface. Warp is classified into six typical forms including diamond, cup, bow, spring (or crook), twist and kink (ASTM, Designation: D9-87, 1995; Ministry of Forestry, New Zealand, 1995; U.S. Forest Products Laboratory, 1955).

- **Diamond** occurs when the square cross-section of a board distorts into a diamond shape; and a **cup** refers the rectangular cross-section of a board changing into a curved strip (ASTM, 1995; Walker, 1993). Both diamonding and cupping result from the difference between tangential and radial shrinkage (the tangential shrinkage is greater than the radial shrinkage). Diamond and cup in radiata pine is not very severe because the difference between tangential and radial shrinkage is small (about 2%)

(Kinimonth and Whitehouse, 1991). Thus the diamonding and the cupping are excluded in this investigation.

- **Bow** is the lengthwise bending of the wide surfaces in a board (Fig. 7.1), while the lengthwise bending of the edge surfaces in a board is defined as **spring** (or **crook**) (Fig. 7.2). Bow and spring are caused by the gradients in longitudinal shrinkage and stiffness (Dahlblom *et al.*, 1994; Kinimonth and Whitehouse, 1991; Hallock and Malcolm, 1972; King, 1954; Cockrell, 1943, 1949).

- **Twist** is defined in terms of the rise of the fourth corner of a surface or a spiral distortion of a board (Fig. 7.3). The twist is normally associated with **spiral grain**, i.e. the angular alignment of the tracheids to the stem axis (Balodis, 1972; Haslett *et al.*, 1991).

- A **kink** is a local distortion associated with a knot or knots and may consist of cup, bow, spring or their combination (Fig. 7.4). The kink in radiata pine may be more serious than that in other species because the knot size of radiata pine is comparatively larger than that in other species (Kinimonth and Whitehouse, 1991).

The bow, spring, twist and the kink are illustrated in Figures 7.1, 7.2, 7.3 and 7.4 respectively.

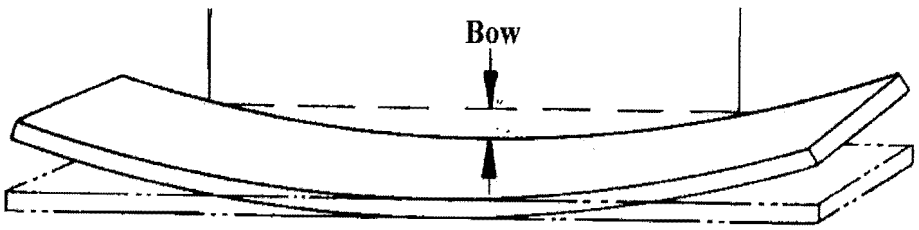

Fig. 7.1. Illustration of bow (after BS 4978:1988).

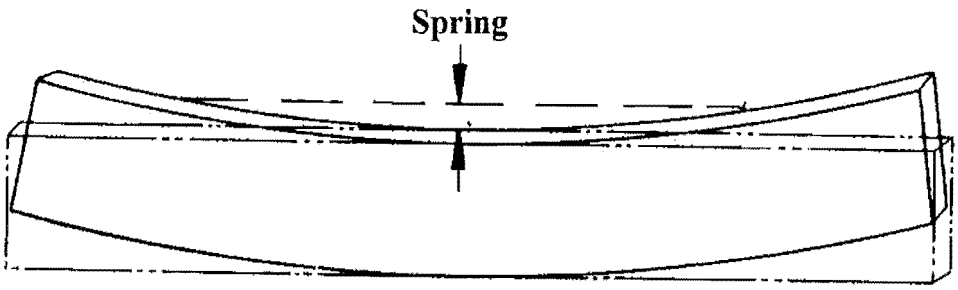

Fig. 7.2. Illustration of spring (crook) (after BS 4978:1988).

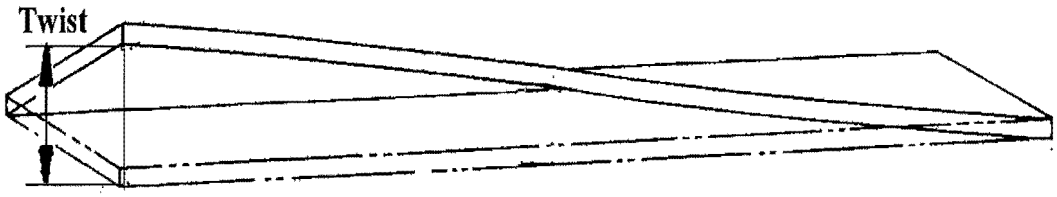

Fig. 7.3. Illustration of twist (after BS 4978:1988).

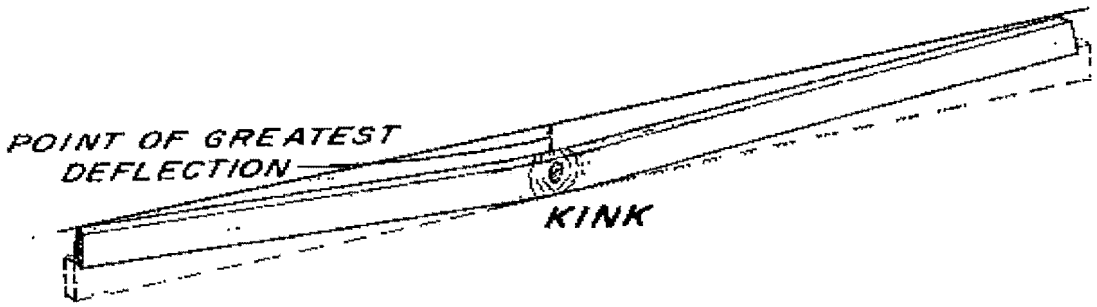

Fig. 7.4. Illustration of kink (after Forest Products Laboratory, USA., 1989).

Warp results in degrade, wastage and rejection of structural timber, and hence a major annual loss to sawmills (Walker, 1993). Unfortunately, the detailed information related to the warp of radiata pine is limited, though the literature regarding the shrinkage is rich. To extend knowledge regarding log quality in terms of warp, this study targeted the average warp profile within stems from butt to upper top log and within logs from the pith to cambium.

The intention of this study is to derive a three-dimensional warp map of bow, spring, and twist within a typical pine stem. Also the influence of knots and spiral grain on warp is investigated. In all tested boards, this study found that: 70% bow and 40% spring did not occur at the half-length location of the board. This deviation from the mid-point is often associated with the knots. The cause of this phenomenon has not been appreciated due to lack of comparably information in clear boards. In other words, we do not know whether the knot is only origin of this phenomenon. Further investigation is proposed for the future. Spiral grain has been shown as the cause of twist (Forsberg and Warensjö, 1999; Perstorper *et. al.*, 1995; Haslett *et. al.*, 1991; Balodis, 1972). This study found that the twist increases with the increase of the spiral grain angle. However, the values of the twist reported here do not correlate well with spiral grain, probably the twist is also affected by other factors. The current study also examined a formula estimating the twist over a given length with respect to the twist in the full-length boards. Unfortunately, the formula proposed by Simpson and Shelly (2000) is not supported by the experimental date of this study because the real warp in the board is more complex than the presumptions of the formula.

The material and experimental methods are introduced in section 7.2. Section 7.3 displays and discusses the experimental results. A final summary is given in section 7.4.

7.2. MATERIALS AND METHODS

7.2.1. Samples and sampling size

1,919 machine stress graded boards, 90 × 35 × 4,200 mm, from 62 radiata pine trees were used to evaluate the variations in warp. The processing of these boards is covered in chapters 2 and 3. The sample size (1919) used for warp studies was less than total number of the boards (1988) that were machine stress graded, because 69 boards broke during the machine stress grading due to big knots. After machine stress grading, the location of every board in the logs was confirmed by rebuilding each log. Then all dried boards were left to equilibrate to the equilibrium moisture content (about 12%).

7.2.2 Methods for measuring warp

Once at the equilibrium moisture content (about 12%), the warp of each board was measured on an aluminum L-plate mounted on a wooden worktable. The aluminum surface was an extruded L-plate that was leveled and calibrated to insure a deviation of less than 0.1mm along its 5.0 meter length.

The bow of each board was measured as the maximum distance between the aluminium reference-plane and the lower surface of the curved sample as shown in Figure 7.5. Note that the bow does not always occur at the mid-point of the member, and the number of boards whose bow did not occur at the mid-span was recorded in this study. The cause of bow occurring off the mid-point has not received adequate consideration although this study observed that this phenomenon often accompanied the knot or the knot appeared in the adjacent zone.

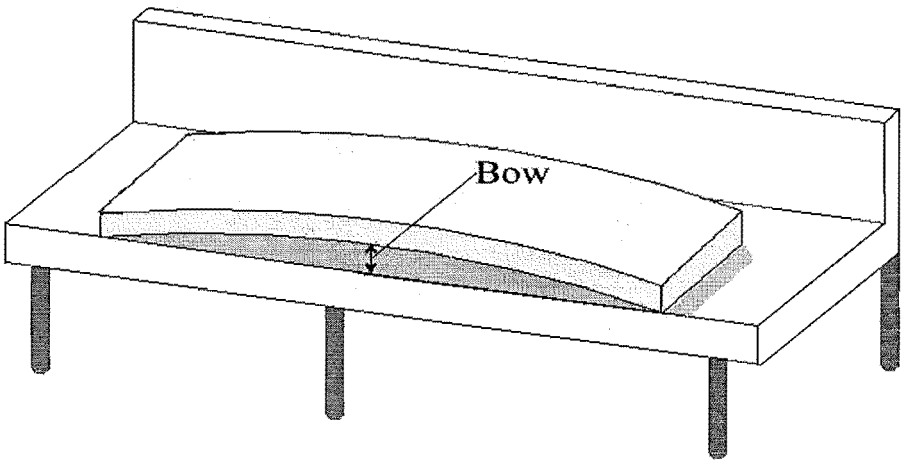

Fig. 7.5. The measurement of bow.

To measure spring, the ends of the concaved edge of the sample touched the edge plane of the worktable and the maximum distance between the edge of the board and the edge of the reference plate was the spring (Fig. 7.6). As with measuring bow, the number of boards whose maximum spring did not occur at the mid-span was recorded.

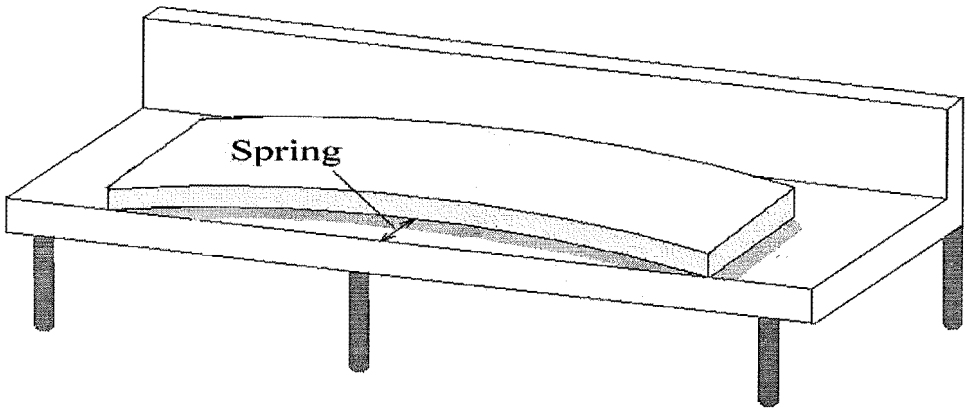

Fig. 7.6. The measurement of spring.

Two readings of twist were taken, from the full- and half-length of each sample, in order to investigate the influence of length on the twist. By placing each piece on the reference plane and fixing one end with a G-clamp, the rises at the other free-end and at the half-length points were measured as the full- and half-length twists. Sometimes both corners at the free-end rose above the reference plane, then the difference between the two values was taken as the full-length twist. This method was also applied to the half-length twist (Fig. 7.7).

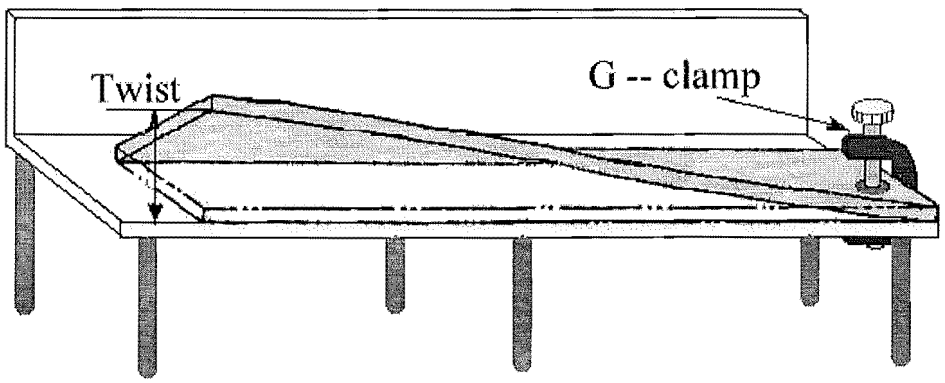

Fig. 7.7. The measurement of twist.

The spiral grain angle for each board was measured in a clear wood zone using a protractor. The measuring method depended on the saw pattern of the board, which are described as below.

- **Measurement of spiral grain on flat sawn board**

The wide surface of the board is the measuring surface for spiral grain when the board is flat sawn. First, a baseline is drawn parallel to the longitudinal direction of the board, i.e. the longitudinal direction of the tree, on the board face, and then the deviation of the grain from this baseline is the spiral grain angle (Fig. 7.8).

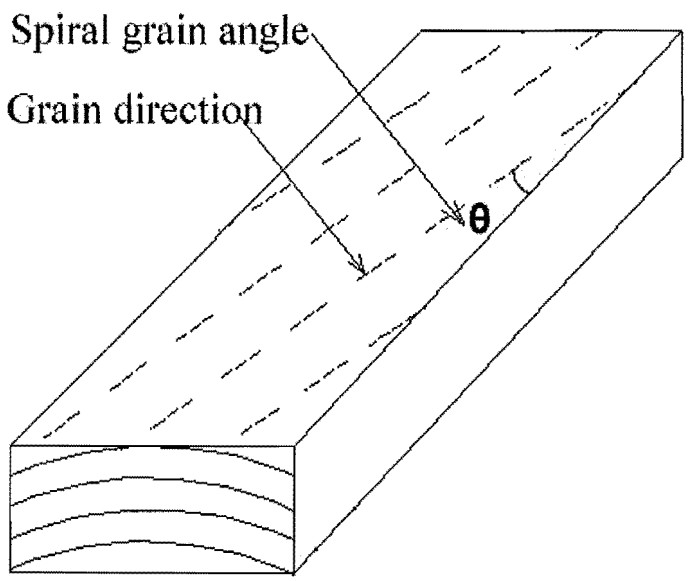

Fig. 7.8. Measurement of spiral grain angle in flat-sawn boards.

- **Measurement of spiral grain on quarter sawn board**

When board is quarter sawn, the measuring surface for the spiral grain angle is the edge of the board. On the edge face, a baseline is drawn parallel to the longitudinal direction and the angle between the grain and this straight line is the spiral grain angle (Fig. 7.9).

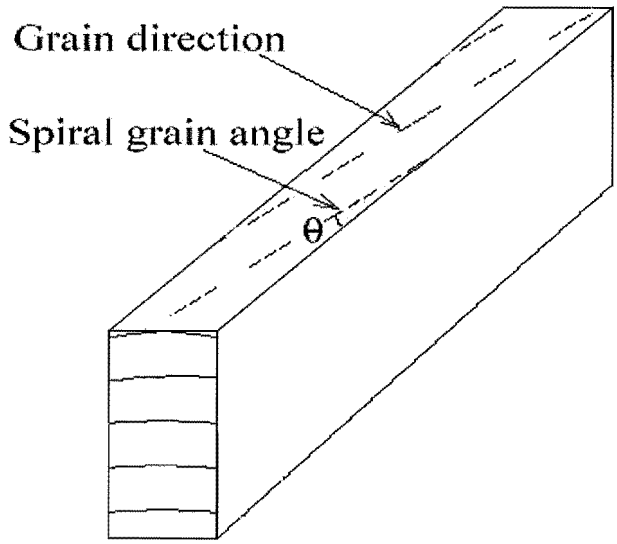

Fig. 7.9. Measurement of spiral grain angle in quarter-sawn board.

- **Measurement of spiral grain angle in mixed sawn board**

When end faces of a board are neither tangential nor radial, the saw pattern of the board is called mixed sawn. In this case, the true spiral grain angle is derived from the combined effect of grain deviation on both the face and the edge surfaces of the board. The spiral grain angle of mixed sawn board can be calculated from the Equation (7.5).

As shown in Figure 7.10, the true spiral grain angle is ∠BOD. This angle can be determined once the angles ∠AOB and ∠BOC have been measured. From the right-angled triangles ΔABO, ΔBCO and ΔBDO, we find:

$$\tan(\angle BOD) = BD/BO = \frac{\sqrt{AB^2 + BC^2}}{BO} \quad (7.1)$$

$$AB = OB \tan(\angle AOB) \quad (7.2)$$

$$BC = OB \tan(\angle BOC) \quad (7.3)$$

Substituting Equations (7.2) and (7.3) in (7.1), the tangent of the spiral grain angle for mixted sawn board will be expressed as

$$\tan(\angle \text{BOD}) = \sqrt{\tan^2(\angle AOB) + \tan^2(\angle BOC)} \qquad (7.4)$$

thus

$$\angle \text{BOD} = \tan^{-1} \sqrt{\tan^2(\angle AOB) + \tan^2(\angle BOC)} \qquad (7.5)$$

Hence, the spiral grain angle can be calculated from the grain angles on face and edge surfaces.

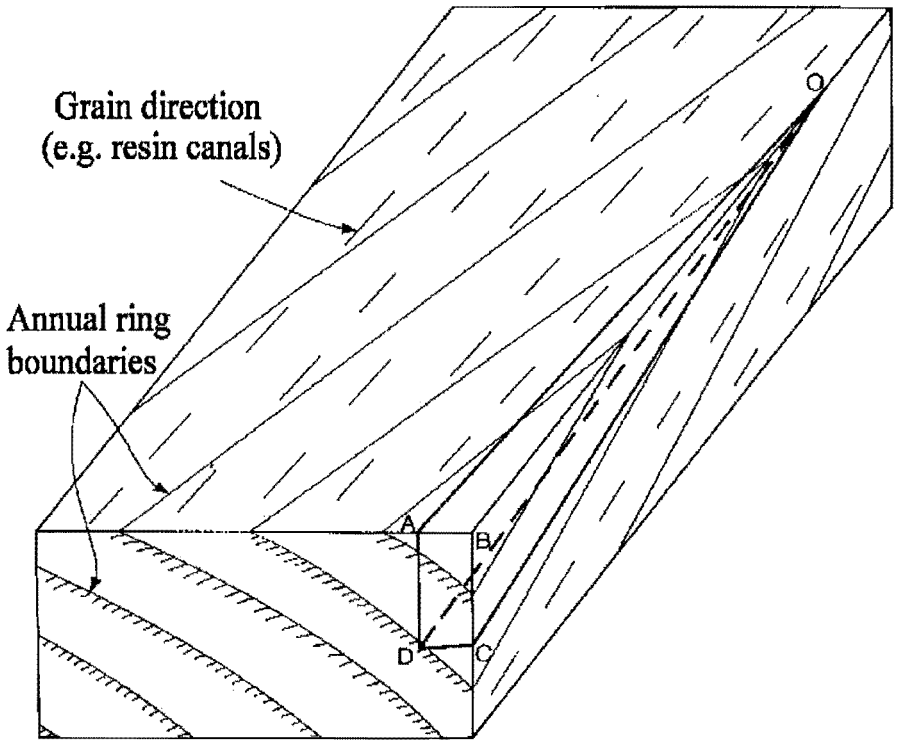

Fig. 7.10. Measurement of the spiral grain angle in mixed-sawn board (after Harris, 1989).

7.3. Experimental results and discussion

This section presents warp maps within radiata pine stems, including variations in average bow, spring and twist up the stem; the variation of average bow, spring and twist within the logs according to radial distance from the pith; and the effects of spiral

grain and board length on twist. A brief discussion about the likely causes of warp in structural timber is given on the basis of the experimental observations.

7.3.1. Variations in average bow, spring and twist up the stem according to log types

The average values for bow and spring both decrease significantly up the stem for the first three logs. Then the average values for bow and spring change little between the top and upper top logs (Fig. 7.11). The worst bow and spring occur in the butt logs with average value of 4.80 mm and 7.40 mm respectively.

The average value for twist increases noticeably with the height up the stem from the butt log to the upper top log (Fig. 7.12). The most severe twist is in the upper top logs where the average value is 10.36 mm.

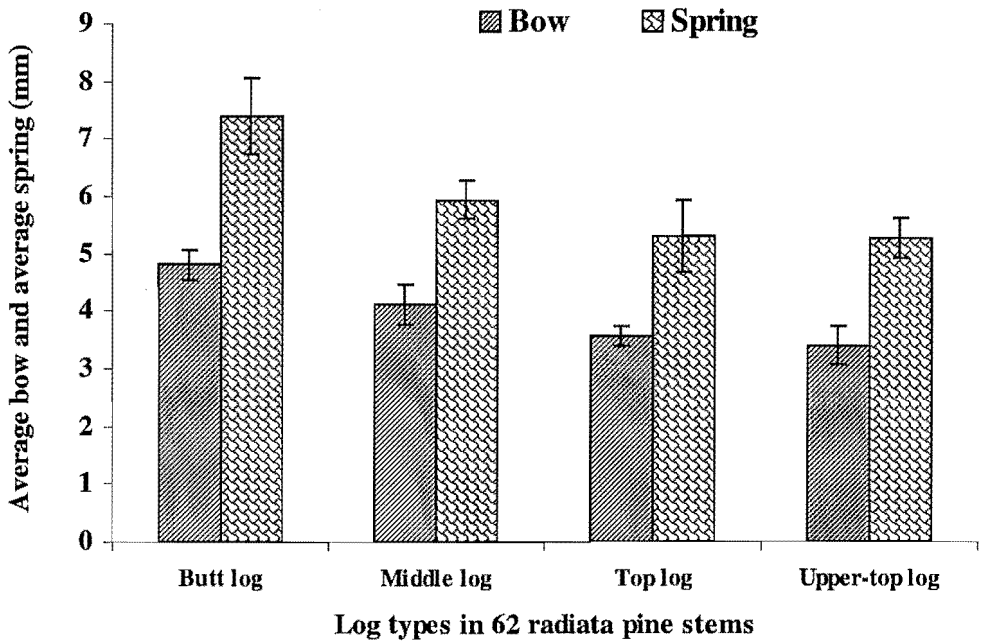

Fig. 7.11. Variations of the average bow and spring in different log types.

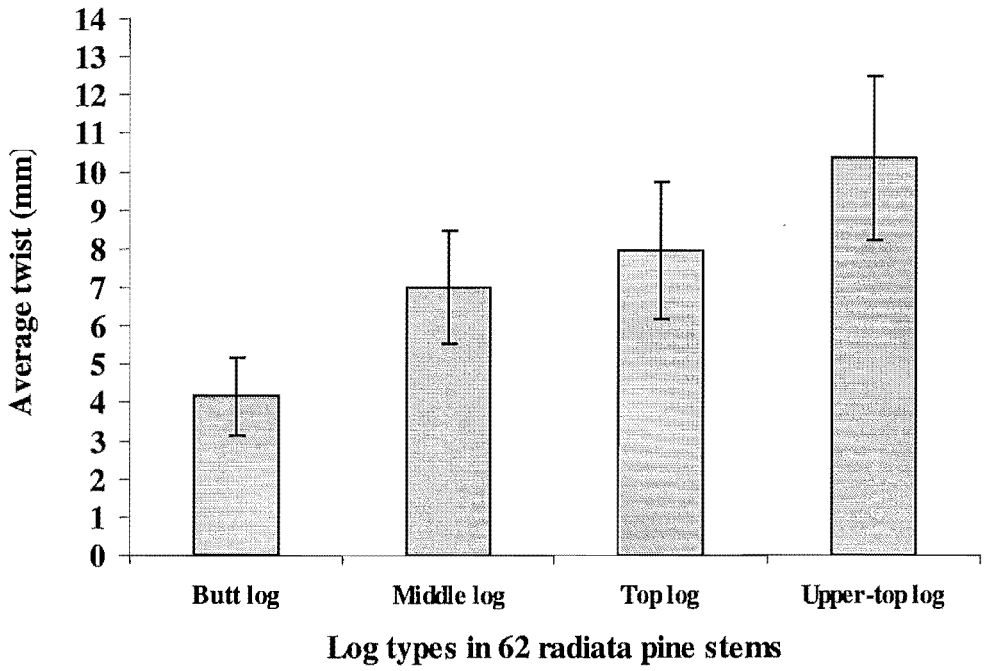

Fig. 7.12. Variations of the average twist in different log types.

7.3.2. Variations of average bow, spring and twist within log types according to the distance from the pith

These experimental observations indicate that in 1348 (70.2%) out of all 1919 boards the maximum bow occur away from the mid-point along the board, and this phenomenon often accompanies margin knots (sometimes in large group knots) or takes place in an adjacent zone of these large knot. The cause of this phenomenon has not been understood well. A likely explanation may be the variation of the diameters in margin knot along the thickness of the board. During moisture desorption, the varying orientation of the grain and so the lateral shrinkage around margin knots would induce longitudinal tensile stresses in the board with a longitudinal shrinkage gradient from one face to the opposite face. This stress gradient imposes a lengthwise bending in the wide faces i.e. bowing. These knots are randomly located along the length of the board and thus causing maximum bow to occur at some point rather than the mid-span.

This study first considers the variation in average bow with the radial distance from pith in different log types. In cross-section, the average bow in the middle and top logs increases with the radial distance from the pith to cambium. However, the average value

of bow does not show any obvious distribution pattern in the butt and upper top logs (Table 7.1). Knots are suspected to be responsible to such an irregular distribution. However, the information in Table 7.1 is not sufficiently conclusive to develop new hypotheses. Therefore, this study suggests that a further research should be developed in the future to explore the influence of knot size, type and number on warp, which may give more detailed evidence for a reasonable hypothesis.

Table 7.1. Average bow within log types according to distance from the pith.

Location from the pith	P1	P2	P3	P4	P5
Av. bow in upper top log (mm)	2.67	4.01	2.81		
Av. bow in top log (mm)	3.14	3.43	4.11		
Av. bow in middle log (mm)	3.29	3.90	4.78	5.22	
Av. bow in butt log (mm)	5.58	4.60	4.92	4.19	3.95
Av. bow in all logs (mm)	3.76	4.00	4.56	4.51	3.95

Large edge knots and group knots located on the edge may be responsible for maximum spring not occurring at the mid-point in 769 (40.1%) out of all 1919 boards. The drying stress gradient due to the diameter change of an edge knot or group knots located in the edge zone is along the width of the board, which leads to a lengthwise bending of edge surface i.e. spring. Compared to bow, spring due to kinking is less severe. The possible explanation is lower frequency of the edge knots in all tested boards (only about 10.5%) (Chapter 6).

In cross-section of the stems, the average spring decreased with the radial distance from the pith. The maximum reduction of the average spring occurred from the pith (position 1) to position 2. Thereafter, the further decreases of the average spring were insignificant. Only one exception was found at position 4 of the middle logs, at where the average spring increased a small amount (0.85 mm) from adjacent wood zone (position 3) (Table 7.2).

Table 7.2. Average spring within log types according to distance from the pith.

Location from the pith	P1	P2	P3	P4	P5
Av. spring in upper top log (mm)	6.12	4.99	4.25		
Av. spring in top log (mm)	7.51	4.55	4.49		
Av. spring in middle log (mm)	7.35	5.47	5.46	6.31	
Av. spring in butt log (mm)	10.55	7.04	6.54	6.30	6.09
Av. spring in all logs (mm)	8.03	5.59	5.58	6.30	6.09

The pattern for distribution of twist in the radial direction is fairly simple and clear. The average twist decreased with the radial distance from the pith. The maximum rate of reduction in average twist was observed between the pith (position 1) and position 2 (Table 7.3).

Table 7.3. Average twist (in the full length of the board) within log types according to distance from the pith.

Location from the pith	P1	P2	P3	P4	P5
Av. twist in upper top log (mm)	15.7	8.08	5.16		
Av. twist in top log (mm)	14.1	6.86	4.39		
Av. twist in middle log (mm)	12.51	6.65	4.33	3.74	
Av. twist in butt log (mm)	8.59	3.74	2.95	2.73	1.45
Av. twist in all logs (mm)	12.47	6.14	3.86	3.04	1.45

7.3.3. Influence of spiral grain angle on twist

Haslett *et al.* (1991) reported that the mean spiral grain angle increased up the stem of radiata pine, typically from an average of 2° at 0 m to 6° at 16 m; and this increase brought an increase in twist. Cown *et al.* (1991b) stated that the spiral grain angle of 25-year-old radiata pine stems increased significantly from butt to 6 m level; and the increase was insignificant above the 6 m level. In agreement with the work of Cown, the average spiral grain angle in this study was found to increase with the height up the stem from the butt log to middle log. Thereafter, there was not any noticeable change up the stem (Table 7.4).

In this study, the average twist was found to increase with an increase in the spiral grain angle along the vertical direction. However, average twist did not always vary regularly with the spiral grain angle. There was a large increase in average twist associated with

only a slight rise in the average spiral grain angle from top log to upper top log. This implies that the twist is affected by other factors as well.

Table 7.4. Average twist within 62 radiata pine stems according to log types.

Log type	Spiral grain angle (degree °)	Twist (mm)
Upper top	5.44	10.36
Top	5.36	7.94
Middle	5.26	7.00
Butt	4.44	4.16

7.3.4. Influence of board length on the average twist

Simpson and Shelly (2000) suggested estimating the twist at a given length by the twist of the full length, using the relationship of similar triangles (Fig. 7.13):

$$t_1 = t_2 \frac{L_1}{L_2} \tag{7.6}$$

where

t_1 and t_2 are the amounts of twist at board lengths L_1 and L_2 respectively;

L_1 and L_2 are the board lengths.

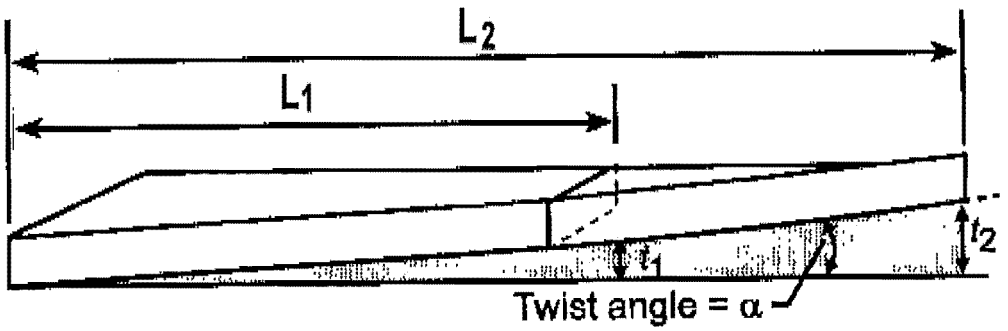

Fig. 7.13. Estimating the twist at a given length by the twist in full length board (after Simpson and Shelly, 2000).

Equation (7.6) assumes that the axis of the twisted board is a straight line. This presupposition is only true in a pure-twist board. However, in practice, spring, bow and twist often occur in same board. In other words, the real board axis generally diverges from a straight line due to spring and bow in the board. In addition, the length effect of structural timber also leads to the errors when applying equation (7.6), since a longer board contains more natural defects and consequently the probability of severer bow and spring. The following experimental data demonstrates the degree to which Simpson and Shelly's (2000) equations falls short of perfection.

The twist at full-length should be twice as great as that at half-length according to Simpson and Shelly's (2000) equation (7.6). The data of the half-length twist (actual experimental data at half-length) and half of the full-length twist are listed in Table 7.5. The large average absolute errors indicates that Equation (7.6) may be inapplicable for practical use.

Table 7.5. Errors between measured twist and estimated twist at the half-length of boards.

Log types in stem	Board location	Av. twist at half-length location (mm)	Half of the average full-length twist (mm)	Av. absolute error (mm)
Upper top log	P1	8.44	7.85	0.59
	P2	4.26	4.04	0.22
	P3	2.31	2.58	0.27
Top log	P1	7.21	7.05	0.16
	P2	3.31	3.43	0.12
	P3	2.28	2.2	0.08
Middle log	P1	6.49	6.26	0.23
	P2	3.27	3.33	0.06
	P3	2.12	2.17	0.05
	P4	1.88	1.87	0.01
Butt log	P1	4.63	4.3	0.33
	P2	2.14	1.87	0.27
	P3	1.65	1.48	0.17
	P4	1.53	1.36	0.17
	P5	0.93	0.72	0.21

7.4. SUMMARY

Average warp profiles, arising from bow, spring, twist and kinking, in radiata pine were investigated, in order to address their significance effects on the industrial profit and the lack of other systematic studies.

In the vertical direction, bow and spring decrease with height up the stem. Butt logs display the worst values for bow and spring, whereas twist increases with the height of stem. The rate of change in twist does not always correspond exactly with that of spiral grain angle, which implies that there may be other factors playing important roles.

In the radial direction, twist and spring decline from the pith. The only exception for spring is at position 4 of the middle logs. Bow is a more variable in the radial direction: the average value increases from the pith to cambium in middle and top logs, and varies irregular in butt and upper-top logs. This behavior might be explained by difference in longitudinal shrinkage across the thickness direction within individual boards due to the localised effects of a large knot or knot cluster.

Kinking may be a contributing factor for 70% of all maximum bow and 40 % of all maximum spring occurring at some distance from the expected mid-span. For bow, kinking is often associated with margin knots; while edge knots mainly cause kinking in spring. According to general warp theory, differences in longitudinal shrinkage and stiffness are the causes of bow and spring – and this can occur in clear, knot-free board. This study concludes that margin knots may create the additional localized bowing in structural timber, while edge knots may create additional localized spring. Radiata pine, as a fast growth species, displays more severe warp compared to many other species due to the presence of very large knots in the stem wood. Therefore, eliminating the negative influence of knots on the wood quality should be emphasized in the further research.

Chapter 8

OVERALL SUMMARY AND RECOMMENDATION

This study focused on the investigations of stiffness, strength and warp as well as the effects of knots on the mechanical properties and stability in radiata pine. The results of this study give detailed timber quality maps in terms of stiffness, strength and warp, which provides useful information for the increase of log value, non-destructive estimation of timber strength and genetic selection.

Sixty-two radiata pine trees from a 27-years old, unpruned, single plantation were used for this study. These trees were cut to give butt, middle, top and upper top logs, and the log diameters were measured to estimate the merchantable volumes of logs. 1,988 boards from these logs were kiln-dried and dressed to 90 × 35 × 4,200 mm for machine stress grading. Throughout the process, the identities of individual logs and boards were kept by tagging them. The location of each board in the logs was confirmed by reassembling each log after machine stress grading. Moisture contents (about 12%) of boards were in equilibrium with the environment before measuring warp. The timber specimens were tensile tested to get the ultimate tensile strength (UTS). After testing destructively, the failure features of the weakest point were studied in detail.

This chapter comments the experimental results of this study. On the basis of the experimental facts, conclusions are drawn and the ideas for future research are proposed as follows.

8.1. MAIN CONCLUSIONS AND RECOMMENDATION REGARDING THE STIFFNESS AND STRENGTH OF RADIATA PINE STRUCTURAL TIMBER

Regarding the stiffness and the strength of radiata pine structural timber, the main results of this study and the objectives for the future research are described below.

1) Log volume is not a potential predictor of log stiffness

The average log volumes for different log types are presented in Chapter 2, and the relationship between the log volume and the log stiffness is displayed in Chapter 3. This study found that most cross-sections of radiata pine logs were best approximated as ellipses, especially in butt logs. Considering the ends shape and the taper of radiata pine stems, this study used a formula for a truncated elliptical cone or a formula of the truncated circular cone instead of a formula for a cylinder to calculate the log volume. On the basis of the experimental facts, the log volume is not considered as a reliable indicator of log stiffness due to the poor correlation between them as analysed in Chapter 3 (Fig. 3.9, 3.10). It means that, under same growth conditions (same harvesting age, same growth environment), fast growth is not at the expense of reduction of stiffness. This is quite encouraging for genetic selection.

2) Butt logs are problem logs due to the lowest stiffness

Compared with other log types, butt logs are problem logs due to the lowest average stiffness in all wood zones. Chapter 3 exhibits a detailed timber quality map in terms of stiffness, including the mean stiffness in different log types according to the radial distance from the pith (Table 3.1); the variation of local average stiffness at 152 mm intervals over stems (Fig. 3.6); and local average stiffness varies with respect to the mean stiffness of the stem (Fig. 3.7). All experimental results show that the lowest average stiffness exist in the all wood zones in the butt logs. The part from groundline up to 2.4 m or 2.7 m is particularly emphasized in this thesis because of the presence of very low local average stiffness. These very low local average stiffnesses should be attributed to the high microfibril angle located predominantly in butt log. Therefore, this study suggests leaving the base 2.4 m or 2.7 m for other end-uses rather than for construction, then the value of remaining part of the traditional butt log can be increased.

3) Boxed-pith timber is a challenge for forestry industry

The boxed-pith boards (boards cut in P1) have the lowest stiffnesses and strengths, maximum springs and twists in all wood zones for all log types, which are shown in Table 3.1, 7.2, 7.3 and Fig. 4.7. Isolating the least-stiff 20% of logs into a different log category, the value of the remaining logs can be raised (Fig. 3.8). This method would increase the average stiffness of boxed-pith board in all remaining log types. Unfortunately, the highest average stiffness value of the boxed-pith boards in the remaining log types is still less than the boundary stiffness value of F5 structural grade (6.9 GPa), even if the least-stiff 20% of logs have been removed. The challenge for the sawmill is to find appropriate uses for this poor quality tail.

4) Wood density alone may not reflect the mechanical properties of radiata pine structural timber

This thesis (Chapter 3 and Chapter 4) presents timber quality maps in terms of stiffness and strength. In the vertical direction, butt logs have the lowest average stiffness, and the middle logs rather than butt logs exhibits the highest average strength. In cross-section, the average strengths of the boards do not always increase with the radial distance from the pith. These strength profiles do not match the typical density map (wood density in radiata pine increases with the radial distance from the pith and decreases with the height up the stem). It means that wood density may not reflect the mechanical properties of radiata pine, because: 1) the denser butt logs display the lowest stiffness among all log types; 2) the denser butt logs are not the strongest logs; 3) the average strengths do not always increase from pith. Further investigation about the relationship between wood density, stiffness and strength in structural timber is proposed. In this study, small clear wood samples have been cut from the zone adjacent to the failure point in each board for measuring wood density in the future studies.

5) Non-destructive estimation of strength at the weakest point in structural timber is possible

Estimating the failure strength at the weakest point of a board includes two aspects: non-destructive estimating the failure strength value at the weakest point as stated in Chapter 5, and identifying the weakest point of the board as reported in Chapter 6. This study concludes that: compared with other variables, the local stiffness at the failure point best indicates the strength value at the weakest point of each board due to the strong correlation; while the features of knots are key indicators for determining the location of the weakest point because nearly 99% of the boards broke at a knot zone. In other words, one may estimate the weakest point of a board from the features of knots, then the failure strength according to the quantitative relationship between the failure strength and the local stiffness at that point.

The failure features of knots were revealed using these approaches: the failure frequency of different knots types, failure patterns and the failure angles. The experimental discoveries are listed below:

- the margin knots displayed the highest failure frequency (42.7%) in all knot types, and only an insignificant number of the face knots are involved (0.3%) (Table 6.1).
- most of the group knots failed in corewood (boards located in P1 and P2) (Table 6.1).
- failed knots in tension displayed two broken patterns, i.e. boundary-broken pattern and plane-broken pattern. The failure frequency in boundary-broken was much higher than that in plane-broken pattern (Table 6.2).
- boundary-broken pattern was the main failure form for encased knots due to the bark separating the knot wood and the adjacent wood. In other words, the boundary of the encased knot is the weakest site of the knot.
- in the boundary-broken pattern, the failure angle range ($40\sim50^0$) appeared frequently and was always associated with the lowest average failure strength. In the plane-broken pattern, the failure angle range associated with the lowest average failure strength varies with the knot types. For margin knots, the angle ranged between 40 ~ 50^o. For through arris knots, the angles ranging between 60 ~ 70^o appeared

frequently with the minimum average failure strength, whereas the lowest average failure strength corresponded with a failure angles from 80 ~ 90° in edge knots.

These three failure features have been confirmed in these tests of radiata pine, which give an insight for estimating the weakest point in radiata pine structural timber and provide useful information for visual grading. The applicability of these physical models for hardwoods or other softwood needs validation.

8.2. MAIN CONCLUSIONS AND DISCUSSIONS REGARDING THE STABILITY OF RADIATA PINE STRUCTURAL TIMBER

This section presents the variations of warp in radiata pine. As a possible element affecting the stability of timber, the influence of knots should be investigated more intensively in the future.

1) Twist varies as a reversed way with spring and bow in vertical direction

Chapter 7 describes a warp variation for radiata pine. Along the vertical direction, the average bow and spring both decreased with the height of the stem, and the butt logs had the worst bow and spring; average twist varied in a reversed way, i.e. increasing with the height of the stem and the most severe twist occurring at the upper top logs (Fig. 7.11, 7.12).

2) Knots may be responsible for irregular warp

Chapter 7 presents a variation of warp with the radial distance from the pith. In the cross-section of the stems, the average twist and spring decreased with the radial distance from the pith in all log types, and only one exception of spring was found at position 4 in the middle logs (Table 7.2, 7.3). However, the average value of bow did not show any obvious distribution pattern in butt and upper top logs (Table 7.1). The information obtained in this study is not sufficient to explain this behavior of bow. Two factors are suspected to responsible for such an irregular distribution.

- The diameter variation of margin knots in the thickness direction of board may cause extra bow, and this extra bow distributed unevenly due to the irregular appearance of margin knots on the boards.
- In retrospect detailed control of the kiln-drying schedule accompanied by regular inspection should have been a pre-requisite for this study. However, drying was undertaken at the TITC (Timber Industrial Training Centre), Rotorua, with no supervision from Canterbury.

Therefore, this study recommends that a further research should be conducted to explore the influence of knot size, type and number on warp, to obtain more detailed evidences for a reasonable hypothesis.

Chapter 7 also shows that: 70.2% of maximum bow and 40.1% of maximum spring did not occur at the mid-point of board; and for bow this phenomenon often accompanied with the margin knots, for spring this phenomenon was frequently associated with edge knots. The cause of this phenomenon has not been understood well. A likely explanation is the disturbance of knots. The lateral longitudinal shrinkage around a knot produces a longitudinal contraction in the board and sometimes leads to the maximum deflection in the vicinity of the knotty area. The maximum deflections due to knots are rarely at the mid-span of the boards, since knots are randomly located along the length of the boards.

REFERENCES

Addis Tsehaye. 1995. Within-and between-tree variations in the wood quality of radiata pine. PhD thesis, University of Canterbury, New Zealand

Addis, T., A. H. Buchanan and J. C. F. Walker. 1995. Stiffness and tensile strength variation within and between radiata pine trees. Journal of the Institute of Wood Science. 13 (5): 513 -518

Addis, T., A. H. Buchanan and J. Cha. 1998. Effects of length and grade on in-grade tensile strength and stiffness properties of radiata pine timber. J. Korean Wood Sci. and Tech. 26(1): 16-23

ASTM. 1995. Standard methods of static tests of lumber in structural sizes. ASTM Designation D198-94. American Society for Testing and Materials.

ASTM D9-87. 1995. Standard terminology relating to wood. ASTM Designation: D9-87. Annual Book Vol. 04.10 (Wood). American Society for Testing and Materials.

AS 1720.1: 1997. Timber structures Part 1: design methods. Standards Association of Australia. North Sydney, N.S.W.

AS 1748: 1978. Specification for mechanically stress–graded timber. Standards Association of Australia. North Sydey, N.S.W.

AS 1749: 1978. Australian standards rules for mechanical stress grading of timber. Standards Association of Australia. North Sydey, N.S.W.

AS 2858: 1986. Australian standard for Timber-Softwood-Visually stress- graded for structural purposes. Standards Association of Australia. North Sydney, N.S.W.

AS/NZS 4063. 1992. Timber - Stress-graded – In-grade strength and stiffness evaluation. Australian/New Zealand standard. North Sydney NSW Australia and Wellington. New Zealand.

Avery, T. E. and Burkhart, H. E. 1994. Forest Measurements. McGraw-Hill. New York, 290 pp.

Balodis, V. 1972. Influence of grain angle on twist in seasoned boards. Wood Science. 5(1): 44-50

Bamber, R.K. and Burley, J. 1983. The wood properties of radiata pine, Commonwealth Agriculture Bureau, Slough. U.K. 84 pp

Barrett, J.D. and Kellogg, R.M. 1986. Lumber quality from second growth managed forests. In: juvenile wood: what does it mean to forest management and forest products (edited by D.Robertson). Proceedings 47309, Forest Products Research Society. Madison

Barrett, J.D. and Kellogg, R.M. 1991. Bending strength and stiffness of second-growth Douglas-fir dimension lumber. Forest Prod. J. 41 (10): 35-43

Bendtsen, B.A. and Senft, J.F. 1986. Mechanical and anatomical properties in individual growth rings of plantation-grown eastern cottonwood and loblolly pine. Wood and Fiber Sci.18(1):23-38

Benham, P. P., Warnock, F. V. 1973. Mechanics of solids and structures. Pitman Publishing, Canada. 664 pp

Beijing Forestry University. 1982. Wood Science. The State Forest Press, China

Bier, H. 1983. The strength properties of small clear specimens of New Zealand-grown timbers. FRI Bulletin 41. Forest Research Institute. New Zealand

Bier, H. and Collins, M.J. 1985. Bending properties of 100 × 50 mm structural timber from a 28-year-old stand of New Zealand radiata pine. New Zealand Journal of Timber Construction. 1(3): 13-20

Bodig, J. and Goodman, J. R. 1973. Prediction of elastic parameters for wood. Wood Science, 5(4): 249-264

Bodig, J. and Jayne, B. A. 1982. Mechanics of wood and wood composite. Van Nostrand Reinhold. New York. 712pp

Breyer, D E. 1980. Design of wood structures. McGraw-Hill Book Company, New York. 542 pp

BS 4978: 1988. British standard specification for softwood grades for structural use. British Standards Institution.

Buchanan, A.H. 1990. Bending strength of lumber. Journal of Structural Engineering. 116 (5): 1213-1229

Bunn, E.H. 1981. The nature of the resource. New Zealand Journal of Forestry 26 (2): 162-99

Cave, I.D. 1968. Anisotropic elasticity of the plant cell wall. Wood Sci. and Tech. 2(4): 268-78

Cave, I.D. 1969. The longitudinal Young's modulus of *Pinus Radiata*. Wood Science and Technology. 3 (1): 40-48

Cave, I.D. and Walker, J.C.F. 1994. Stiffness of wood in fast grown plantation softwoods: the influence of microfibril angle. Forest Products Journal. 44(5): 43-48

Cockrell, R.A. 1943. Some observations on density and shrinkage of ponderosa pine wood. Amer. Soc. Mech. Engin. Trans. 65: 729-739

Cockrell, R.A. 1949. Further observations on longitudinal shrinkage of softwoods. Forest Prod. Res. Soc. Proc. 1949. 455-459

Cowdrey, D.R. and Preston, R.D. 1966. Elasticity and microfibril angle in the wood of Sitka spruce. In: Proc. of the Royal Soc. B166 (1004): 245-272

Cown, D. J. and McConchie, D.L. 1983. Radiata pine wood properties survey (1977-82). New Zealand Forest Service, FRI Bulletin No. 50. Forest Research Institute. New Zealand

Cown, D.J., McConchie, D.L., and Young, G.D. 1991a. Radiata pine wood properties survey. FRI Bulletin No. 50 (Revised edition). Forest Research Institute. New Zealand

Cown, D.J., Young, G.D., and Kimberley, M.O. 1991b. Spiral grain patterns in plantation-grown *pinus radiata.* New Zealand Journal of Forestry Science. 21(2/3): 206-216

Cown, D.J. 1992. Corewood (juvenile wood) in *Pinus radiata* – should we be concerned? NZ Journal of Forestry Science 22(1): 87-95

Cramer, S.M. and Goodman, J.R. 1983. Model for stress analysis and strength prediction of lumber. Wood and Fibre Sci. 15(3):338-349

Cramer, S.M. and Goodman, J.R. 1986. Failure modelling: A basis for strength prediction of lumber. Wood Fiber Sci. 18(3): 446-459

Cramer, S. M., Fohrell, W. B., McDonald, K. A., and Stahl, D. C. 1988. Exploring the relationship between local slope of grain angle and initial fracture in lumber subject to tensile load. Proceedings of 1988 International Conference on Timber Engineering, Seattle. 2:566-575.

Dabholkar, A.Y. 1980. Analysis of wood with knots and cross grain. PhD thesis, Department of Civil Engineering, Colorado State University, Ft. Collins, CO.

Danborg, F. 1994a. Drying properties and visual grading of juvenile wood from fast grown *Picea abies* and *Picea sitchensis*. Scand. J. For.Res.9: 91-98

Dahlblom, Q., Peterson, H., and Ormarsson, S. 1994. Improving wood dying technology. 4th IUFRO Int. Wood Drying Conf. New Zealand. 165-172

Department of Statistics, New Zealand. 1996. New Zealand Official Yearbook. Statistics New Zealand. 592 pp

Doyle, D.V. and Markwardt, L.J. 1967. Tension parallel-to-grain properties of southern pine dimension lumber. Research Paper FPL 84. U.S. Products Forest Laboratory

Ellis, J. C. and Kimbeerley, M. O. 1995. Volume estimation of export pulplogs. New Zealand J. of Forestry Sci. 25 (2): 123-32.

Fenton, R. R. 1967. A timber grade study of first rotation pinus radiata (D. Don) from Kaiangarroa State Forest, NZFS FRI Technical Paper No. 54, Wellington

Fewell, A.R. 1984. Timber stress grading machines. Building Research Establishment Information Paper 17/84, Garston, UK.

Forest Products Laboratory. 1987. Wood Handbook: Wood as an engineering material. Agric. Handb. 72. USDA Forest Service, Washington, DC

Forest Products Laboratory, USA. 1989. Handbook of wood and wood-based materials for engineers, architects and builders. Hemisphere Publishing Co., New York.

Forsberg, D. 1997. Shape stability of sawn wood of Norway spruce in relation to site parameters, wood characteristics and market requirements. Dept. of Forest-Industry-Market Studies, Swed. Univ. of Agri. Sciences, Uppsala. Report 45, ISSN 0284379X. (In Swedish with English summary). 80 pp

Forsberg, D. and Warensjö, M. 1999 Grain angle variation - A major determination of twist (*Picea abies* (L.) Karst.). Doctoral thesis. Swedish University of Agricultural Sciences. Uppsala.

Goodman, J. R. and Bodig, J. 1970. Orthotropic elastic properties of wood. Journal of the Structural Division, ASCE 96 (St 11): 2301-2319

Goodman, J. R. and Bodig, J. 1980. Tension behaviour of wood-An anisotropic, inhomogeneous material. Final Report to the National Science Foundation. Colorado State University, Fort Collins, CO.

Gordon, J.E. 1978. Structures, or why things don't fall down. Plenum Press, London

Grant, D.J., Anton, A., and Lind, P. 1984. Bending strength, stiffness, and stress-grade of structural Pinus radiata: effect of knots and timber density. New Zealand Journal of Forestry Science 14 (3): 331-48

Grant, D.J. and Anton, A. 1984. Strength and stiffness of Australian-grown stress-graded Pinus Radiata with cross-sections of 35 × 150 mm and 35 × 200 mm. New Zealand Journal of Forestry Science 14(1): 135-45.

Green, A.E. and Zerna. W. 1968. Theoretical Elasticity, 2nd ed. Oxford University Press. 368 pp

Gunnerson, R.A., Goodman, J.R., and Bodig, J. 1972. Plate tests for the determination of elastic parameters of wood. Wood Sci. 5(4): 241-248

Hallock, H. and Malcolm, F.B. 1972. Sawing to reduce warp in plantation red pine studs. U.S.D.A. Forest service research paper. FPL 164 (1972). Forest Products Laboratory, Forest Service, U.S. Department of Agriculture

Hamilton, G. J. 1985. Forest Mensuration Handbook. Forestry Commission Booklet No.39. London

Harris, J. M. 1961. The dimensional stability, shrinkage intersection point and related properties of New Zealand timbers. Technical Paper 36. New Zealand Forest Service. 17pp

Harris, J. M. 1965. A survey of the wood density, tracheid length and latewood characteristics of radiata pine grown in New Zealand. New Zealand Forest Service, Technical Paper No.47.

Harris, J.M. 1989. Spiral grain and wave phenomena in wood formation. Springer Series in Wood Science, Springer-Verlag, New York. 214 pp

Haslett, A. N., Simpson, I. G., and Kimberley, M. O. 1991. Utilisation of 25-years-old *Pinus radiata.* Part 2: Warp of structural timber in drying. New Zealand J. of Forestry Sci.. 21(2/3): 228-233

Hearmon, R. F. S. 1948. Elasticity of wood and plywood. Forest Products Research, Department of Scientific and Industrial Research, London. Special Report No.7

Hibbeler, R. C. 1999. Structural Analysis. Prentice Hall, New Jersey, USA. 600 pp

Hinds, H. V. and Reid, J. S. 1957. Forest trees and timbers of New Zealand. Government Printer. Wellington. 207pp

Hirakawa, Y. and Fujisawa, Y. 1996. The S_2 microfibril angle variations in the vertical direction of latewood tracheids in sugi trees (in Japanese). Mokuzai Gakkaishi 42: 107-14

Hsu, N. N. and Tang, R. C. 1975. Distortion and internal stresses in lumber due to anisotropic shrinkage. Wood Sci.. 7(4): 298-307

Kennedy, R. 1995. Coniferous wood quality in the future: concerns and strategies. Wood Science and Technology. 29(4):321-338

Kinimonth, J.A. 1961. Checking of intergrown knots during seasoning of radiata pine sawn timber. Technical Paper No. 30. New Zealand Forest Service.

Kinimonth, J. A. and Whitehouse, L. J. 1991. Properties and use of New Zealand radiata pine. Ministry of Forestry, New Zealand.

King, Woodrow W. 1954. Alleviating bow and crook in southern yellow pine dimension with chemicals. Forest Prod. J. 4(5): 271-276

Kunesh, R.H. and Johnson, J.W. 1972. Effect of single knots on tensile strength of 2-by 8-inch Douglas-fir dimension lumber. Forest Products Journal, 22(1): 32-36

Liu, H. 1998. A developed model for the simulation of drying deformation in radiata pine boards. PhD thesis. Lincoln University. New Zealand.

Liska, J.A. 1965. Research progress on the relationships between density and strength. Proceedings of the Symposium on Density: A key to wood quality. USDA Forest Serv. Forest Prod. Lab., Madison, WI p89-97

Madsen, B. 1992. Structural behaviour of timber. Timber Engineering Ltd., North Vancouver, British Columbia, Canada

Matheson, A.C., Yang, J. L., and Spencer, D. 1997. Breeding radiata pine for improvement of sawn product value. Timber management toward wood quality and end-product value. IV-19 ~ IV-26. CTIA/IUFRO International Wood Quality Workshop-1997.

McAdoo, J. C. 1969. Computer simulation of small-log mill process. Forest Products Journal. 19(4): 34-35

McConchie, D. and Metcalfe, H. 1999. Obtaining an estimate of log density in conjuction with marvl assessments. Emerging technology for evaluating wood quality for processing. 3rd Wood Quality Symposium. Rotorua, New Zealand, 30th November 1999. Melbourne, Australia, 2nd December 1999

Middleton, G.R. and Munro, B.D. 1989. Log and lumber yields. In (edited by R.M. Kellogg): Second – growth Douglas-fir: its management and conversion value, Special publication No. SP-32, Forintek Canada Corp., Vancouver

Ministry of Forestry, New Zealand, 1995. A Guide to the New Zealand and Australia Timber grading rules. Ministry of Forestry. Wellington, New Zealand

Nestic, R. and H. R. Miler 1991. Shrinkage induced stresses in adhesive joints of glued laminated timber. J. Inst. Wood Sci.. 12(4): 225-231

NZS 3603: 1993. New Zealand timber structures standard. Standards Association of New Zealand, Wellington, New Zealand.

NZS 3618: 1984S. 1984. Specification for mechanical stress grading of timber. Standards Association of New Zealand, Wellington, New Zealand.

NZS 3631. 1988. New Zealand timber grading rules. Standards association of New Zealand, Wellington, New Zealand.

Panshin, A.J. and Dezeeuw, C. 1970. Textbook of wood technology. Vol.1 Third Edition. McGraw-Hill Book Company. New York. 705pp

Pape, R. 1999. Influence of thinning on spiral grain in Norway spruce grown on highly productive sites in southern Sweden. Silva Fennica 33(1): 3-12

Pearson, R.G., Kloot, N.H., and Boyd, J.D. 1966. Timber engineering design handbook. Jacaranda Press Pty Ltd, Sydney

Pellicane, P.J. and Stanfill-McMillan, K., Tichy, R.J. 1987. Effects of knots near the fingers of finger-jointed dimension lumber. Forest Prod. J. 37(5): 13-16

Pellicane, P. J. and Franco, N. 1994. Modelling wood pole failure part2. Material and geometric considerations. Wood Sci. and Tech.. 28(4): 261-274

Perstorper, M., Pellicane, I.R., Kliger, R., and Johansson, G. 1995. Quality of timber products from Norway spruce Part 2. Influence of spatial position and growth characteristics on warp. Wood Science and Technology 29:339-352

Perstorper, M. 1996. Lengthwise variation in grading parameters and comparison with bending strength tests. Proceedings 10th International Symposium on Nondestructive Testing of Wood (edit J.L. Sandoz), Lausanne, Presses Polytechniques et Universitaires Romandes, Lausanne, p341-50.

Phillips, G.E., Bodig, J., and Goodman, J.R. 1981. Flow grain analogy. Wood Science. 14(2): 55-64.

Price, E. W. and P. Koch 1980. Kiln time and temperature affect shrinkage, warp and mechanical properties of southern pine lumber. Forest Products J.. 30(8): 41-47

Samson, M. 1993. Modelling of knots in logs. Wood Sci. & Tech.. 27(4): 429-437.

Shelbourne, C.J.A. 1997. Genetics of adding value to the end-products of radiata pine. Proceedings of IUFRO' 97 GENETICS OF RADIATA PINE, Rotorua, New Zealand, 1-4 December 1997 (FRI Bulletin No.203). 129~141.

Siau, J. F. 1971. Flow in wood. Syracuse University Press, Syracuse, USA. 131 pp

Siau, J. F. 1984. Transport process in wood. Springer-Verlag, New York. 245pp

Siau, J. F. 1995. Wood: influence of moisture on physical properties. Department of Wood Science and Forest Products, Virginia Polytechnic Institute and State University, USA. 227pp

Simperingham, P. 1997. A structural engineer's approach to forestry production. Capturing the benefits of forestry research: Putting ideas to work. Proceedings of the Workshop 1997. Wood Technology Research Centre. University of Canterbury

Simpson, W. T. and Shelly, J. R. 2000. Method for adjusting warp measurements to a different board dimension. Research Note FRL–RN–0273, Forest Products Laboratory, USDA, USA

Skaar, C. 1972. Water in wood. Syracuse University Press, Syrancuse, USA. 218pp

Skaar, C. 1988. Wood - water relations. Springer-Verlag, New York. 283pp.

Sorensson, C.T., Cown, D.J., Ridoutt, B.G., Tian, X. 1997. The significance of wood quality in tree breeding: A case study of radiata pine in New Zealand. Timber management toward wood quality and end-product value. IV-35. CTIA/IUFRO International Wood Quality Workshop.

Steven, M.C. and Goodman, J.R. 1986. Failure modelling: A basis for strength prediction of lumber. Wood and Fiber Sci. 18(3): 446-459

Stohr, H.P. 1983. Twist – where do we go from here? Mededeling, Fakulteit-Bosbou, Universiteit Stellenbosch. No. 98, Vol. II. Pp.704-729 in Jubilee Symp. Faculty of For., Univ. Stellenbosch, 23-24 Sept. 1982

Summitt, R. and Sliker, A. 1980. CRC handbook of materials science, vol.4: Wood, Boca Raton, FL: CRC Press, Inc.

Talor, W. F. 1989. The effect of drying temperature and humidity of moisture variation and warp of south pine dimension lumber. Proceedings of the International Wood Drying Symposium. Washington, USA. 101-106.

Tang, R.C. 1984. Stress concentration around knots in laminated beams. Wood Fiber Sci. 16(1): 57-71.

Tustin, J. and Wilcox, M. 1978. The relative importance of branch size and wood density to the quality of Douglas-fir framing lumber. A review of Douglas-fir in New Zealand. FRI Symposium No. 15, Rotorua

U.S. Forest Products Laboratory. 1955. Wood handbook, U.S. Dept. Agr., Agr. Handbook No. 72, 528 pp.

U.S. Forest Products Laboratory. 1974. Wood handbook: wood as an engineering material. Dept. of Agriculture, Washington, DC

Walford, G.B. 1982. Comparison of the tensile and bending strength of 100 x 50 mm radiata pine. FRI Bulletin No. 21

Walford, G.B. 1985a. Strength/density relationship for Pinus caribaea and Pinus elliotti from Fiji. FRI Bulletin No.90. New Zealand. 17pp.

Walford, G.B. 1985b. The mechanical properties of New Zealand-grown radiata pine for export to Australia. FRI Bulletin No.93. New Zealand. 27pp.

Walford, G.B. 1991. Mechanical properties. Chapter 8. Properties and Uses of New Zealand Radiata pine. Edited by Kininmonth, J.A. and Whitehouse, L.J.. New Zealand Ministry of Forestry.

Walker, J.C.F. 1975. Wood as a material for construction and other purposes. School of Forestry, University of Canterbury, unpublished lecture notes in Wood Science, 123 pp.

Walker, J. C. F. 1993. Primary wood processing: principles and practice. Chapman & Hall, London. 595pp

Walker, J.C.F. and Butterfield, B.G. 1995. The importance of microfibril angle for the processing industries. N.Z. Forestry. 40(4): 34-40.

Walker, J.C.F. 1998. Corewood: docking the dog's tail. Part 2, The need to particularise. New Zealand Forestry. 42(5): 4-6.

Wangaard, F.F. 1950. The mechanical properties of wood. John Wiley and Sons. Inc. New York. 377pp.

Wiedenbeck, J. K., K. Hofmann, P. Peralta, C. Skaar, and P. Koch 1990. Air permeability, shrinkage, and moisture sorption of lodgepole pine stemwood. Wood and Fibre Science. 22(3): 229-245.

Williamson, J. A. 1982. Bending Strength of *Pinus radiata*. Report No. 297. Department of Civil Engineering. University of Auckland, New Zealand.

Woxblom, L. 1993. Quality variations in wall studs – A study conducted at five sawmills in southern Sweden. Dept. of Forest-Industry-Market Studies, Swed. Univ. of Agri. Sciences, Uppsala. Report 28, ISSN 0284379X. (In Swedish with English summary). 50 pp.

Zandbergs, J.G. and Smith, F.W. 1988. Finite element fracture prediction for wood with knots and cross grain. Wood and Fiber Sci. 20(1): 97-106.

Zhang, S.Y. 1994. Mechanical properties in relation to specific gravity in 342 Chinese woods. Wood and Fiber Science 26(4): 512-526.

Zhang, S.Y. 1995. Effect of growth rate on wood specific gravity and selected mechanical properties in individual species from distinct wood categories. Wood Science and Technology 29(4): 451-465.

Zhang, S.Y. 1997. Wood quality: its definition, impact, and implications for value-added timber management and end uses. CTIA/IUFRO International Wood Quality Workshop. p I-17 ~ I-39.

Zhang, S.Y., Corneau, Y., and Chauret, G. 1997. From tree volume to lumber value. Precommercial Thinning Workshop, Laval University, Sainte-Foy.

Zhou, H., Smith, I. 1991. Factors influencing bending properties of white spruce lumber. Wood and Fiber Science 23 (4): 483-500.

Zobel, B.J., Van Buijtenen, J.P. 1989. Wood variation: its causes and control, Springer-Verlag, Berlin. 363pp.

Appendix 1. The colour code of F-grade (after AS 1748: 1978)

F-grade	Corresponding colour
F4	Red
F5	Black
F7	Blue
F8	Green
F11	Purple
F14	Orange
F17	Yellow
F22	White
F27	Colour not yet allocated
F34	Colour not yet allocated

Appendix 2. Structural design properties for F-Grades (after AS 1720.1-1997)

Stress grade	Characteristic strength, MPa					Characteristic short duration average modulus of elasticity parallel to the grain, GPa (E)	Characteristic short duration average modulus of rigidity for beams, GPa (G)
	Bending (f_b)	Tension parallel to grain (f_t)		Shear in beam (f_s)	Compression parallel to grain (f_c)		
		Hardwood	Softwood				
F34	100	60	50	7.2	75	21.5	1.43
F27	80	50	40	6.1	60	18.5	1.23
F22	65	40	35	5	50	16	1.07
F17	50	30	26	4.3	40	14	0.93
F14	40	25	21	3.7	30	12	0.8
F11	35	20	17	3.1	25	10.5	0.7
F8	25	15	13	2.5	20	9.1	0.61
F7	20	12	10	2.1	15	7.9	0.53
F5	26	9.7	8.2	1.8	12	6.9	0.46
F4	13	7.7	6.5	1.5	9.7	6.1	0.41

Appendix 3. Summary of permissible KAR in structural grades (after AS 2858: 1986)

Structural grade	F-grade	Face knots	Edge knots	Other knots
No.1	F14	KAR <= 25%	KAR <= 25%	KAR <= 15%
No.2	F11	KAR <= 33%	KAR <= 40%	KAR <= 25%
No.3	F8	KAR <= 40%	KAR <= 50%	KAR <= 30%
No.4	F7	KAR <= 50%	KAR <= 60%	KAR <= 40%
No.5	F5	KAR <= 60%	KAR <= 66%	KAR <= 45%

**** <= means not exceeding**

Other knot includes all knots that are not fit the definitions of face and edge knots (AS 2858: 1986)